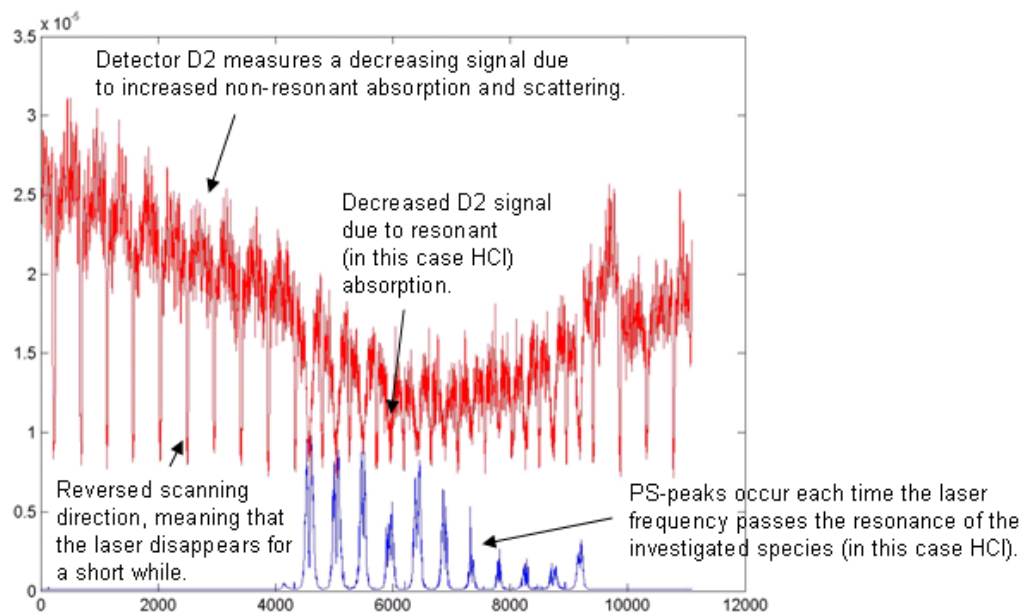
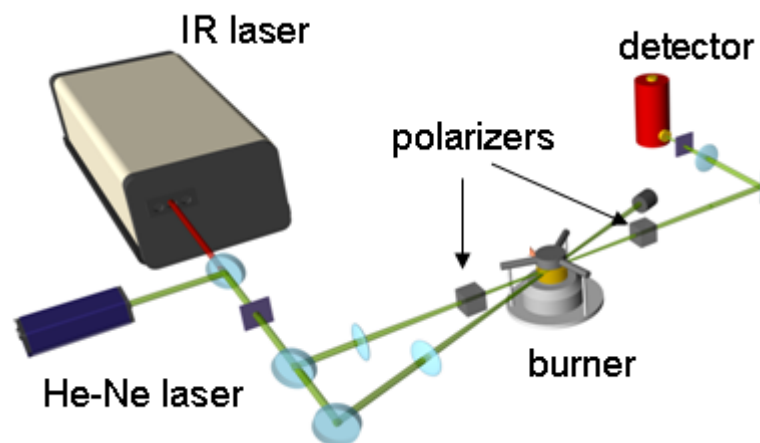
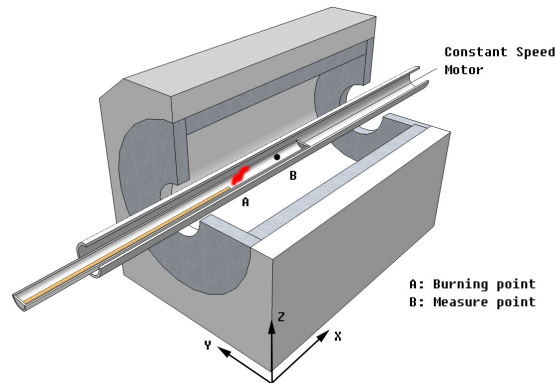


# In-situ measurements of toxic gases in a tube furnace

Zhongshan Li (Lunds Tekniska Högskola), Zhiwei Sun (LTH), Bo Li (LTH), Marcus Aldén (LTH), Heimo Tuovinen (SP), Michael Försth (SP)

Brandforsk project 303-071



# In-situ measurements of toxic gases in a tube furnace

Zhongshan Li (Lunds Tekniska Högskola), Zhiwei Sun (LTH), Bo Li (LTH), Marcus Aldén (LTH), Heimo Tuovinen (SP), Michael Försth (SP)

## Abstract

Infrared Polarization Spectroscopy (IRPS) was used to detect and quantify HCl and HCN in an 800 mm long tube furnace. Pieces of a PVC-carpet or pellets of nylon 6,6 were continuously fed into the furnace producing a heavy smoke. This constitutes a very harsh environment from a diagnostic point of view due to the high smoke density and relatively long length of the furnace. Despite this it was possible to quantify HCl and HCN concentrations in the smoke down to a levels of 50 ppm using IRPS. The explanation for this success is twofold. Firstly the IRPS method is inherently almost noise free due to the use of crossed polarisers, creating a virtually zero background. Secondly the problem with laser beam attenuation due to scattering in the smoke, especially with soot particles, decreases in importance with the fourth power of the laser wavelength. This means that infrared measurements represent a great advantage over measurements in the ultraviolet or visible wavelength range.

It is concluded that IRPS shows great promise as a new diagnostics tool in fire technology for small-scale as well as for large scale experiments. Furthermore the *in situ* nature of the method should be emphasized since this means that valuable information is obtained that can not be extracted from sampling methods such as MS/GC or FTIR for example. This information is important, for example, in egress calculations and analysis of fire chemistry. The method can easily be adapted for other gases such as HF, NO, NO<sub>2</sub>, HBr, CO and SO<sub>2</sub>.

Key words: fire, toxicity, tube furnace, IRPS, polarization spectroscopy, chemistry

Sökord: brand, toxicitet, rörugn, IRPS, polarisationsspektroskopi, kemi

**SP Sveriges Tekniska Forskningsinstitut**  
SP Technical Research Institute of Sweden

SP Report 2009:50  
ISBN  
ISSN 0284-5172  
Borås 2009

# Contents

<b>Abstract</b>	<b>3</b>
<b>Contents</b>	<b>4</b>
<b>Preface</b>	<b>5</b>
<b>Summary</b>	<b>6</b>
<b>1 Introduction</b>	<b>7</b>
<b>2 Methods</b>	<b>9</b>
2.1 Infrared polarization spectroscopy, IRPS	9
2.2 Measurements of HCl in a premixed CH <sub>4</sub> /O <sub>2</sub> /Ar flame	10
2.3 Measurements in a tube furnace	11
2.3.1 The tube furnace	11
2.3.2 Operating conditions	13
2.3.3 IRPS experimental setup and interpretation	16
2.4 Modelling	20
<b>3 Results</b>	<b>22</b>
3.1 Measurements in a premixed CH <sub>4</sub> /O <sub>2</sub> /Ar flame	22
3.2 Measurements in a tube furnace	22
3.2.1 PVC-carpet, measurement of HCl	22
3.2.2 Nylon 6,6, measurement of HCN	24
3.3 Modelling	29
<b>4 Conclusions</b>	<b>31</b>
<b>Appendix A Complete results from measurements in the tube furnace</b>	<b>33</b>
<b>Appendix B Reaction mechanism</b>	<b>58</b>
<b>References</b>	<b>75</b>

## **Preface**

The Swedish Board for Fire Research (Brandforsk) sponsored this project with reference number 303-071 which is gratefully acknowledged. Brandforsk is owned by the Swedish government, assurance companies, local authorities and industry and has as mission to initiate, finance and follow-up different types of fire research.

## Summary

It has been shown that IRPS (Infrared Polarization Spectroscopy) in combination with absorption measurements is a useful laser diagnostic technique for fire technology. The technique enables time resolved *in situ* measurements of toxic gases such as HCl and HCN in a tube furnace filled with hot sooty combustion gases. This is a very harsh environment and it can therefore be expected that IRPS can also be applied to many other geometries that are used by the fire community.

In the first part of the study the technique was applied to a small scale laboratory burner. The rationale for this simplified test was to see what signal levels could be expected and whether quantitative measurements would be possible. Based on this experiment quantitative measurements were deemed possible and the detection limit was estimated to be less than 50 ppm based on the signal to noise ratio of 10.

The second and main part of the project consisted of *in situ* measurement inside a tube furnace. The purpose of conducting measurements in a tube furnace is that it is possible to model a variety of ventilation and temperature conditions that might occur during a real fire. These are important parameters that strongly influence the production of toxic gases. If the combustion would be studied in well ventilated conditions in the open air the amounts of toxic gases produced are typically much lower than for more realistic under-ventilated conditions. The fuels used in the study were small pieces of a PVC-carpet and nylon 6,6 pellets. This constitutes a very harsh environment from a diagnostic point of view due to the high smoke density and relatively long length of the furnace. Despite this it was possible to quantify HCl and HCN concentrations in the smoke using IRPS. The explanation for this success is twofold. Firstly the IRPS method is inherently almost noise free due to the use of crossed polarisers, creating a virtually zero background. Secondly the problem with laser beam attenuation due to scattering in the smoke, especially with soot particles, decreases in importance with the fourth power of the laser wavelength. This gives infrared measurements a great advantage as compared to measurements in the ultraviolet or visible wavelength range, due to their relatively long inherent wavelength.

It is concluded that IRPS shows great promise as a new diagnostics tool in fire technology for small-scale as well as for large scale experiments. Furthermore, the *in situ* nature of the method should be emphasized since this means that valuable information is obtained that can not be extracted from sampling methods such as MS/GC or FTIR. This information is important, for example, in egress calculations and the analysis of fire chemistry. The method can easily be adapted for other gases such as: HF, NO, NO<sub>2</sub>, HBr, CO and SO<sub>2</sub>.

Further work should focus on better understanding of chemistry of toxic gases as well as on using the techniques for other applications than a tube furnace, such as the cone calorimeter (ISO 5660) [1] or the room-corner test (ISO 9705) [2].

In order to develop the technique further it would be useful to test a single mode laser system which would enable single-shot measurements and thereby also enable studies of mixing conditions in the combustion zone and in the fire gases.

# 1 Introduction

Typically two thirds of fire related fatalities are due to smoke inhalation [3]. Therefore it is important to understand how toxic gases are produced and how to avoid them. There are presently a number of powerful CFD (Computational Fluid Dynamics) codes which successfully predict the transport of fire smoke inside a building in a fire. However, the amount of toxic gases produced cannot be predicted in any detail by the most common application of these programs, but is needed as input. Therefore, to take full advantage of these programs there is a need for quantitative data on the production rate and chemistry of the toxic gases produced in a fire. This is especially important since the use of CFD-programs is widespread among fire safety consultants and researchers and plays an important role in the design of new buildings. Information concerning the concentrations of toxic molecules is not only used in CFD-programs but also in egress (i.e. evacuation) models. Typical egress models compute incapacitation in a fire environment based on the concentration of a number of toxic gases [4]. For full scale experiments [5] where the toxic gases are transported in the hot fire gases, the chemistry for these gases must be known in order to draw conclusions concerning the toxicity at different times and positions of species produced from different materials. Another example from recent years are *in vitro* experiments with fire gases performed using human lung cells [6] as well as entire lung systems from guinea pigs [7]. When gases are transported to the alveoli, wall effects become important as the diameter of the respiratory system decreases. In order to study such effects high spatial resolution such as that provided by laser diagnostics is imperative.

The toxicity of fire smoke is not constant over time and space but depends on the distance from the fire and the transport conditions of the smoke. At elevated temperatures, such as in fire situations, the smoke chemistry is important near the fire implying that concentration of important toxic species, e.g. HCN [8-10], will differ between the sampling location and the measurement chamber. If the detailed chemistry of the production and destruction of molecules is to be studied it is necessary to have detailed knowledge of the exact composition in space as well as in time. Traditionally, toxic molecules, such as HCl and HCN have been measured using FTIR (Fourier Transform Infrared Spectroscopy). FTIR can easily be applied to a variety of situations using custom made sampling probes. On the other hand the method measures values that are partially averaged in both time and space. Furthermore, the measurements are conducted in a chamber that is physically separated from the sampling point, at least by the length of the probe. This means that reactive molecules can react or stick to the probe on their way to the measurement chamber. This is typically a problem with acid gases [11].

While a large body of information exists on gas chemical kinetics for well ventilated combustion, typical for energy production purposes, the level of knowledge is significantly lower concerning the processes involved in fire situations, where ventilation is often poor. The Purser Furnace apparatus [12, 13] enables different fire stages to be created on a small scale in the laboratory, which gives the possibility of using various advanced techniques to do *in-situ* measurements. Several studies have been undertaken where the yield of toxic molecules in a tube furnace has been measured as a function of fuel, equivalence ratio and temperature [14-16]. In these studies the fire smoke was diluted and homogenized in a mixing chamber after exiting the furnace. Gas concentrations were then determined indirectly or directly by sampling from the mixing chamber with subsequent analysis using FTIR-spectroscopy of the gas or by spectrophotometric or chromatographic analysis of bubbler solutions. This means that no information about the spatial information on the gas concentrations can be obtained. Furthermore the time resolution becomes relatively poor due to the mixing in the mixing chamber. Using laser diagnostics it is possible to study the chemistry *in situ*. Thus, laser

diagnostics and chemical modelling are often the combination of choice in combustion sciences [17]. In many cases laser diagnostics exhibit a superior sensitivity compared to other techniques.

Several laser-based diagnostics techniques have been applied widely elsewhere in combustion science for *in situ* measurements, such as: Laser-Induced Fluorescence (LIF), Coherent Anti-Stokes Raman Spectroscopy (CARS), Degenerate Four-Wave Mixing (DFWM) and so on, due to their merits of non-intrusiveness, high temporal and spatial resolution and species-selected detection. For species like HCN and HCl, which have no electronic transitions accessible for conventional LIF techniques in the UV/visible, Tunable Diode-Laser Absorption Spectroscopy (TDLAS) in the near-IR region, mid-infrared DFWM (IR-DFWM) and Infrared Polarization Spectroscopy (IRPS) have been broadly utilized [18, 19]. Although the TDLAS technique can provide high detection sensitivity, the line-of-sight nature of the method makes it inappropriate for spatially resolved measurements.

Various laser techniques have been developed and applied to the measurement of, e.g., temperature, species concentration and velocities in recent years. These techniques have been important in the diagnostics of various phenomena in combustion [20]. Several techniques have shown outstanding features, e.g., non-intrusiveness in combination with high temporal ( $\sim 10$  ns) and spatial ( $\sim 50$ - $100$   $\mu\text{m}$ ) resolution. These techniques presently represent our most important tools in the understanding of high temperature reactions in general and combustion processes in particular.

In this work, IRPS was used to measure the production of the toxic gases in a tube furnace under different ventilation conditions, temperatures and positions along the furnace. Polyvinyl chloride (PVC) carpet and pure Nylon 6.6 pellets were burned and the production of HCl and HCN, respectively, was measured. In addition, the line-integrated Absorption Spectra (AS) along the tube were recorded simultaneously.



## 2 Methods

### 2.1 Infrared polarization spectroscopy, IRPS

Polarization Spectroscopy (PS) is a widely used non-linear sub-Doppler spectroscopic technique [21], which was firstly reported by Wieman and Hänsch [22]. In a representative setup of PS, a co-propagating strong pump and a weak probe beam, usually derived from the same laser, are tuned to optical transitions of the studied species and crossed at the measurement volume. The induced bi-refringence, due to the polarized optical pumping, is detected. As for most coherent techniques the PS-signal propagates as a laser-like beam. This is an advantage when discriminating the signal from background noise due to non-coherent scattering and fluorescence. Furthermore, the very low background noise is also due to the use of crossed polarizers. Another technique, degenerate four-wave mixing (DFWM), is a similar mature non-linear laser spectroscopic technique for trace molecular species sensing [23]. DFWM has previously been employed in the detection of various important molecules, e.g. HF [24], HCl [25], NO<sub>2</sub> [25], C<sub>2</sub>H<sub>2</sub> and CH<sub>4</sub> [26] in non-reactive gas flows. However, the complexity of a DFWM setup in the mid-IR has hindered the application of IR-DFWM to reactive gas flows.

With almost all the merits of laser diagnostic techniques, like high temporal and spatial resolution, species specific detection and low detection limits, PS has been widely used in combustion and plasma diagnostics [27, 28]. Mid-IR Polarization Spectroscopy (IRPS) has been recently applied to detect various species, e.g. CO<sub>2</sub> [29, 30], C<sub>2</sub>H<sub>2</sub> [31], CH<sub>4</sub> [32, 33], C<sub>2</sub>H<sub>6</sub> [33] and H<sub>2</sub>O [29] in flames, by probing molecular fundamental vibration transitions. An advantage of PS compared with other non-linear techniques, e.g. DFWM and CARS, is the relatively simple experimental setup. This is represented by the automatic phase matching with crossing of only two beams [18] and the overlap of the signal beam with the probe beam which can be used to guide the signal detection by slightly opening the analyzing polarizer. This experimental simplicity is important due to the lack of beam viewer in the mid-IR.

However, most PS studies heretofore have been limited to the ultraviolet/visible spectral region by probing electronic transitions. Probing the molecular ro-vibrational transition by infrared (IR) excitation has always been attractive to the combustion diagnostic community. Many important combustion species such as CO<sub>2</sub>, CO, H<sub>2</sub>O, CH<sub>4</sub> etc., which are ‘dark’ as they post no conveniently accessible electronic transitions, are detectable in the mid-IR spectral range. Due to limited availability of proper IR laser sources, low sensitivity of the infrared detectors and the relatively low fluorescence quantum yields, only limited laser-based combustion diagnostic experiments in the mid-infrared spectral region via ro-vibrational transitions have been reported. Infrared Polarization Spectroscopy (IRPS) is an absorption based, crossed-beam, coherent signal measurement technique with possibility to achieve high sensitivity and high contrast against thermal background. As such it has proved to be a proper technique to probe molecular ro-vibrational transitions in the mid-infrared spectral range. In the last five years, IRPS has been applied to detect CO<sub>2</sub> [14, 15] and CH<sub>4</sub> [16] in non-reactive flows, CH<sub>4</sub> and C<sub>2</sub>H<sub>6</sub> [17] as fuel and CO<sub>2</sub> and H<sub>2</sub>O [18] as combustion products in atmospheric pressure flames. Very recently C<sub>2</sub>H<sub>2</sub> [19] has been detected as a combustion intermediate in a CH<sub>4</sub>/O<sub>2</sub> low pressure laminar flame. The detection of OH as a minor species in a low pressure flame has also been reported [20].

## 2.2 Measurements of HCl in a premixed CH<sub>4</sub>/O<sub>2</sub>/Ar flame

The first experiments were performed in a laboratory flame. This is a much simpler and more accessible geometry than the setup with the tube furnace described in Section 2.3 and is therefore a good geometry for a test of concept before full blown experiments were conducted.

A schematic view of the experimental setup is shown in Figure 1. The injection-seeded single-longitudinal-mode Nd:YAG laser (Spectra Physics, PRO 290-10) operated at a repetition rate of 10 Hz. The second harmonic at 532 nm from the Nd:YAG laser was used to pump a tunable dye laser (Sirah, PRSC-D-18) with styryl 11 dye. The residual fundamental beam at 1.064  $\mu\text{m}$  from the Nd:YAG laser after frequency doubling was differentially frequency mixed in a LiNbO<sub>3</sub> crystal with the tunable dye laser output centered at 800 nm generating the required IR laser beam around 3.2  $\mu\text{m}$  with a pulse energy of about 1 mJ. To visualize the IR beam path a HeNe laser beam was overlapped with the horizontally polarized IR beam through a CaF<sub>2</sub> plate. A co-propagating geometry PS setup, with an angle between the two beams of 5 degrees, was utilized. The probe beam, a 7% reflection of the IR beam from a CaF<sub>2</sub> beam splitter, was focused with a lens of 90 cm focal length over the sample. The transmitted part of the IR beam was reflected by an aluminium mirror and focused with a 55 cm lens to serve as the pump beam. A quarter wave or half wave plate was placed before the focusing lens in the pump beam to alter the polarization of the pump beam to be circularly polarized. Two crossed infrared polarizers (YVO<sub>4</sub>) were used as polarizer and analyzer. The extinction ratio,  $6.6 \cdot 10^{-7}$ , of the polarizer pair was measured with an previously published novel method [34]. The transient PS signal was detected using a liquid nitrogen cooled InSb (Judson, J10D) photovoltaic infrared detector. A 3 GHz analogue bandwidth digital oscilloscope (Lecroy, WaveMaster 8300) was used to time integrate and store the transient PS signal from the IR detector.

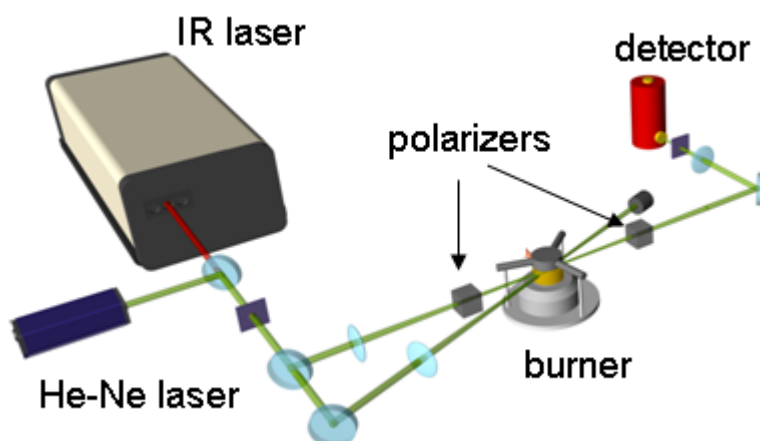


Figure 1 Schematic experimental setup for IRPS detection of HCl in a laboratory flame.

The measurements were performed at atmospheric pressure in a premixed CH<sub>4</sub>/O<sub>2</sub>/Ar flame, burning on a 3-cm-diameter McKenna-type flat burner. The gas flow was controlled with three mass flow meters for Ar, CH<sub>4</sub>, and O<sub>2</sub> with speeds of 16.8, 1.9, and 3.8 l/min, respectively. Hydrogen chloride was created by seeding chloroform into the flame. Two independent Ar conduits were utilized, one of them bubbled through the liquid chloroform (in an ice bath), in order to control the amount of chloroform seeding

while keeping the same total Ar gas flow. The IRPS measurements were performed at 1 cm above the burner surface. The results are presented in Section 3.1.

## 2.3 Measurements in a tube furnace

The purpose of conducting measurements in a tube furnace is that it is possible to model a variety of ventilation and temperature conditions that might occur during a real fire. These are important parameters that strongly influence the production of toxic gases. If the combustion were studied under well ventilated conditions in the open air, the amounts of toxic gases produced would typically be much lower than for more realistic under-ventilated conditions.

### 2.3.1 The tube furnace

The tube furnace used was a Carbolite AGD 12, see Figure 2.



**Figure 2** The Carbolite AGD 12 tube furnace used in the experiments [35].

A schematic view of the furnace is shown in Figure 3. The geometry and operation are similar to the Purser furnace standardized test [16, 36]. The length of the furnace was 80 cm. A quartz tube with a length of 170 cm was fixed in the furnace and protruded on both sides from the furnace. The inner and outer diameter of the quartz tube were 42 and 47 mm, respectively. An 80 cm long silica boat containing the investigated fuel was delivered into the quartz tube with speeds of 2 or 4 cm/s, in the positive x-direction as defined in Figure 3, driven by a step motor. The inner and outer widths of the boat were 36 and 41 mm, respectively. The boat was dragged through the furnace instead of pushed. The conventional method of entry of the boat is to push but the laser optics placed in front of the tube, see Figure 10, made it easier to pull the boat into the tube. The constant speed of the boat ensures a continuous fuel feed to the burning point A, see Figure 3, whose position is normally  $x = 15 \sim 20$  cm with the set temperatures 670°C, 750°C, and 910°C used in this study. *In situ* measurements inside the furnace were performed and therefore the mixing box prescribed in reference [36] was not used.

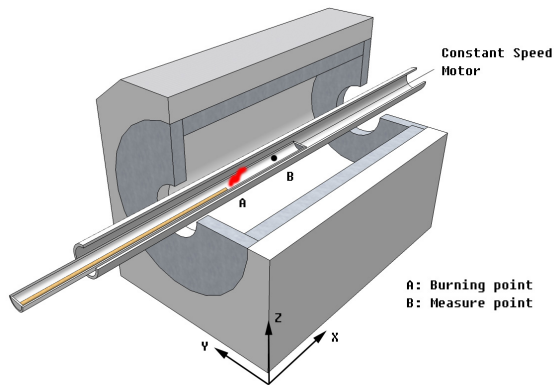


**Figure 3** Schematic view of the cross section of the tube furnace setup. See the text for a detailed description.

The fuels used in the study were pieces of a PVC-carpet and nylon 6,6 pellets (the pellets were purchased from Northern Industrial Plastics). The PVC content of the carpet was approximately 50%. The thickness of the carpet was 2.7 mm and its area weight 2.9 kg/m<sup>2</sup>. The carpet was cut into ~1.5 mm wide stripes, depending on the fuel load. The nylon 6,6 pellets had dimensions of ~2-4 mm and density ~1140 kg/m<sup>3</sup>. The fuel was distributed as homogeneously as possible in the boat in order to keep the fuel load,  $\rho_{load}$ , constant, see Section 2.3.2.1 and Figure 4.

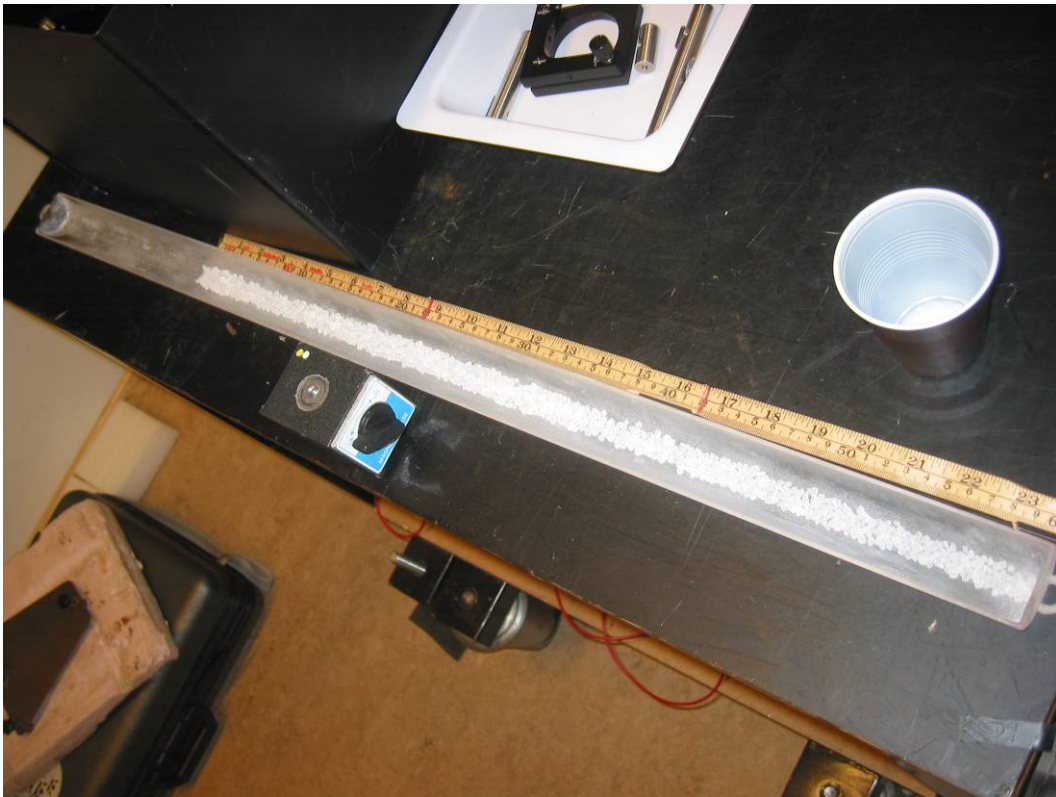


**Figure 4** Distribution of nylon 6,6 pellets in the silica boat.

The air flow through the quartz tube was varied between 0.5, 2, 2.5, 10 and 30 l/min. In some of the measurements nitrogen was mixed with the air in order to increase the equivalence ratio without creating an exceedingly slow air flow through the furnace. The

gas flows were controlled by mass flow controllers (Bronkhorst), and the mixed gas was pumped into the quartz tube in the x direction, see Figure 3 and Figure 10. In order to get a well controlled air flow through the furnace modified for the inclusion of the laser beams, a plexiglas box was built, see Figure 10. The air entered the box through a conduit and the laser beam entered through a CaF<sub>2</sub> window. The plexiglas box was connected to the quartz tube of the furnace via an air-tight seal.

## 2.3.2 Operating conditions

The operating conditions for all tests are presented in Table 1 in Appendix A. The set temperature of the oven was varied between 670°C, 750°C, and 910°C. The actual temperature profile in the middle of the quartz tube was measured using a type K thermocouple. This measurement had to be repeated for each air flow used since the temperature inside the quartz tube is sensitive to the air flow inside the tube for any given set temperature. The set temperature is the temperature indicated by a thermocouple at a position that is not affected by the air flow.

The calculation of equivalence ratio from the operating parameters in Table 1 is given below.

### 2.3.2.1 Mass loss concentrations

The mass loss concentration is given by the following equation:

$$C_{m_{loss}} = \frac{\dot{m}_{loss}}{g} [\text{gm}^{-3}] \quad (1)$$

where  $g$  [ $\text{lmin}^{-1}$ ] is the gas flow through the furnace and  $\dot{m}_{loss}$  is the mass-loss rate [ $\text{mgmin}^{-1}$ ] of the fuel in the combustion process. The mass-loss rate is given by

$$\dot{m}_{loss} = \frac{d}{dt} (m_{load} - m_{res}) \quad (2)$$

where  $m_{load}$  is the fuel mass [ $\text{mg}$ ] entering the furnace and  $m_{res}$  [ $\text{mg}$ ] is the mass of the fuel residues after the boat exits the furnace. This can be calculated as:

$$\dot{m}_{loss} = (\rho_{load} - \rho_{res}) \dot{b} = \rho_{loss} \dot{b} \quad (3)$$

where  $\rho_{load}$ ,  $\rho_{res}$ , and  $\rho_{loss}$  [ $\text{mg}\cdot\text{mm}^{-1}$ ] are the linear densities of entering fuel, exiting fuel, and their difference, respectively.  $\dot{b}$  [ $\text{mm}\cdot\text{min}^{-1}$ ] is the boat advance rate. In most, but not all, of the experiments in this study the fuel was completely combusted and therefore  $\rho_{loss} = \rho_{load}$ .

The gas flows in this study were different mixtures of air and N<sub>2</sub>. For the relative oxygen supply it is not flow of air + N<sub>2</sub> that is of interest but only the flow of air. Therefore the air equivalent mass-loss concentration is introduced as:

$$C_{air, m_{loss}} = \frac{\dot{m}_{loss}}{a} [\text{gm}^{-3}] \quad (4)$$

where  $a$  is the [ $\text{min}^{-1}$ ] amount of air in the gas flow. Obviously for pure air flow  $a = g$ .

### 2.3.2.2 Equivalence ratios

#### 2.3.2.2.1 HCN

For flaming decomposition conditions, such as studied in this project, the equivalence ratio  $\phi$  is of fundamental interest<sup>1</sup>. The equivalence ratio is defined as:

$$\phi = \frac{\left(\frac{\dot{m}_{loss}}{a}\right)_{\text{exp}}}{\left(\frac{\dot{m}_{loss}}{a}\right)_{\text{stoich}}} = \frac{(C_{air, \dot{m}_{loss}})_{\text{exp}}}{(C_{air, \dot{m}_{loss}})_{\text{stoich}}} \quad (5)$$

The reason why  $\dot{m}_{loss}$  and not  $\dot{m}_{load}$  is used is that the gas-phase combustion conditions depend on the amount of the solid fuel that is pyrolyzed or vaporized, rather than the amount that is actually fed into the furnace.

Nylon 6,6 is made by reacting hexamethylene diamine ( $\text{C}_6\text{H}_{16}\text{N}_2$ ) with adipic acid ( $\text{C}_6\text{H}_{10}\text{O}_4$ ), see Figure 5.

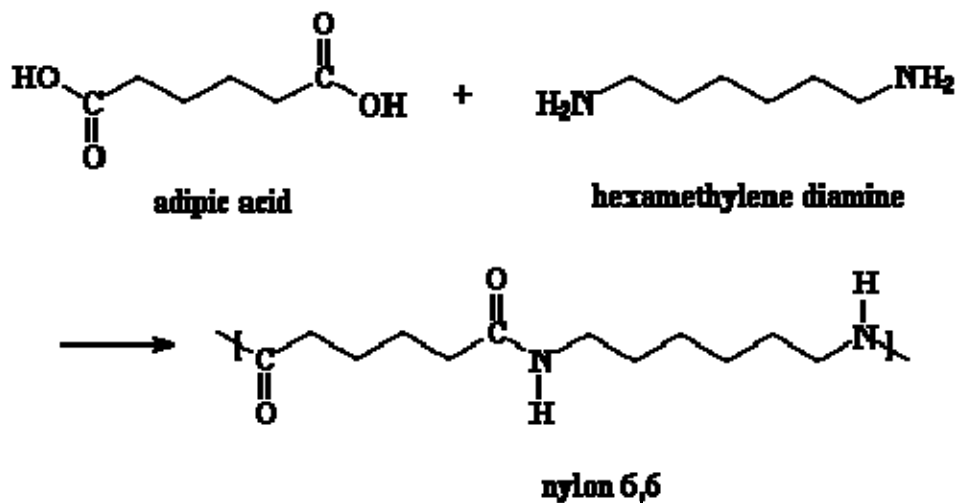
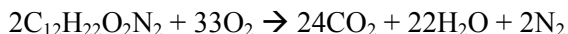


Figure 5 Production of nylon 6,6 from adipic acid and hexamethylene diamine.

The molecular formula for one unit of nylon 6,6 is  $\text{C}_{12}\text{H}_{22}\text{O}_2\text{N}_2$ . The stoichiometry for combustion is therefore:



That is, for two units of consumed nylon 6,6 ( $\text{C}_{12}\text{H}_{22}\text{O}_2\text{N}_2$ ), 33  $\text{O}_2$  molecules are consumed.

<sup>1</sup> The fuel can also react with oxygen under non-flaming conditions. This is however not the case in this study where the temperatures were relatively high. An exception is the initial phase of each experiment when the fuel is heated from room temperature to the furnace temperature as the boat enters the furnace. Non-flaming pyrolysis is not analyzed in this report.

The concentration of O<sub>2</sub> in air is 20.95%. Therefore one mole of oxygen corresponds to 1/0.2095 = 4.77 mole air. Therefore 33·4.77 = 157.51 mole of air is consumed for every two moles of nylon 6,6. The molecular mass of dry air is 28.97 g/mole. The molecular mass of C<sub>12</sub>H<sub>22</sub>O<sub>2</sub>N<sub>2</sub> is:

$$M_{\text{nylon6,6}} = 12 \cdot M_C + 22 \cdot M_H + 2 \cdot M_O + 2 \cdot M_N = 12 \cdot 12.01 + 22 \cdot 1.01 + 2 \cdot 16.00 + 2 \cdot 14.01 \\ = 226.23 \text{ g/mole}$$

This gives a stoichiometric fuel/air mass ratio of:

$$\left( \frac{\dot{m}_{\text{fuel}}}{\dot{m}_{\text{air}}} \right)_{\text{stoich,nylon6,6}} = \frac{2 \cdot 226.23}{157.51 \cdot 28.97} = 0.099 \quad (6)$$

Or, since the density of dry air at atmospheric pressure (101.325 kPa) and room temperature (293 K) is  $\rho_{\text{air}} = 1.20 \text{ kgm}^{-3}$ :

$$(C_{\text{air},m_{\text{loss}}})_{\text{stoich,nylon6,6}} = \left( \frac{\dot{m}_{\text{loss}}}{\dot{a}} \right)_{\text{stoich,nylon6,6}} = \left( \frac{\dot{m}_{\text{loss}}}{\dot{m}_{\text{air}} / \rho_{\text{air}}} \right)_{\text{stoich,nylon6,6}} = \quad (7) \\ \frac{2 \cdot 226.23}{157.51 \cdot 28.97 / 1200} = 119 \text{ [gm}^{-3}\text{]}$$

This gives the equivalence ratio:

$$\phi_{\text{nylon6,6}} = \frac{(C_{\text{air},m_{\text{loss}}})_{\text{exp,nylon6,6}}}{(C_{\text{air},m_{\text{loss}}})_{\text{stoich,nylon6,6}}} = \frac{(C_{\text{air},m_{\text{loss}}})_{\text{exp,nylon6,6}}}{119} \quad (8)$$

where  $(C_{\text{air},m_{\text{loss}}})_{\text{exp,nylon6,6}}$  is given in [gm<sup>-3</sup>] (or [mg l<sup>-1</sup>]). Using Eqs. (3), (4) and (8) we obtain.

$$\phi_{\text{nylon6,6}} = \frac{\rho_{\text{loss}} \dot{b}}{119 \dot{a}} \quad (9)$$

### 2.3.2.2.2 HCl

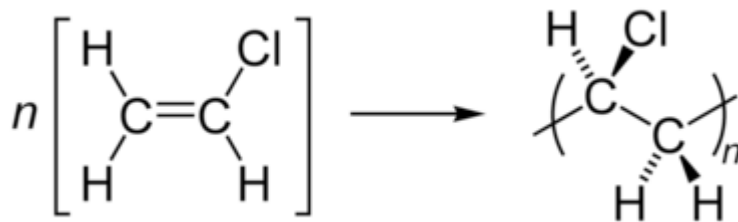
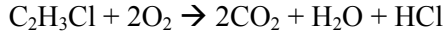


Figure 6 Polymerization of the vinyl chloride monomer into PVC.

The molecular formula for one unit of PVC is  $C_2H_3Cl$ . The stoichiometry for combustion is:



That is, for one unit of consumed PVC ( $C_2H_3Cl$ ), 2  $O_2$  molecules are consumed.

One mole of oxygen corresponds to  $1/0.2095 = 4.77$  mole air. Therefore  $2 \cdot 4.77 = 9.54$  mole of air is consumed for every mole of PVC. The molecular mass of  $C_2H_3Cl$  is:

$$\begin{aligned} M_{PVC} &= 2 \cdot M_C + 3 \cdot M_H + 1 \cdot M_{Cl} = 2 \cdot 12.01 + 3 \cdot 1.01 + 1 \cdot 35.45 \\ &= 62.45 \text{ g/mole} \end{aligned}$$

This gives a stoichiometric fuel/air mass ratio of:

$$\left( \frac{\dot{m}_{fuel}}{\dot{m}_{air}} \right)_{stoich,PVC} = \frac{1 \cdot 62.45}{9.54 \cdot 28.97} = 0.226 \quad (10)$$

Or, using the density of air:

$$\begin{aligned} (C_{air, \dot{m}_{loss}})_{stoich,PVC} &= \left( \frac{\dot{m}_{loss}}{\dot{a}} \right)_{stoich,PVC} = \left( \frac{\dot{m}_{loss}}{\dot{m}_{air} / \rho_{air}} \right)_{stoich,PVC} = \\ &= \frac{1 \cdot 62.45}{9.54 \cdot 28.97 / 1200} = 271 \text{ [gm}^{-3}\text{]} \end{aligned} \quad (11)$$

This gives the equivalence ratio:

$$\phi_{PVC} = \frac{\rho_{loss} \dot{b}}{271a} \quad (12)$$

The PVC content of the carpet was ~50% and therefore the equivalence ratio becomes:

$$\phi_{PVC-carpet} = \frac{\rho_{loss} \dot{b}}{542a} \quad (13)$$

This equivalence ratio is an approximate indication since some of the non-PVC content in the carpet is combustible plasticiser. The major part of the non-PVC content is, however, non-combustible filler.

### 2.3.3 IRPS experimental setup and interpretation

A schematic view of the laser spectroscopy setup used for the measurement in the tube furnace is shown in Figure 7. The pump and probe laser beams were crossed at an angle of  $2.2^\circ$ , see point B in Figure 3 and DV in Figure 7. The detection volume was about



15 mm × 1 × mm × 1 mm = 15 mm<sup>3</sup> (x × y × z). The IR laser pulses around 3280 cm<sup>-1</sup> (3.0 μm) for HCN and around 3000 cm<sup>-1</sup> (3.3 μm) for HCl with a line width of 0.025 cm<sup>-1</sup>. The laser frequency was constantly scanned over the resonance. The IR beam was traced by a HeNe laser beam in order to visualize the IR beam in the following optics alignments. The IR laser beam was focused by a f = 1000 mm CaF<sub>2</sub> lens, and then about 7% was reflected by a CaF<sub>2</sub> plate to be used as the probe beam. The transmitted part of laser beam served as pump beam. A quarter-wave plate was placed in the pump beam to polarize the pump beam circularly. Two YVO<sub>4</sub> infrared polarizers were positioned, one before and one after the detection volume, crossed to each other in the probe beam. After passing the probe volume the pump beam was blocked in a beam dump. Part of the probe laser beam reflected from the second polarizer was detected simultaneously in order to record the total absorption along the tube, which gave the Absorption Spectrum (AS). The PS and AS signals were collected with two independent liquid-N<sub>2</sub>-cooled InSb detectors, time-integrated and stored in a 1 GHz bandwidth digital oscilloscope. The furnace was fixed on a table which could be moved in three directions (x, y, z). This enabled measurements at almost any point in the oven. A photograph of the laboratory is shown in Figure 10.

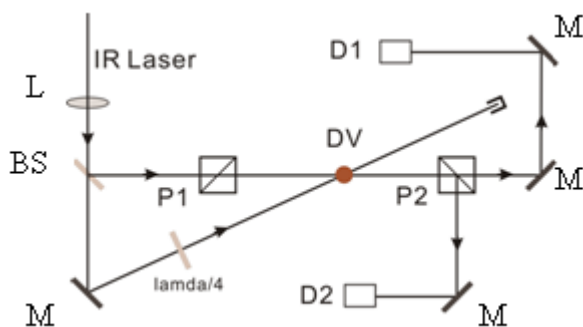


**Figure 7 Schematic view of the laser spectroscopic setup. IR laser is the circular laser beam from the laser system, BS beam splitter, P1 and P2 polarizers, D1 detector for the IRPS-signal, D2 detector for the absorption measurements, DV detection volume (inside the furnace, corresponding to point B in Figure 3), M mirrors.**

In order to obtain quantitative information from the PS signal, the integrated intensities of the PS signal was calibrated by HCN or HCl sample gases with known concentrations. In the experiments, the commercial HCN/N<sub>2</sub> (206 ppm HCN by volume) and HCl/N<sub>2</sub> (200 ppm HCl by volume) bottle gases were diluted further by N<sub>2</sub> and used for calibrations. The measurement of calibration gases was performed at room temperature and atmospheric pressure, which differed from the conditions in the furnace tube, see Figure 9. Thanks to the translation table, the furnace could be removed during calibrations. After calibrations the table was repositioned at its original position. This enabled calibrations without re-alignment of the system before measurements in the furnace.

An example of the raw spectra from a measurement in the tube furnace is shown Figure 8.

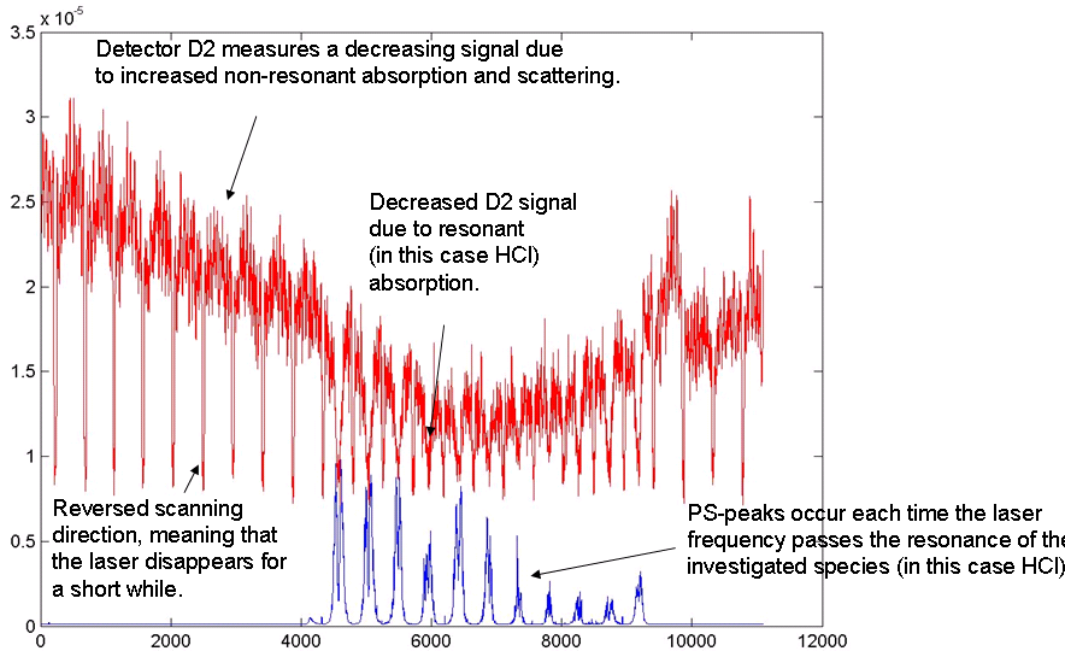


**Figure 8** Example spectra. The red spectrum is the absorption signal and the blue spectrum is the PS-signal. The detector D2 refers to Figure 7. The unit on the y-axis is arbitrary while the unit on the x-axis is [s].

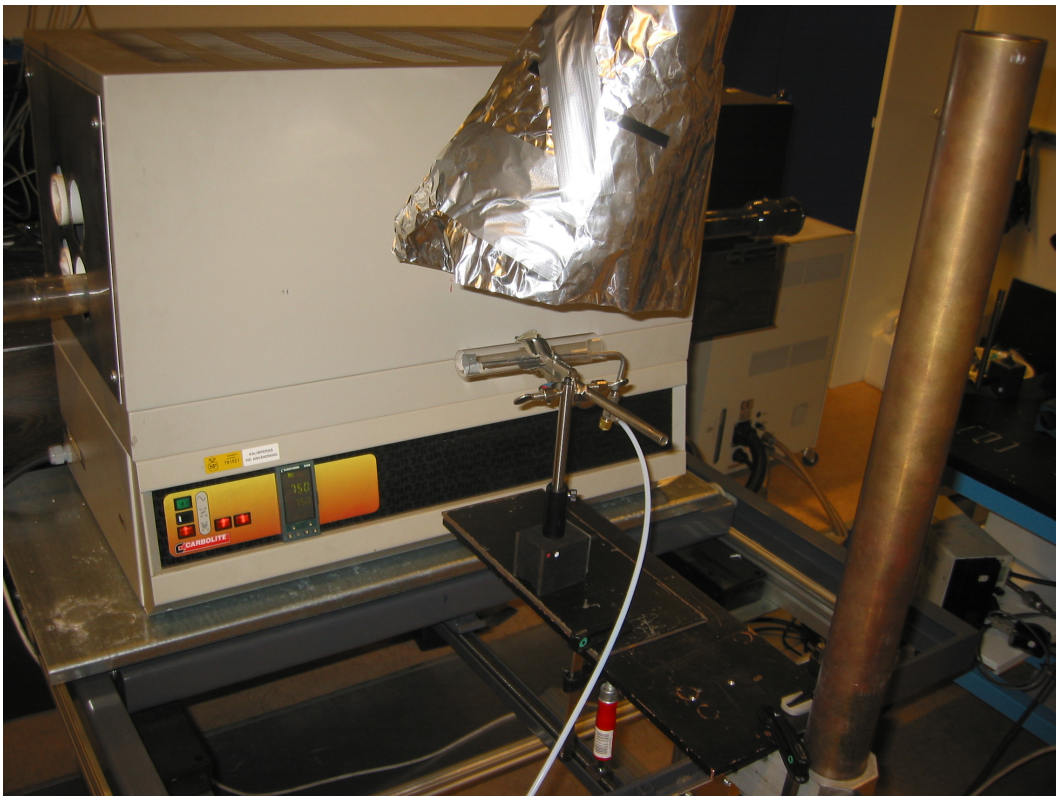


**Figure 9** Photograph of the calibration cell. The translation table was used to remove the furnace from the path of the laser beams. In this way re-alignment of the system was not necessary between calibrations and measurements in the furnace.

A detailed account on the theory for polarization spectroscopy can be found in references [18, 19, 21]. Here a short account is given of how quantitative information can be obtained from a spectra such as the one shown in Figure 8.

Experimentally, PS line-integrated signal under saturated condition [18] can be expressed by the empirical equation [37]:

$$I^{PS} = \alpha \cdot g \cdot c \cdot I^{laser} \cdot \zeta_{JJ'}^2 \cdot N_0^2 \cdot \sigma^2 \quad (14)$$

where  $\alpha$  is a factor corresponding the signal collection efficiency;  $I^{PS}$  is the IRPS line-center signal intensity;  $I^{laser}$  is the probe laser pulse energy;  $g$  is a correction parameter accounting for the spectral overlap between laser profile and the absorption profile of the molecular line;  $c$  is a parameter that corrects for the collision effect under different conditions (temperatures, pressures and buffer gases);  $\zeta_{JJ'}$  is a geometry factor of the probed transition, which depends on the pumping geometry and angular momentum of both the upper and lower states;  $N_0$  is the molecular number density of the probed species; and  $\sigma$  is the absorption cross section of the probed transition. Probing the same transition using the same experimental setup in calibration gas and in the furnace, the parameters  $\zeta_{JJ'}$  and  $I^{laser}$  were assumed to be the same.

Using the mole fraction  $f$  ( $f = N_0/n$ ,  $n$  is the gas molecule number density following the ideal gas law) and by a simple derivation, the mole fraction  $f$  of the investigated species in the furnace can be expressed as

$$f_2 = f_1 \cdot \frac{T_2}{T_1} \cdot \frac{\sigma_1}{\sigma_2} \cdot \left( \frac{\alpha_1}{\alpha_2} \right)^{\frac{1}{2}} \cdot \left( \frac{g_1}{g_2} \right)^{\frac{1}{2}} \cdot \left( \frac{c_1}{c_2} \right)^{\frac{1}{2}} \cdot \left( \frac{I_2^{PS}}{I_1^{PS}} \right)^{\frac{1}{2}} \quad (15)$$

where  $f$  and  $T$  are the mole fraction of detected species and the temperature of gaseous system at the measurement point, respectively, while the subscripts 1, 2 denote in calibration gas and in flames, respectively. The cross sections  $\sigma$  of the investigated transition at different temperatures, such as room temperature and furnace temperature, can be extracted from the HITRAN database [38] and only the relative values are needed here. It should be noted that the value  $\sigma$  both in HITRAN database and in Eq. (15) is for a single molecule considering the thermal population. The furnace temperature profile  $T$  was measured by a thermocouple, see also Appendix A.3. A unit value of 0.266 for  $\alpha_1/\alpha_2$  was adopted in the calibration based on the measurements. This is a result of the fact that the PS signals were weakened 26.6% due to the thermal effects in the furnace including beam expansion and beam steering. The ratios  $g_1/g_2$  and  $c_1/c_2$  were given the values of 1/1.5 and 1/5, respectively, based on investigations of  $C_2H_2$  IRPS signals at high temperatures.

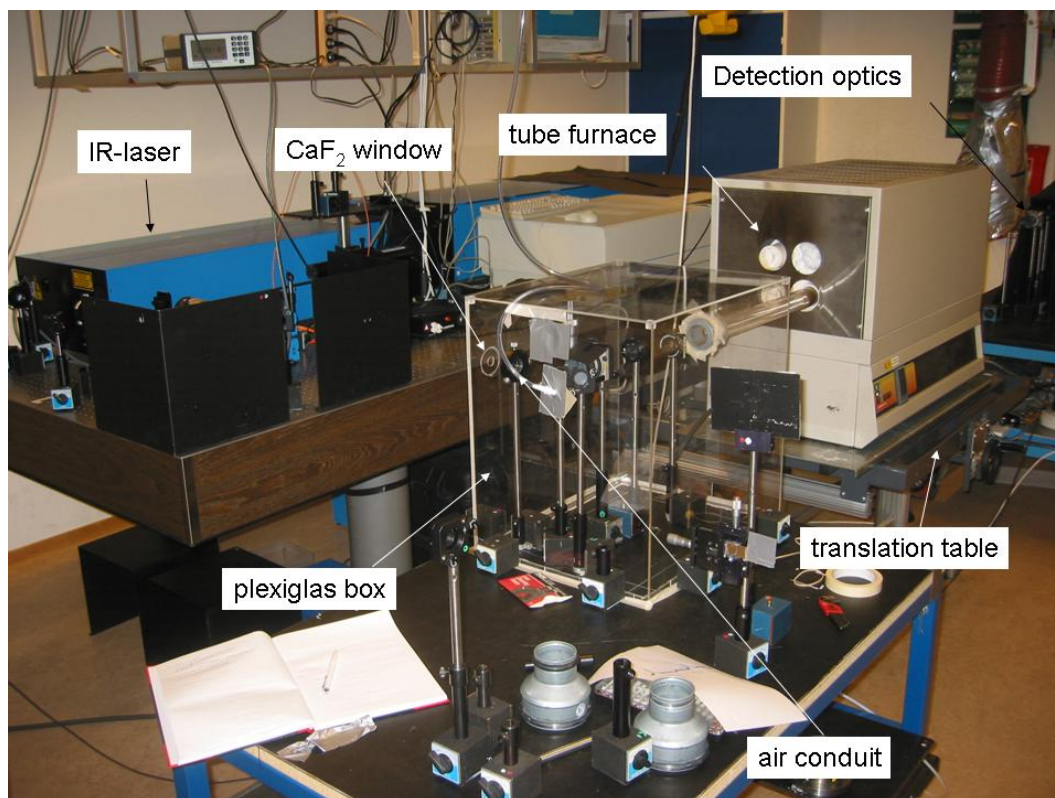


Figure 10 Photograph of the lab.

## 2.4 Modelling

In order to simulate the chemistry, mathematical equations need to be formulated and solved. In this study the Chemkin software package was used for this purpose. Chemkin was developed by Sandia National Laboratories in Albuquerque, New Mexico and Livermore, California [39]. The Chemkin software package was developed to simulate complex chemically reacting flow systems such as combustion, catalysis, chemical vapour deposition and plasma processing. The core of the Chemkin codes consists of packages for dealing with gas-phase reaction kinetics, species transport properties, thermodynamic data, and numerical solution. Chemkin was developed to aid in the incorporation of complex gas-phase chemical reaction mechanisms into numerical simulations. The Chemkin interface allows the user to specify the necessary input through a high-level symbolic interpreter, which interprets the information and passes it to a Chemkin application code. To specify the needed information, the user writes an input file declaring the chemical elements in the problem, the name of each chemical species, a list of chemical reactions (written in the same fashion that a chemist would write them, that is, a list of reactants converted to products), and rate constant information in the form of Arrhenius coefficients. The thermo chemical information is normally obtained from a data base [40]. However, the user may also specify thermodynamic data for species that do not exist in the data base. The transport software package [41] provides a multi-component, dilute-gas treatment of the gas-phase transport properties. It also includes the effects of such phenomena as thermal diffusion. It has the capability of calculating, as a function of temperature, the pure species viscosity, pure species thermal conductivity, and binary diffusion coefficients for every gas-phase species in the mechanism. The Chemkin thermodynamic data base [40] contains polynomial fits with respect to temperature to entropy,  $S$ , enthalpy,  $H$ , and heat capacity,  $c_p$ , at 1 atmosphere pressure. The actual geometry module used was a perfectly stirred reactor (PSR) [42]. The numerical solution is obtained with the Twopnt (pronounced "two point") program [43]. Twopnt is a computer program that finds steady-state solutions for systems of differential equations.

The purpose of the chemical simulations was to investigate whether it is possible to model the destruction of HCN in the hot gases as evidenced in Section 3.2.2 and also in reference [8]. The reaction mechanism used is mainly based on GRI-MECH 3.0 [44] with additions from Kantak *et al.* [45] and from Dagaut *et al.* [9] for parts of the N<sub>2</sub> chemistry and for HCN oxidation, respectively. The full reaction mechanism is given in Appendix B.

## 3 Results

### 3.1 Measurements in a premixed CH<sub>4</sub>/O<sub>2</sub>/Ar flame

The experimental setup is described in Section 2.2. Figure 11 shows the PS-signal as a function of HCl concentration in the flame. The HCl number density was estimated by assuming that all chlorine atoms in the chloroform (CHCl<sub>3</sub>) were converted to HCl in the flame [46] where the measurements were made. The rationale for this simplified test was to see what signal levels could be expected and whether quantitative measurements will be possible. In order to conduct quantitative measurements it is important to understand the relationship between the signal strength and the concentration. According to the theory for PS [18] the signal strength depends quadratically on the concentration. This is shown to actually be the case in Figure 11 where the solid line is a good quadratic fit to the experimental values.

Based on this experiment quantitative measurements seems possible and a detection limit of less than 50 ppm was estimated based on an signal to noise ratio of 10 in this measurement.

The results have been published in references [47] and [48].

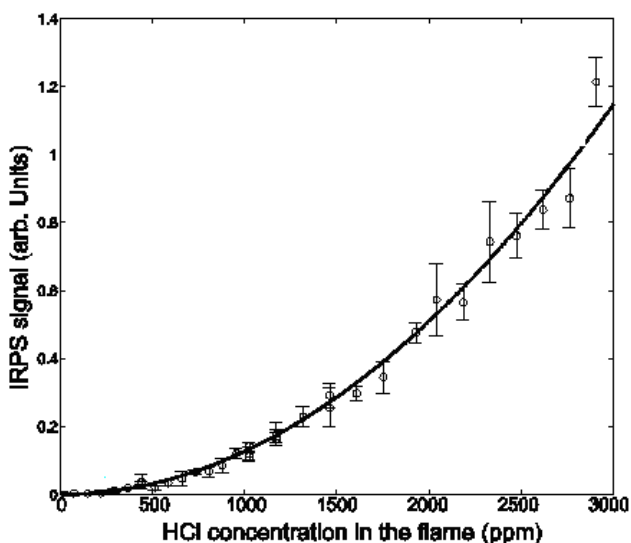


Figure 11 PS-signal as a function of HCl concentration in the flame. The solid curve is a quadratic fit to the measurements point.

### 3.2 Measurements in a tube furnace

A complete list of the measurements as well as all spectra and results are given in Appendix A. In this section some examples are given.

#### 3.2.1 PVC-carpet, measurement of HCl

Results for combustion of PVC-carpet in an oven with set temperature of 670°C and at  $x = 400$  mm, that is in the middle of the oven, are shown in Figure 13. The temperature at this position was measured as 506°C with an air flow of 30 l/min. It should be noted that

the absorption is very high, close to one, and it is still possible to measure the HCl concentration with PS. The absorption measurements are integrated line-of-sight measurements of what the probe beam encounters through the furnace. The red markers correspond to non-resonant absorption and scattering. This can, for example, be due to absorption and scattering with soot particles. The red markers are therefore not a measure of the amount of HCl or HCN. The blue markers correspond to the resonant absorption. This means that they represent the total integrated line-of-sight absorption due to HCl or HCN, depending on what the laser wavelength at resonance is. See also Figure 12 which shows the raw spectra from the measurement.

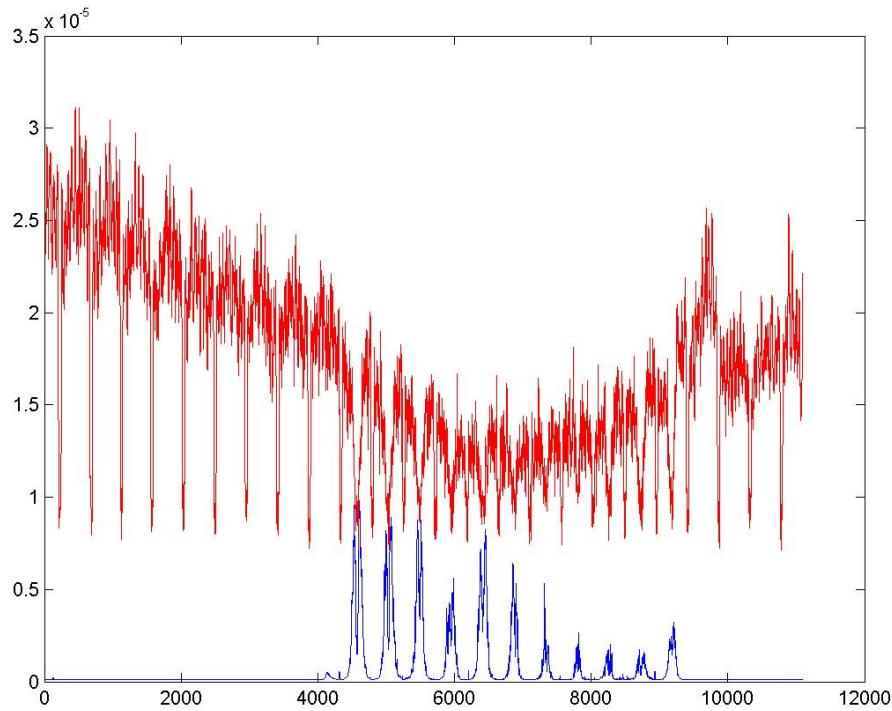


**Figure 12** Raw spectra for the results presented in Figure 13 . The red spectrum is the absorption signal and the blue spectrum is the PS-signal. The unit on the y-axis is arbitrary while the unit on the x-axis is [s].

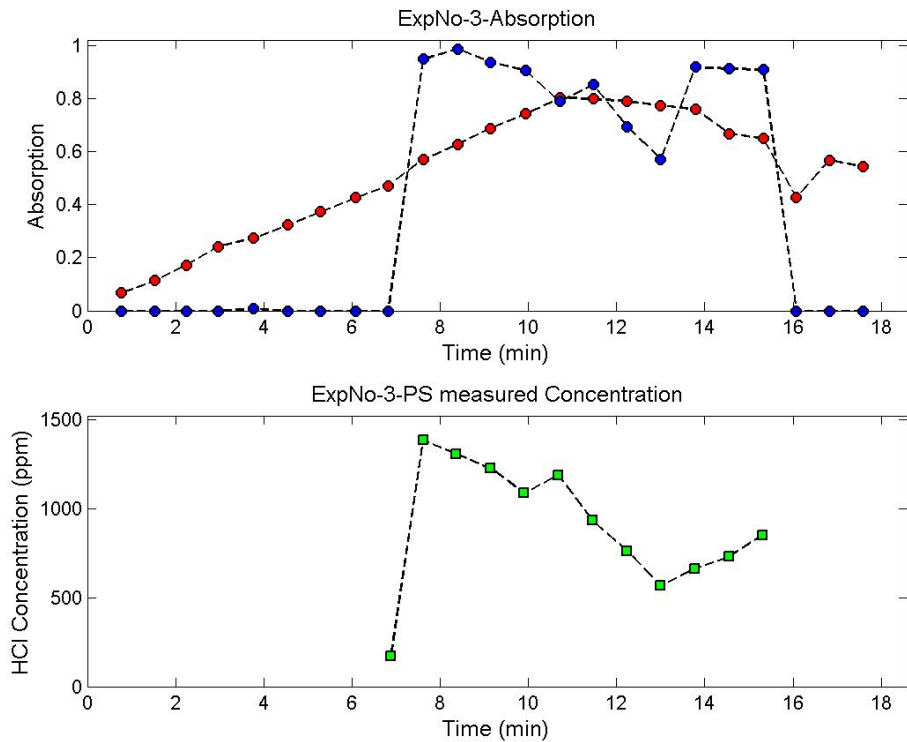


**Figure 13 Measurement at  $x=400$  mm, that is in the middle of the oven. The combustion was well ventilated and the set temperature of the furnace was  $670^{\circ}\text{C}$ . The red absorption curve corresponds to non-resonant absorption or scattering. The blue absorption curve corresponds to resonant absorption.**

### 3.2.2 Nylon 6,6, measurement of HCN

The dependence of HCN levels on temperature is illustrated in Figure 15 and Figure 16. An example or raw spectrum for HCN measurements is shown in Figure 14.



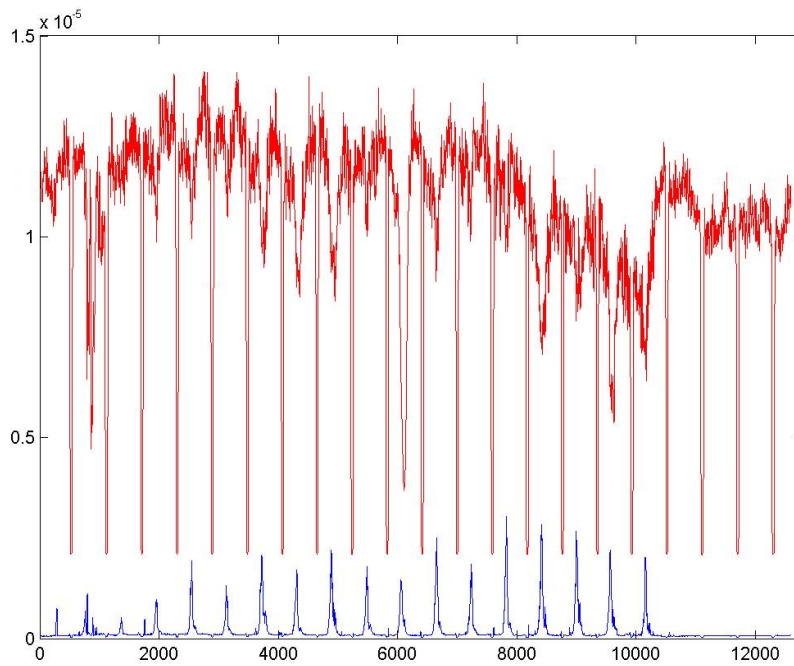


**Figure 14** Raw spectra for the results presented in Figure 15. The red spectrum is the absorption signal and the blue spectrum is the PS-signal. The unit on the y-axis is arbitrary while the unit on the x-axis is [s].

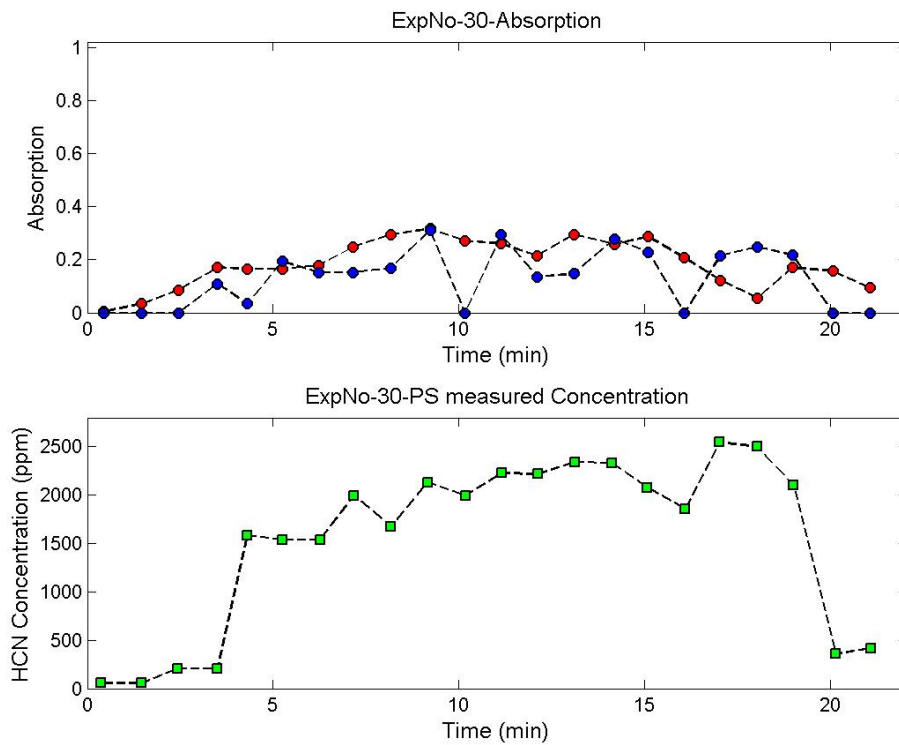


**Figure 15** Measurement at  $x=600$  mm, that is in the downstream part of the oven,  $\theta = 1$  and the set temperature of the oven was  $750^{\circ}\text{C}$ . The red absorption curve corresponds to non-resonant absorption or scattering, and the blue to resonant absorption.

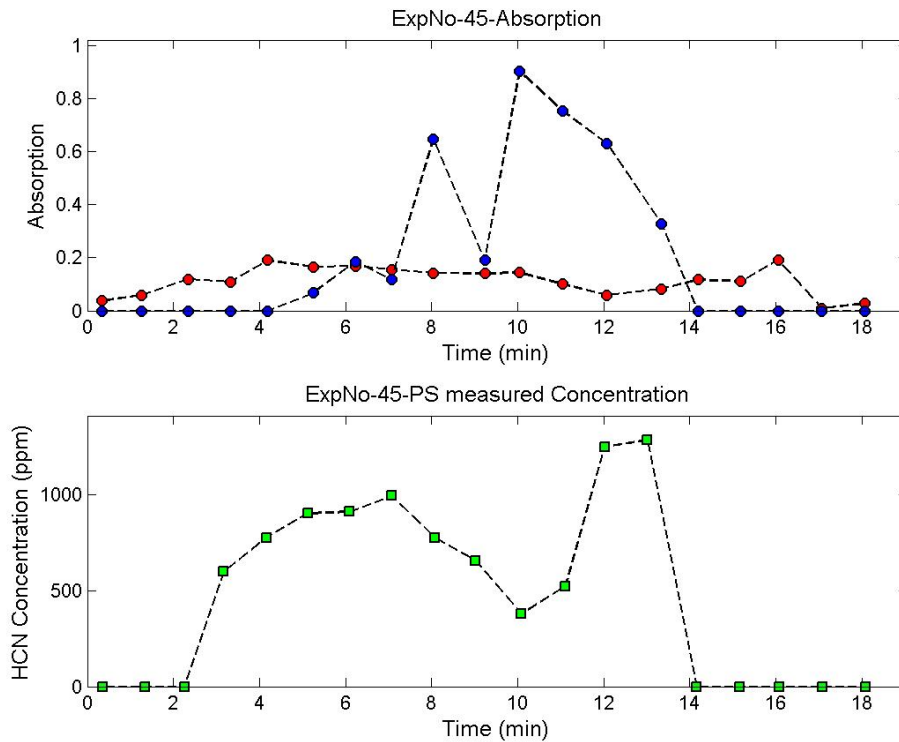


**Figure 16** Measurement at  $x=600$  mm, that is in the downstream part of the oven,  $\theta = 1$  and the set temperature of the oven was  $910^{\circ}\text{C}$ . The red absorption curve corresponds to non-resonant absorption or scattering, and the blue to resonant absorption.

When Figure 15 is compared to Figure 16 it is seen that the total integrated amount of HCN (blue markers) increases with increasing temperature. On the other hand the measured concentration of HCN at  $x = 600$ , i.e., far downstream of the combustion, the concentration has decreased with increasing temperature. An explanation for this is that more HCN is produced in the combustion process when the temperature increases but at the same time the destruction of HCN in the hot gases increases with temperature [8]. This explanation is supported by the simulations in Section 3.3.

Figure 17 and Figure 18 show the dependence of HCN-levels on the equivalence ratio.

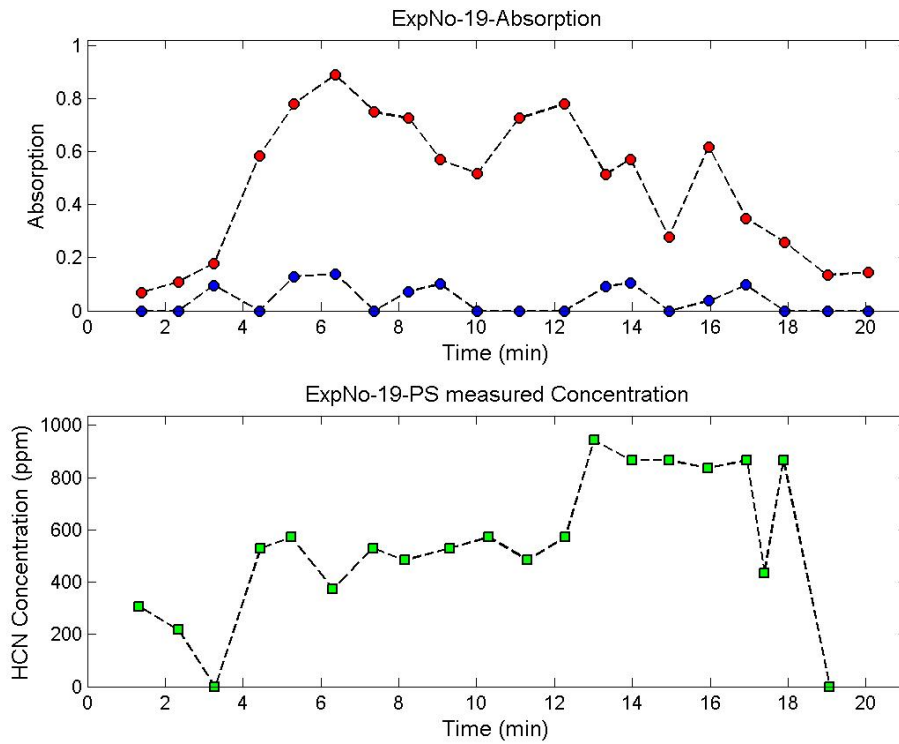


**Figure 17** Measurement at  $x=530$  mm, that is in the downstream part of the oven,  $\theta = 0.5$  and the set temperature of the oven was  $750^{\circ}\text{C}$ . The red absorption curve corresponds to non-resonant absorption or scattering, and the blue to resonant absorption.

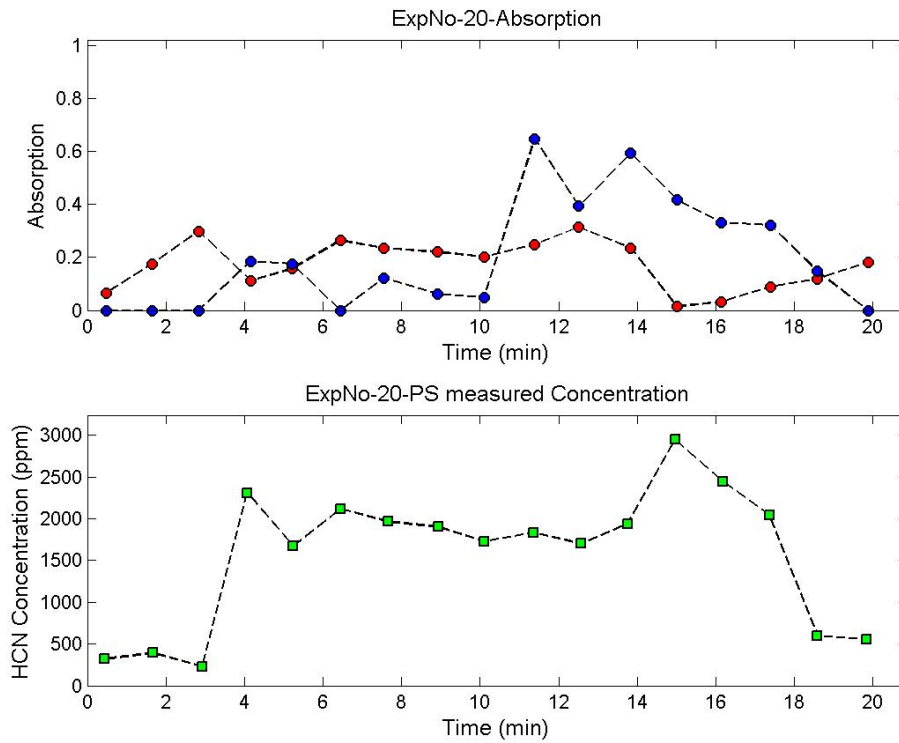


**Figure 18** Measurement at  $x=530$  mm, i.e., in the downstream part of the oven,  $\theta = 1$  and the set temperature of the oven was  $750^{\circ}\text{C}$ . The red absorption curve corresponds to non-resonant absorption or scattering, the blue to resonant absorption

Comparing Figure 17 with Figure 18 it is observed that the amount of HCN, both totally integrated (blue markers) as well as measured at  $x = 530$  mm with PS, increases significantly when the equivalence ratio increases from 0.5 to 1. This is in agreement with the fact that the HCN production is larger when there is less oxygen available. The increase in HCN measurement can be due both to increased production in the combustion zone but also due to decreased destruction in the hot gases.

The destruction of HCN in the hot gases [8] is further supported by the concentration curves in Figure 19 ( $x = 600$  mm) and Figure 20 ( $x = 700$  mm) which show that the HCN concentration decreases as the measurement point is moved downstream.

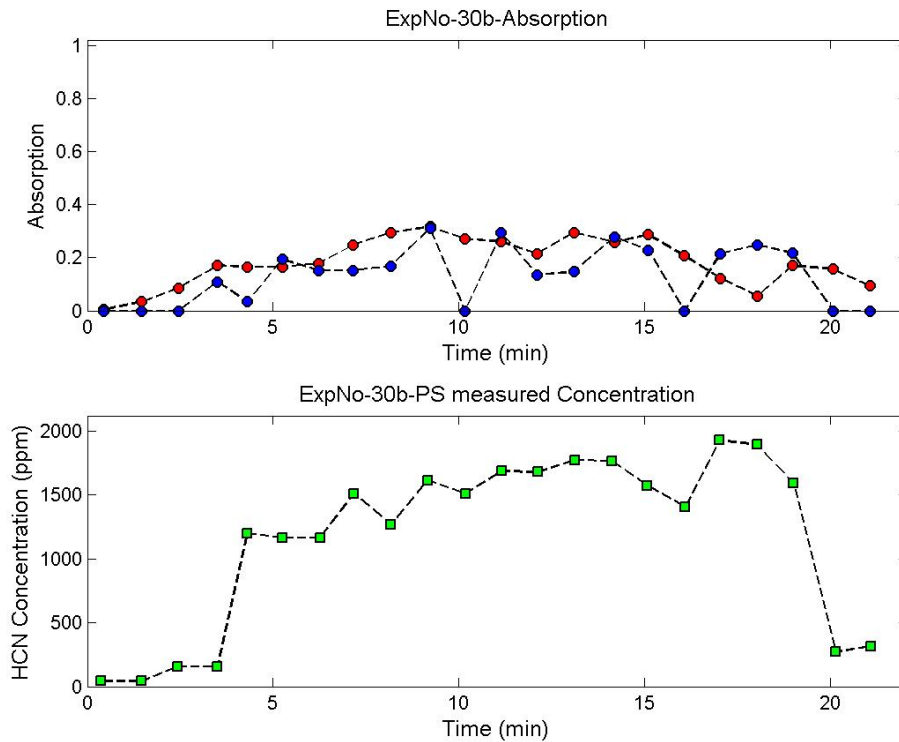


**Figure 19 Measurement at  $x=600$  mm, that is in the downstream part of the oven,  $\theta = 1$  and the set temperature of the oven was  $750^\circ\text{C}$ . The red absorption curve corresponds to non-resonant absorption or scattering, the blue to resonant absorption.**

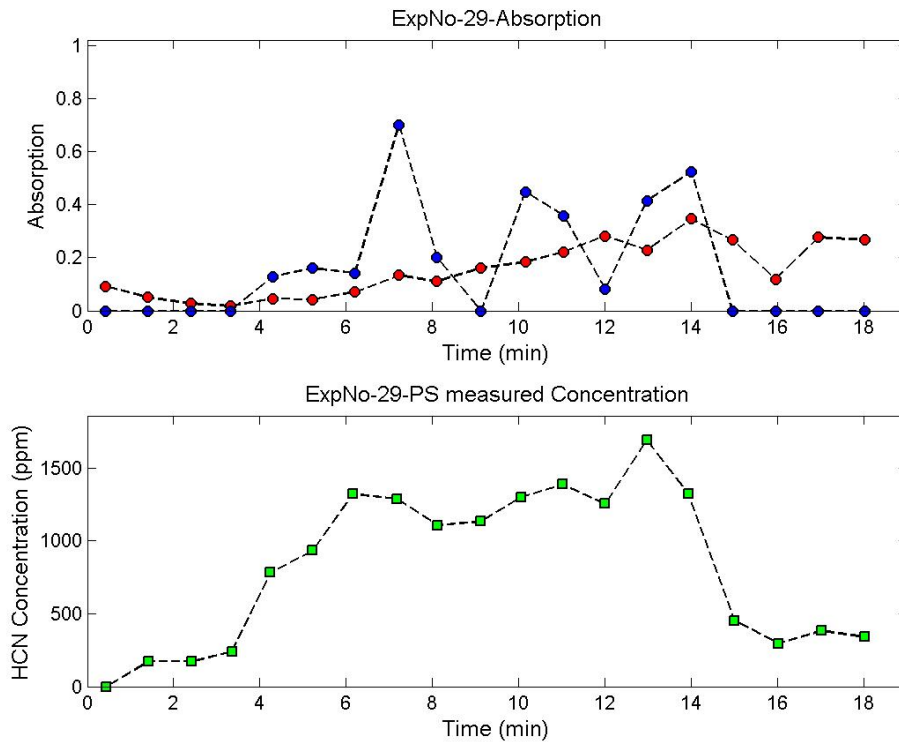


**Figure 20** Measurement at  $x=700$  mm, that is in the downstream part of the oven,  $\theta = 1$  and the set temperature of the oven was  $750^{\circ}\text{C}$ . The red absorption curve corresponds to non-resonant absorption or scattering, the blue to resonant absorption.

A general conclusion from the measurements is that the variation in time is relatively high, both for the pointwise IRPS-measurements but also for the integrated resonant absorption measurements. This phenomenon is difficult to detect when measurements are conducted in the mixing box which is traditionally the case in the tube furnace [36]. Parts of these results have been published in reference [49].

### 3.3 Modelling

The purpose of the modelling with Chemkin was to determine whether it is possible to reproduce the destruction of HCN in the hot fire smoke. This decrease in HCN concentration with distance from the fire source was observed in the experiments in the tube furnace, see Section 3.2.2, and has also been observed in earlier works, see reference [8].

The experimental results presented in Figure 18 to Figure 20 show that the HCN concentration decreases with increasing  $x$ , that is downstream in the tube furnace. Although the variation in time is relatively high, a rough estimate is that the HCN concentrations decrease from  $\sim 2000$  ppm at  $x = 530$  mm, to  $\sim 1500$  ppm at  $x = 600$  mm, and finally to  $\sim 1200$  ppm at  $x = 700$  mm. An attempt was made to reproduce this behaviour using the Chemkin PSR module. Residence times of  $0.6$  s for the transport between  $x = 530$  and  $600$  mm, and  $0.9$  s for the transport between  $x = 600$  and  $700$  mm were used. The results are shown in Figure 20 and it is clear that the existing model predicts a far too rapid destruction of HCN compared to the experimental results.

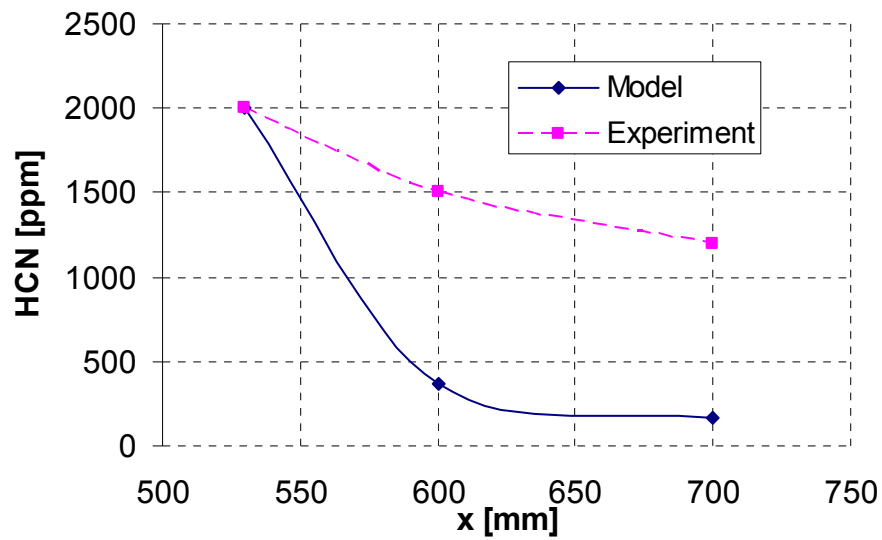


**Figure 21 Comparison between experimental and simulated result for the HCN concentration as a function of position in the furnace,  $\theta = 1$  and the set temperature of the oven was 750°C.**

Further studies of the experimental conditions, for example *in situ* temperature measurements, as well as a refined reaction mechanism is required in order to obtain a better agreement between experiment and model.

## 4 Conclusions

It has been shown that IRPS is a promising laser diagnostic technique for fire technology. The technique enables time resolved *in situ* measurements of toxic gases such as HCl and HCN in a tube furnace filled with hot sooty combustion gases. This is a very harsh environment and it can therefore be expected that IRPS also can be applied to many other geometries that are applicable for the fire community.

In a preparatory experiment the technique was applied to a small scale laboratory burner in order to see what signal levels could be expected and whether quantitative measurements would be possible. Based on this experiment quantitative measurements were deemed possible and the detection limit was estimated to be less than 50 ppm based on the signal to noise ratio of 10.

The second and main part of the project consisted of *in situ* measurement inside a tube furnace. This constitutes a very harsh environment from a diagnostic point of view due to the high smoke density and relatively long length of the furnace. Despite this it was possible to quantify HCl and HCN concentrations in the smoke using IRPS. The explanation for this success is twofold. Firstly the IRPS method is inherently almost noise free due to the use of crossed polarisers, creating a virtually zero background. Secondly the problem with laser beam attenuation due to scattering in the smoke, especially with soot particles, decreases in importance with the fourth power of the laser wavelength. This gives infrared measurements a great advantage as compared to measurements in the ultraviolet or visible wavelength range, due to their relatively long inherent wavelength.

A general conclusion from the measurements was that the variation in time is relatively high, both for the pointwise IRPS-measurements but also for the integrated resonant absorption measurements. This phenomenon is difficult to detect when measurements are conducted in the mixing box which is traditionally the case in the tube furnace.

It was also observed that the concentration of HCN in the hot smoke decreased as the smoke was transported downstream in the furnace. This is in agreement with earlier studies.

Further work should focus on better understanding of chemistry of toxic gases as well as on using the techniques for other applications than a tube furnace, such as the cone calorimeter (ISO 5660) or the room-corner test (ISO 9705).

In order to develop the technique further it would be useful to use a single mode laser system which would enable single-shot measurements and thereby also enable, for example, studies of mixing conditions in the combustion zone and in the fire gases. Using a split furnace, such as the one shown in Figure 22, would facilitate the alignment and calibration procedures for further work in a tube furnace.



**Figure 22 Split furnace [35].**



## Appendix A Complete results from measurements in the tube furnace

### A.1 Summary of measurements

Table 1 lists all measurements that were performed in the project. The numbering is exactly the same as the numbering in all internal project documentation. This means that some of the measurement numbers corresponds to measurements that either failed or were never carried out. The reason for keeping the original numbering is traceability.

**Table 1 Operating conditions for the experiments in the tube furnace.**

Meas No.	Fuel	Mole-cule	T <sub>set</sub> [°C]	$\phi_{rel}$	Air flow [l/min]	N <sub>2</sub> flow [l/min]	$\rho_{fuel}$ [mg/mm]	x <sub>meas</sub> [mm]	Boat speed [mm/min]
1	PVC	HCl	20-670	varying	18.5	0	3.3	400	0
2	PVC	HCl	670	0.01	30	0	4.5	400	40
3	PVC	HCl	670	0.01	30	0	4.1	400	40
4	PVC	HCl	670	0.01	30	0	4.4	400	40
5	PVC	HCl	670	0.01	30	0	3.2	Scan	40
6	PVC	HCl	750	0.01	30	0	6.8	Scan	20
7	PVC	HCl	750	0.02	30	0	6.6	400	40
8	PVC	HCl	750	0.04	10	0	5.1	400	40
9	PVC	HCl	750	1	2	0	27.8	400	40
10	PVC	HCl	750	0.8	0.5	9.5	5.4	400	40
11	PVC	HCl	750	0.04	10	40	5.0	400	40
12	N6,6	HCN	750	0.5	10	0	14.9	400	40
13	N6,6	HCN	750	1	10	0	29.8	400	40
14	N6,6	HCN	750	1	5	5	14.9	400	40
15	N6,6	HCN	750	2	2.5	7.5	14.9	400	40
16	N6,6	HCN	750	2	2.5	7.5	14.9	530	40
17	N6,6	HCN	750	0	0	10	14.9	530	40
18	not used/failed								
19	N6,6	HCN	750	0.5	10	0	14.9	530	40
19b	N6,6	HCN	750	0.5	10	0	14.9	530	40
20	N6,6	HCN	750	1	5	5	14.9	530	40
21	not used/failed								
22	not used/failed								
23	N6,6	HCN	750	0.5	5	5	14.9	530	20
24	N6,6	HCN	750	0	10	0	14.9	scan	40
25	N6,6	HCN	750	1	5	5	14.9	scan	40
26	N6,6	HCN	750	2	2.5	7.5	14.9	scan	40
26b*	N6,6	HCN	750	0.5	10	0	14.9	400	40
27	not used/failed								
28	not used/failed								
29	N6,6	HCN	750	1	5	5	14.9	700	40
29b	N6,6	HCN	750	0.5	10	0	14.9	700	40
30	N6,6	HCN	750	1	5	5	14.9	600	40

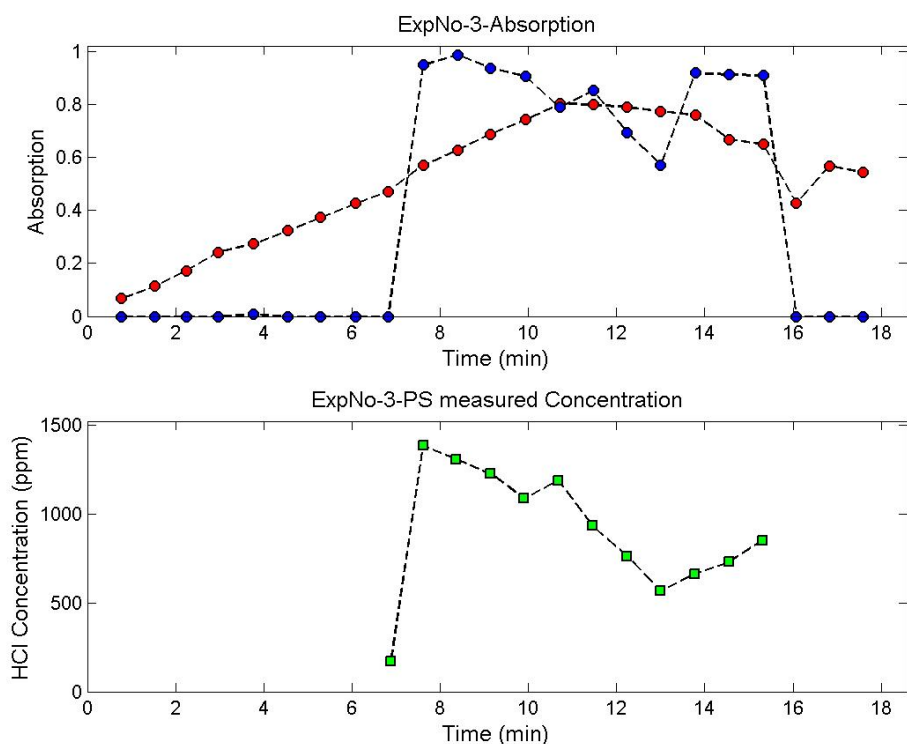
30b	N6,6	HCN	750	1	5	5	14.9	600	40
31	N6,6	HCN	750	1	5	5	15	400	40
32	N6,6	HCN	750	1	5	5	14.9	200	40
33	not used/failed								
34	N6,6	HCN	750	2	2.5	7.5	14.9	700	40
35	N6,6	HCN	750	2	2.5	7.5	14.9	600	40
36	N6,6	HCN	750	2	2.5	7.5	14.9	400	40
37	N6,6	HCN	750	2	2.5	7.5	14.9	200	40
38	N6,6	HCN	910	2	2.5	7.5	14.9	400	40
39	N6,6	HCN	910	2	2.5	7.5	14.9	200	40
40	N6,6	HCN	910	2	2.5	7.5	14.9	400	40
41**	N6,6	HCN	910	2/1	2.5/5.0	7.5/5	14.9	400	40
42	N6,6	HCN	910	1	2.5	5	14.9	400	40
43	N6,6	HCN	910	2	2.5	7.5	14.9	600	40
44	N6,6	HCN	910	2	2.5	7.5	14.9	700	40
45	N6,6	HCN	910	1	5	5	14.9	600	40

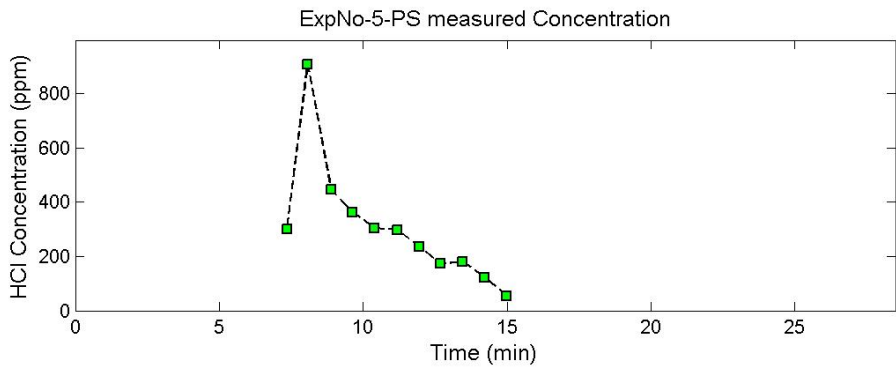
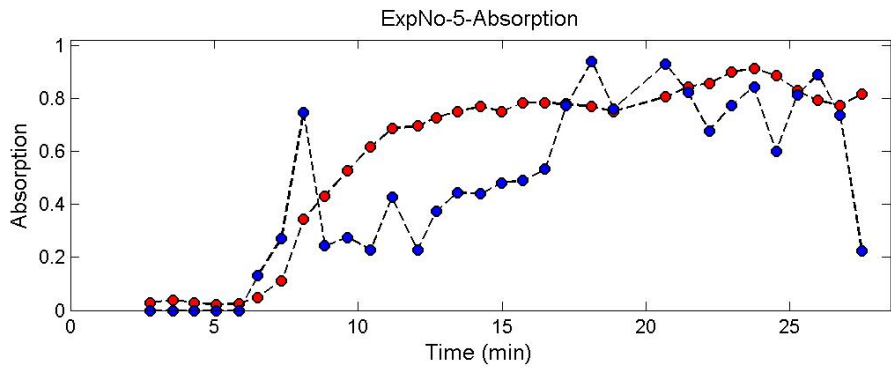
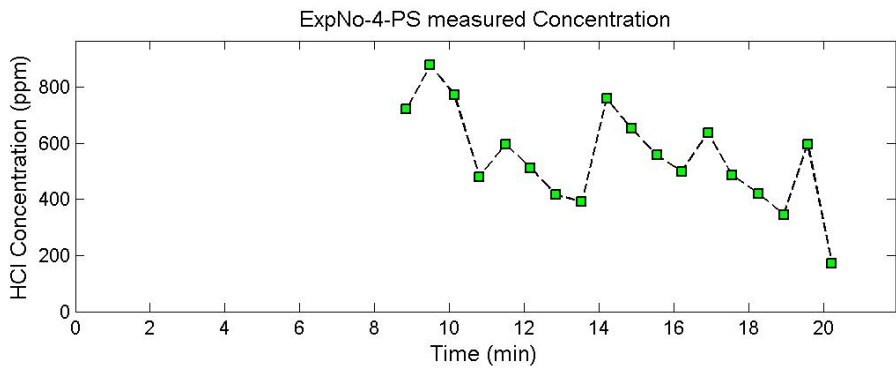
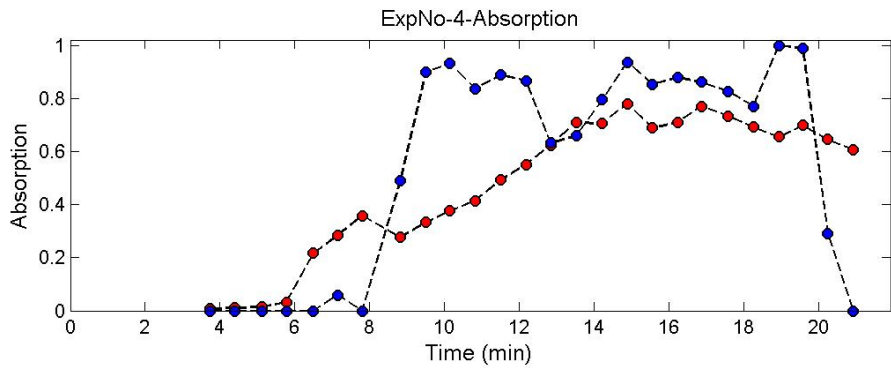
\*Scanning of oven in vertical direction.

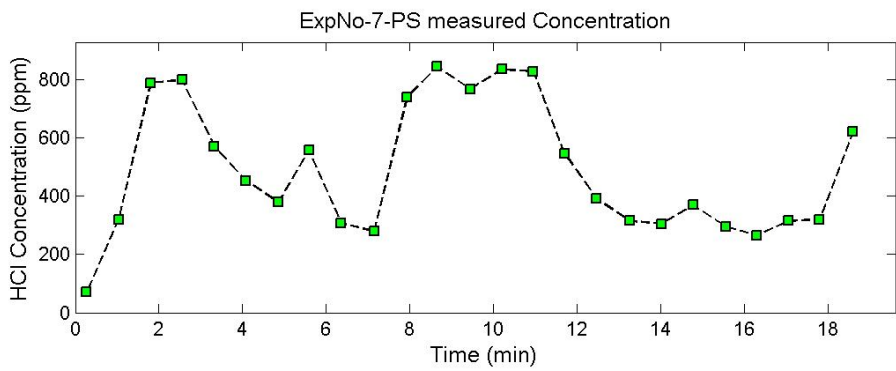
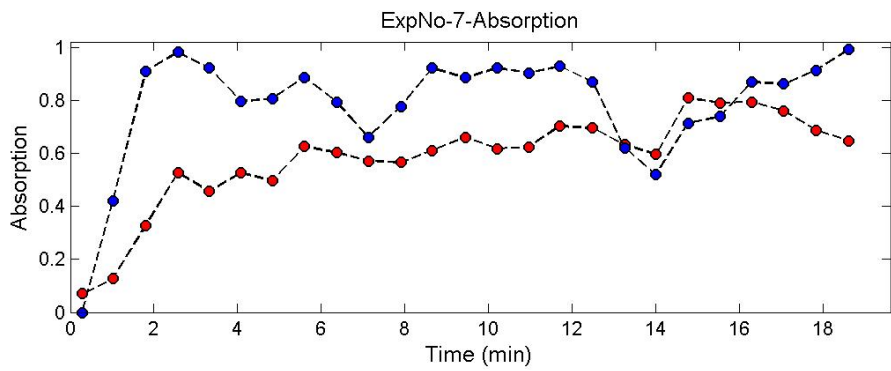
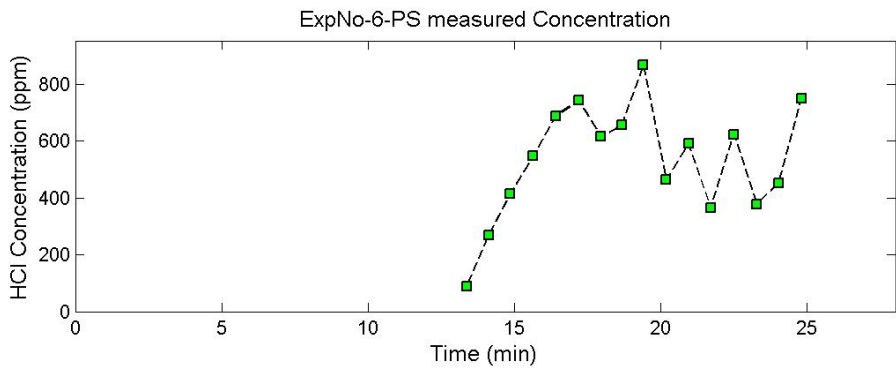
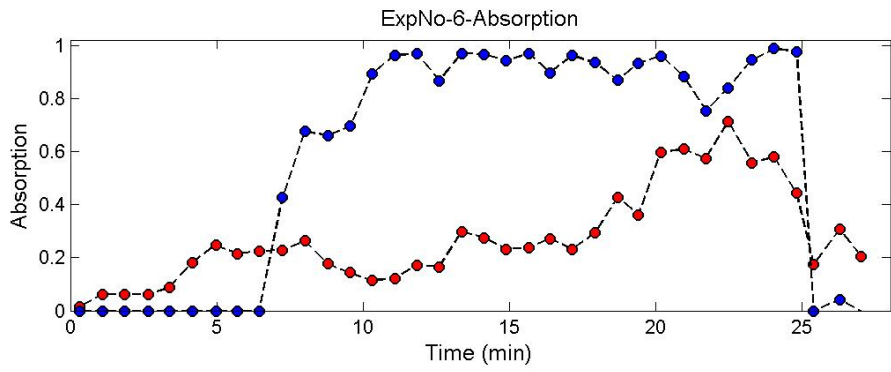
\*\*Varying equivalence ratio.

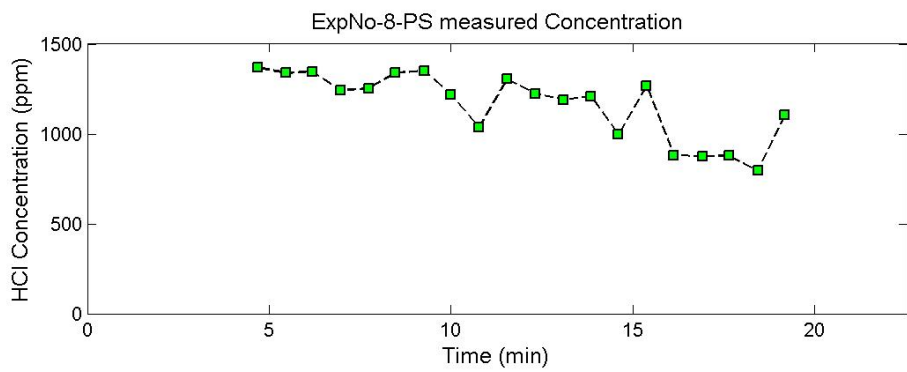
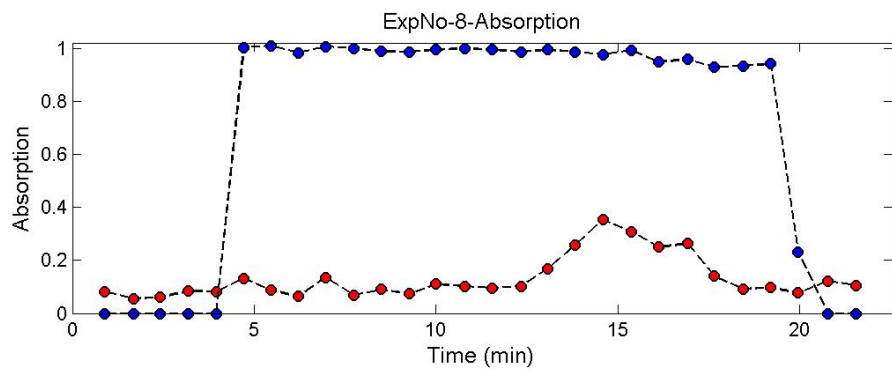
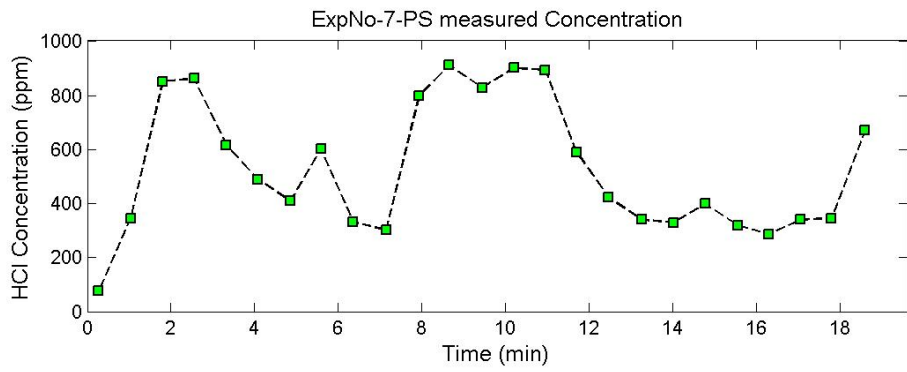
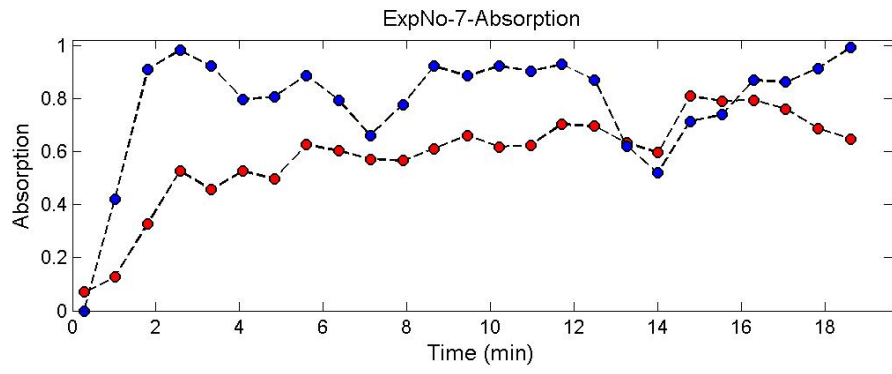
## A.2 Results

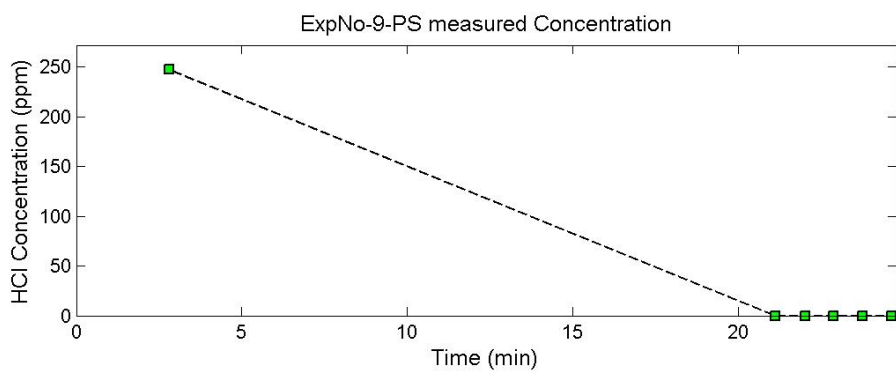
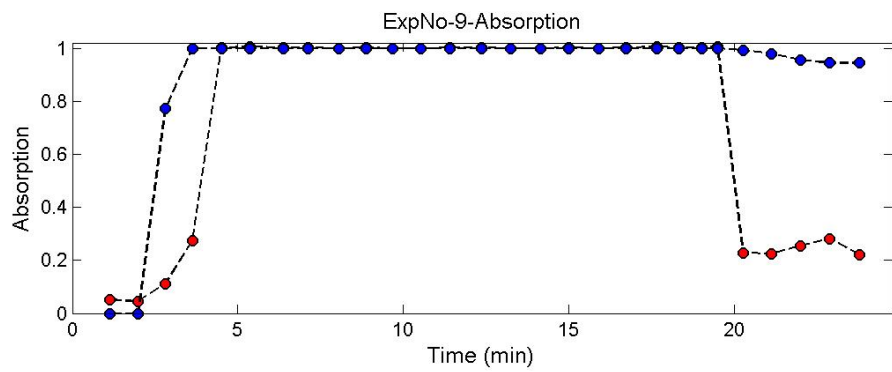
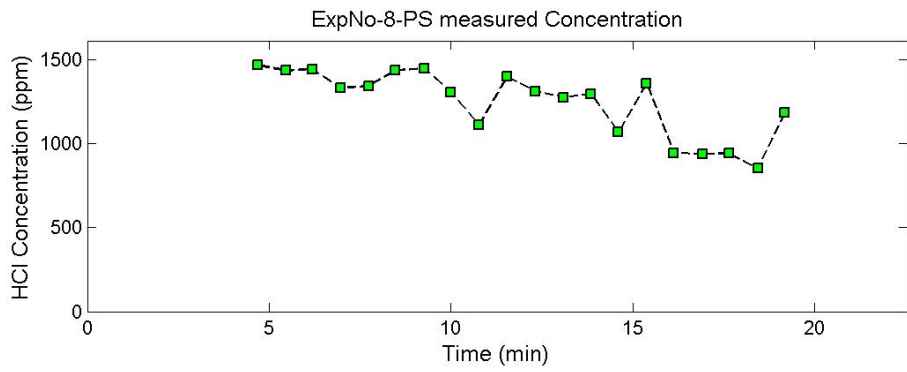
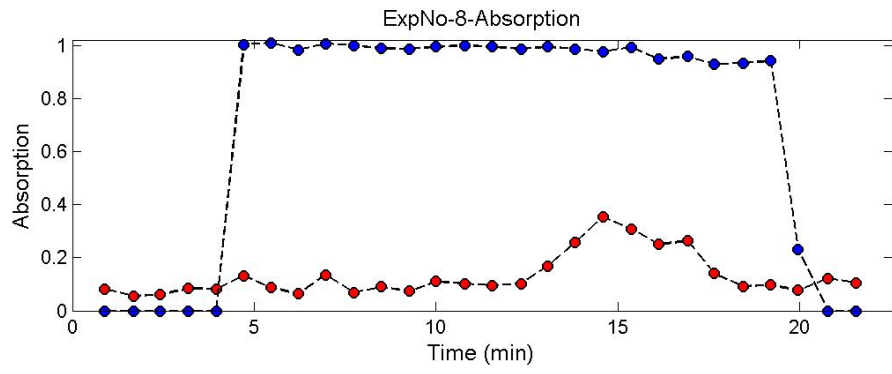
The red markers correspond to non-resonant absorption and scattering. This can, for example, be due to absorption and scattering by soot particles. The red markers are therefore not a measure of the amount of HCl or HCN. The blue markers correspond to the resonant absorption. This means that they represent the total integrated line-of-sight absorption due to HCl or HCN, depending on what the laser wavelength at resonance is. See also Figure 12 which shows a raw spectra from the measurement. The green markers correspond to the pointwise IRPS concentration measurements.

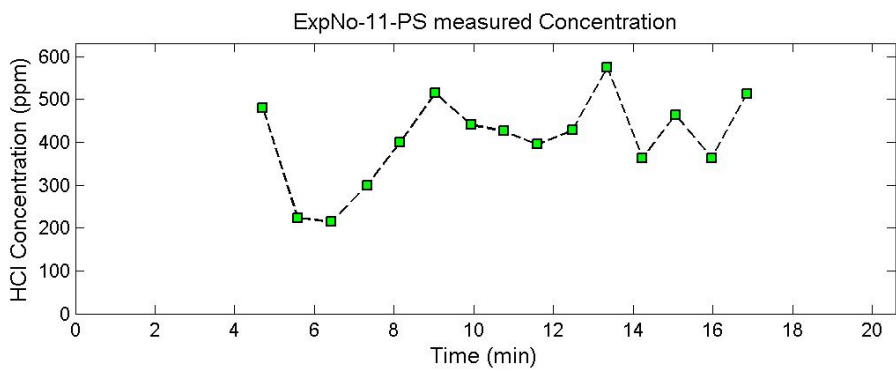
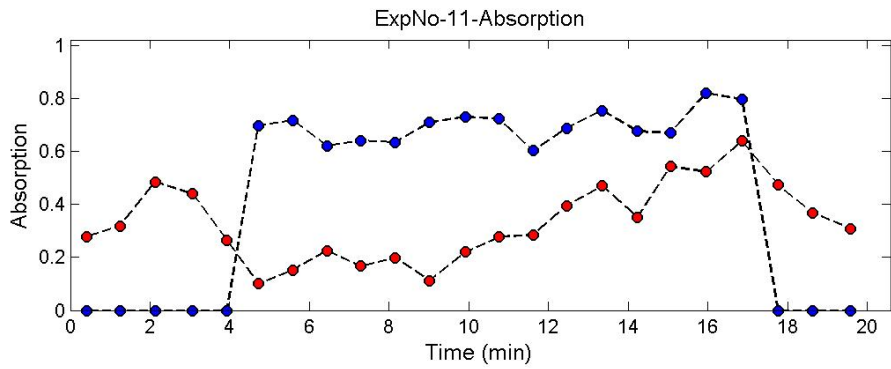
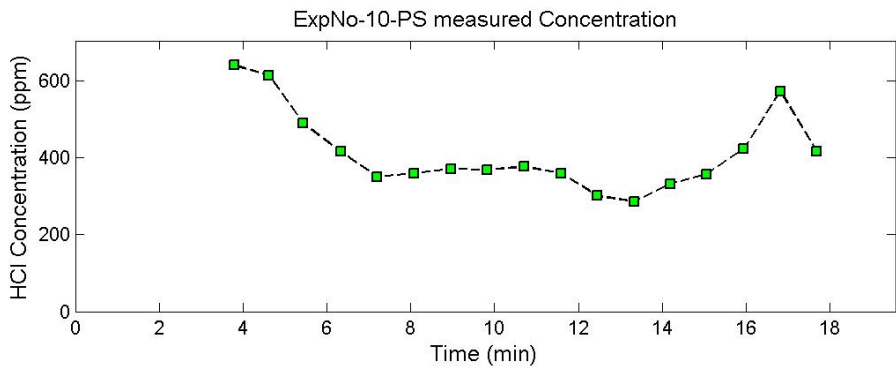
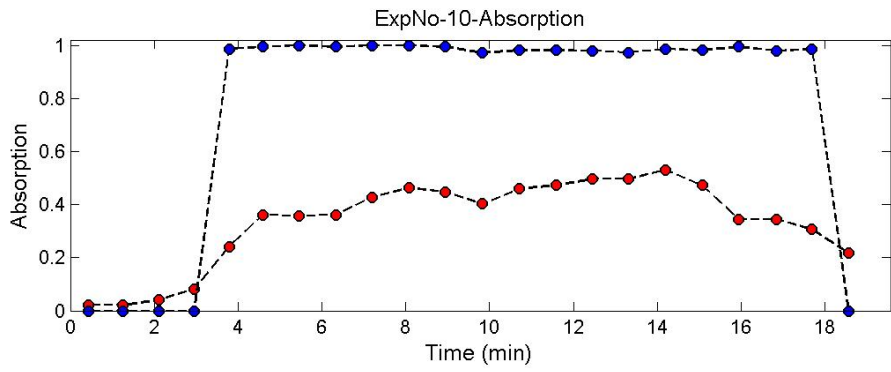


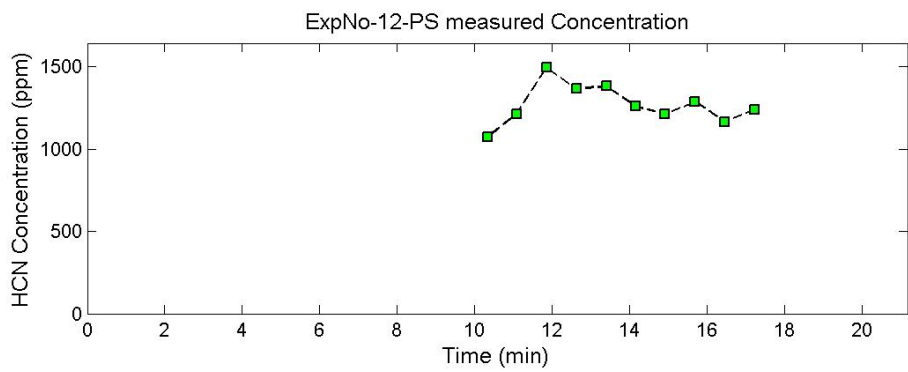
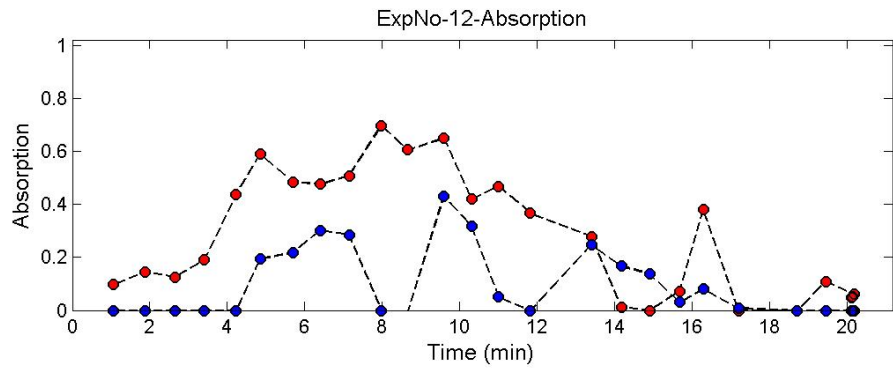
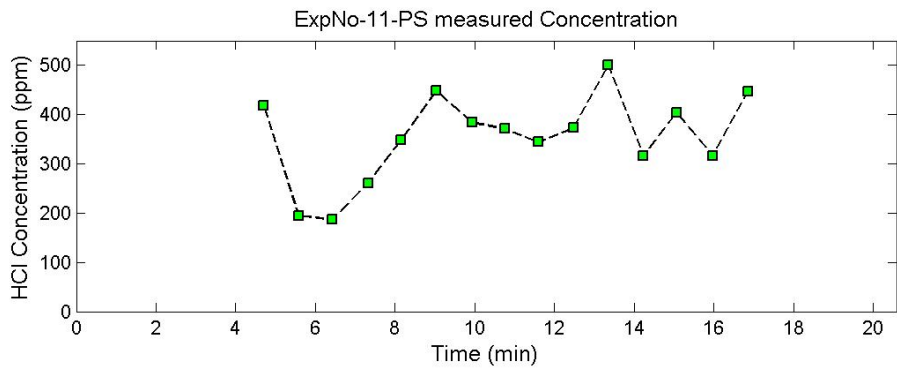
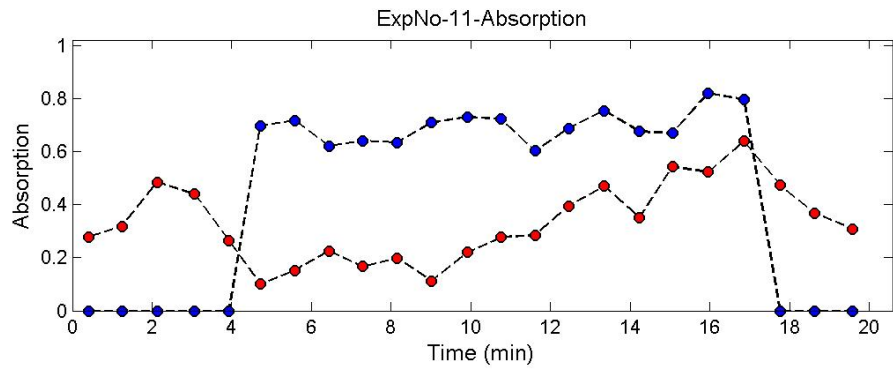




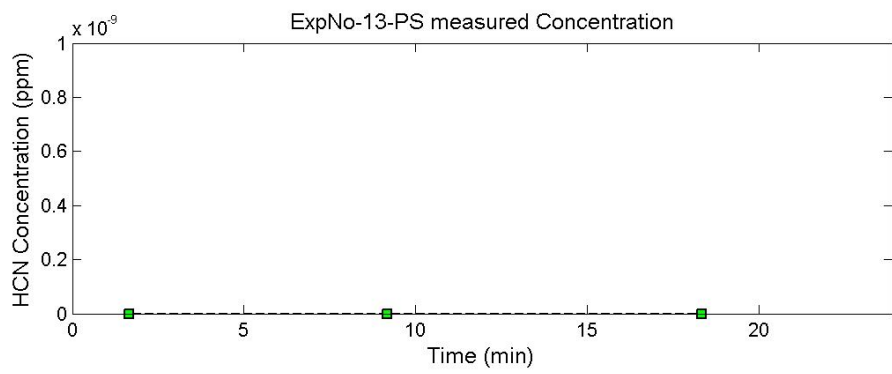
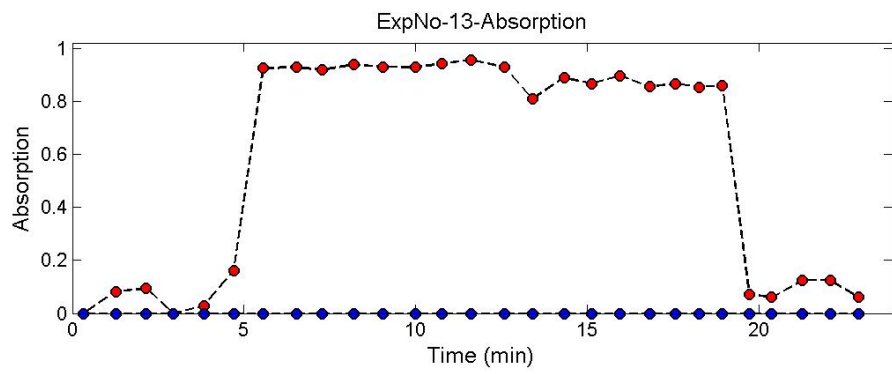
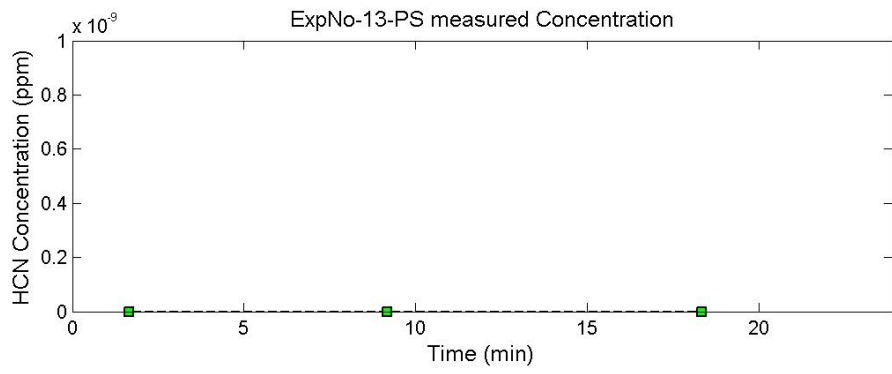
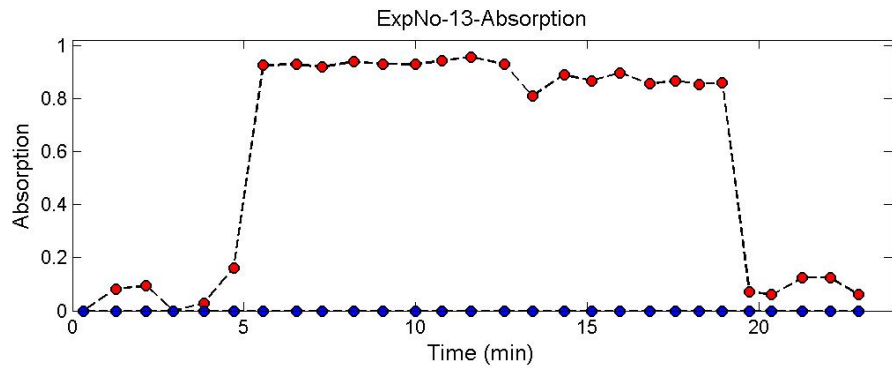


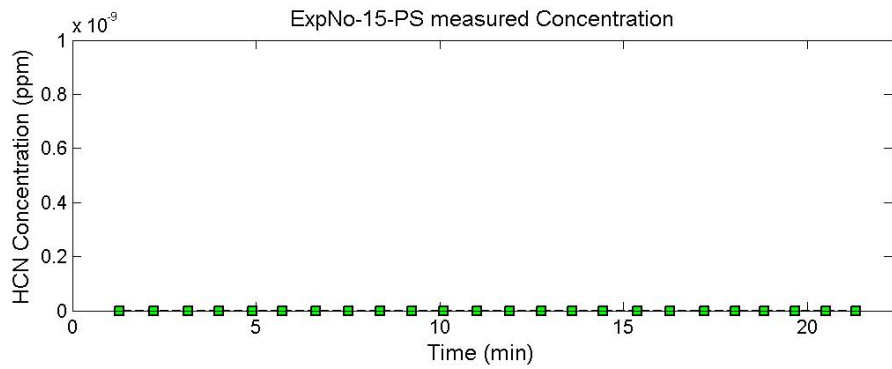
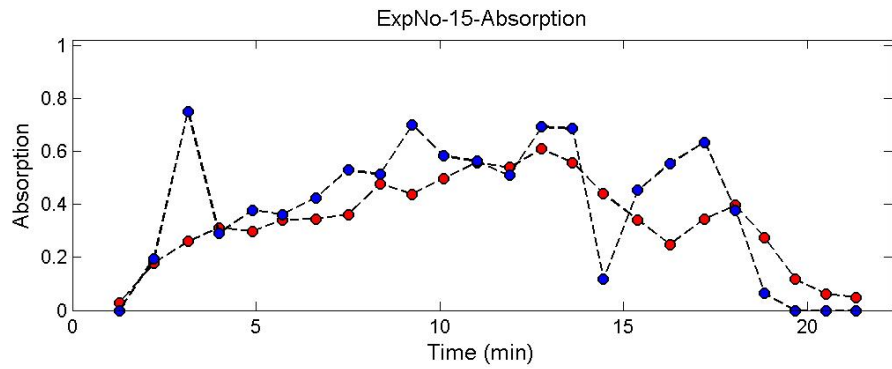
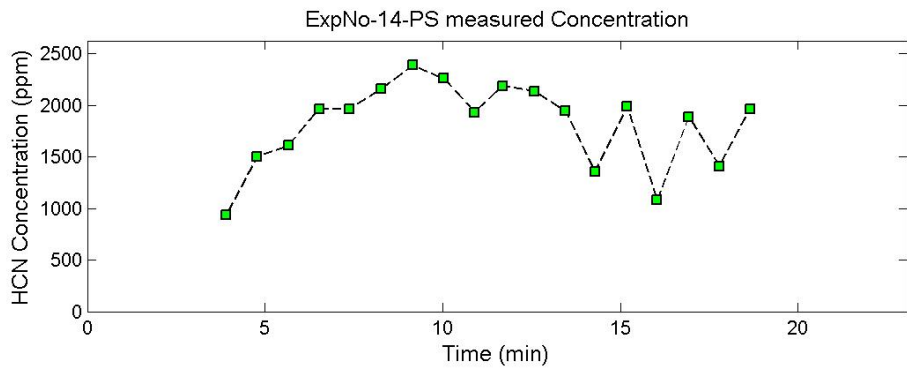
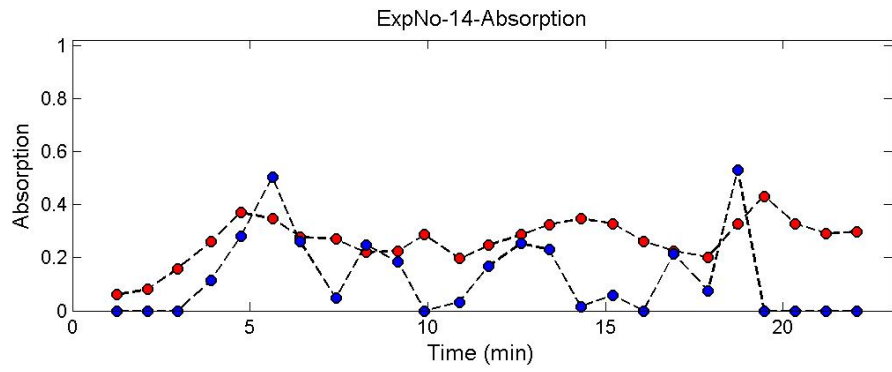


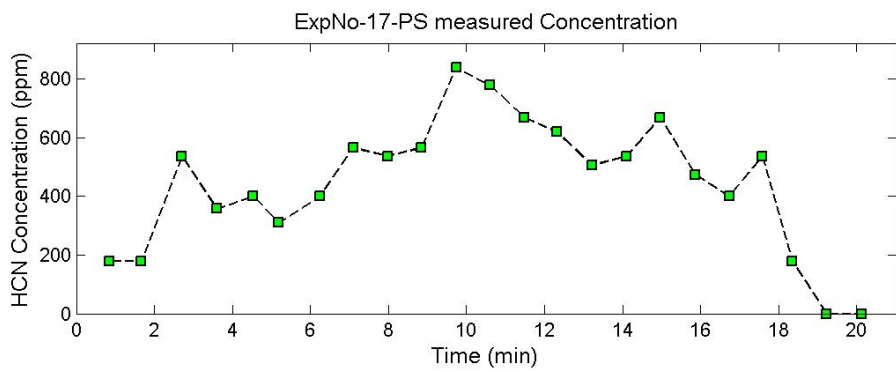
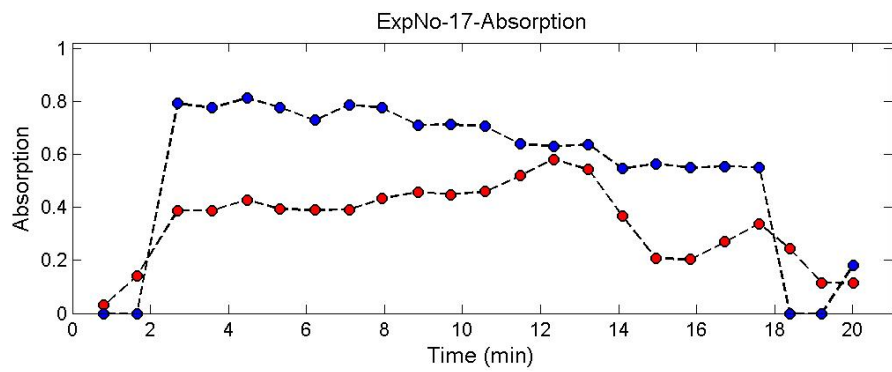
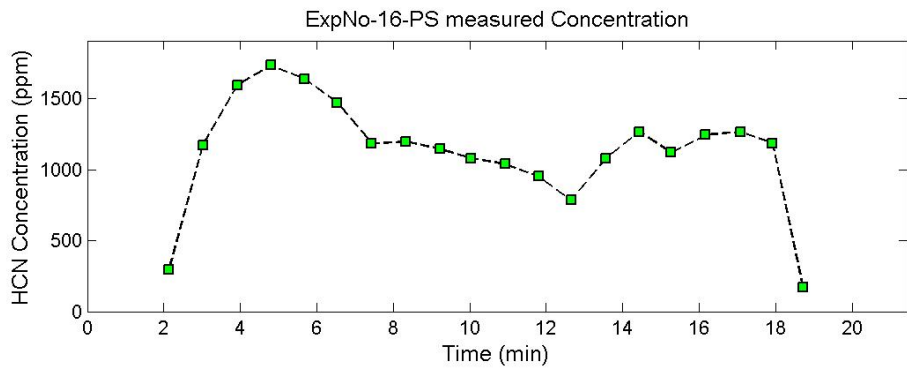
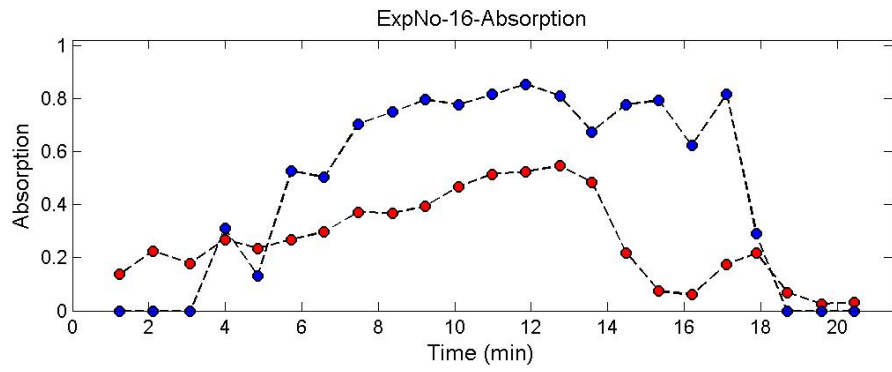


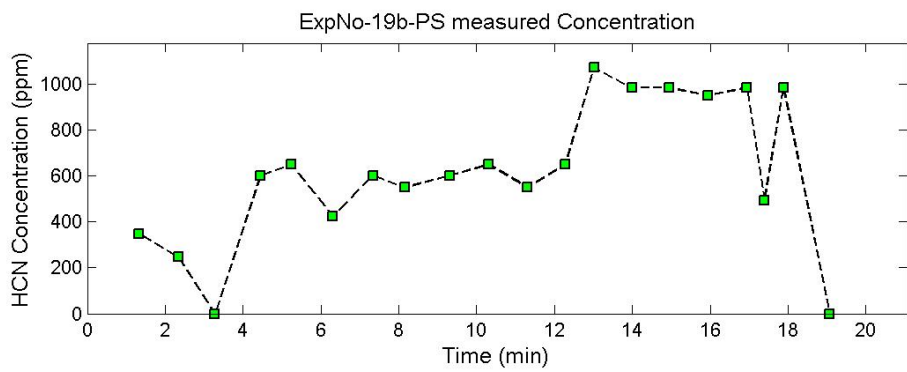
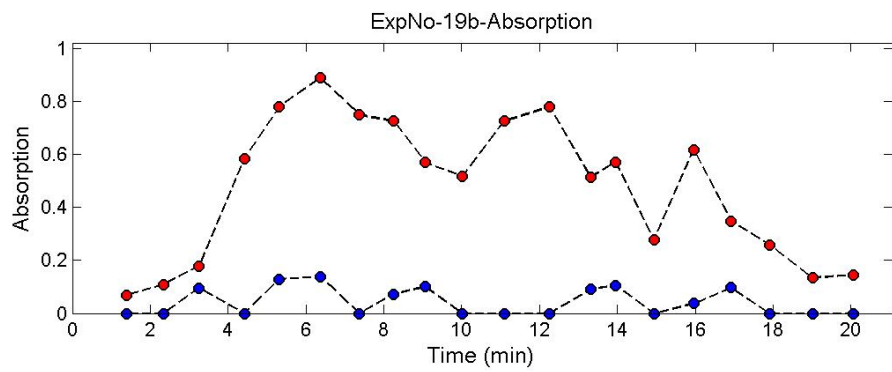
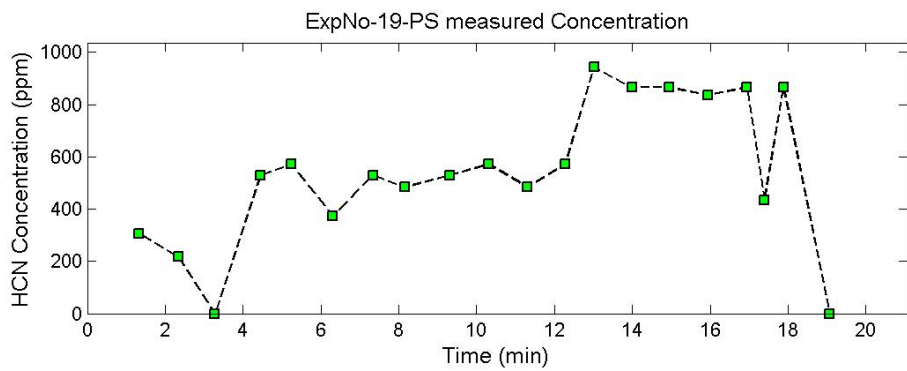
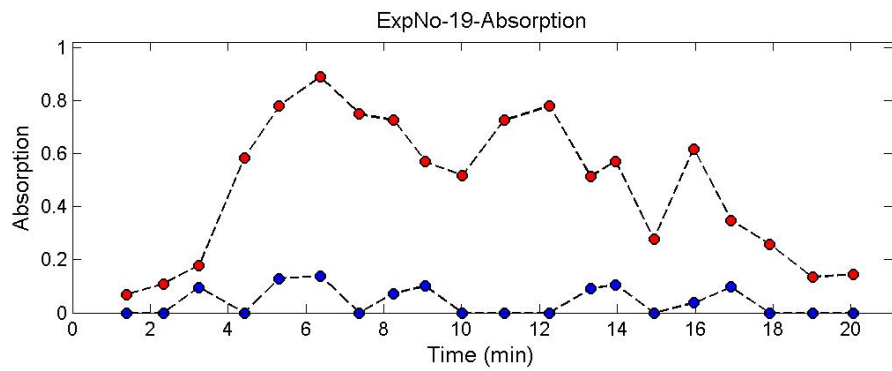


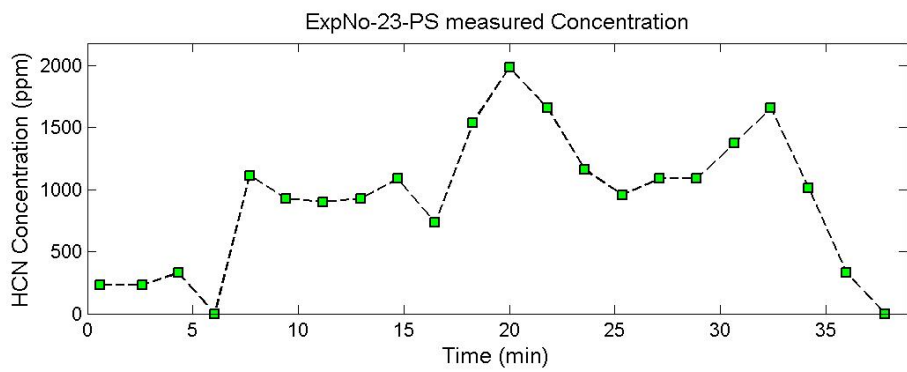
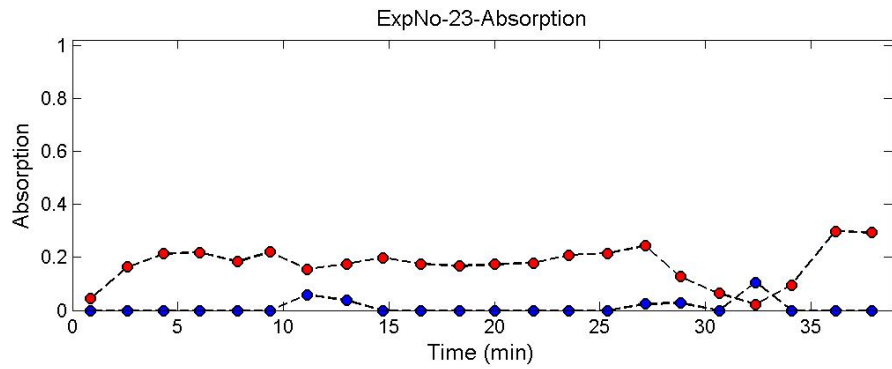
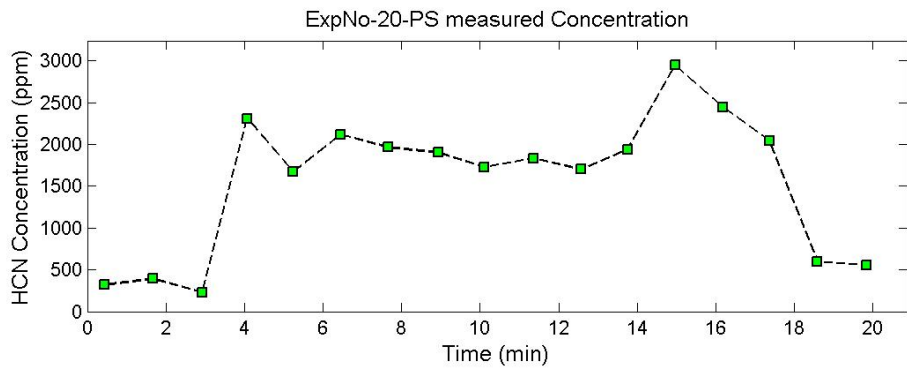
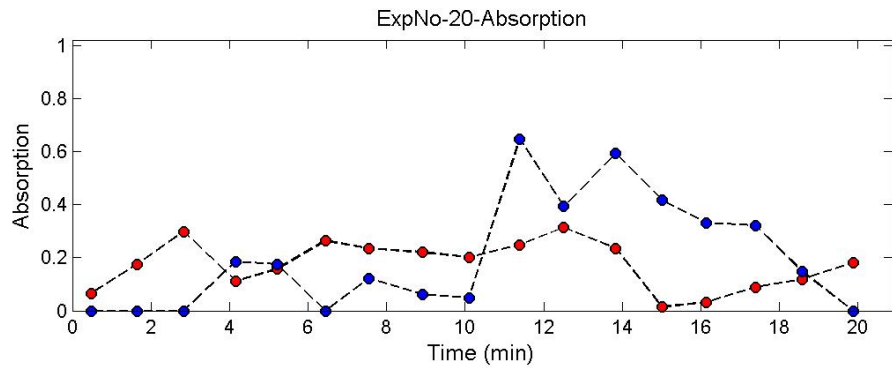


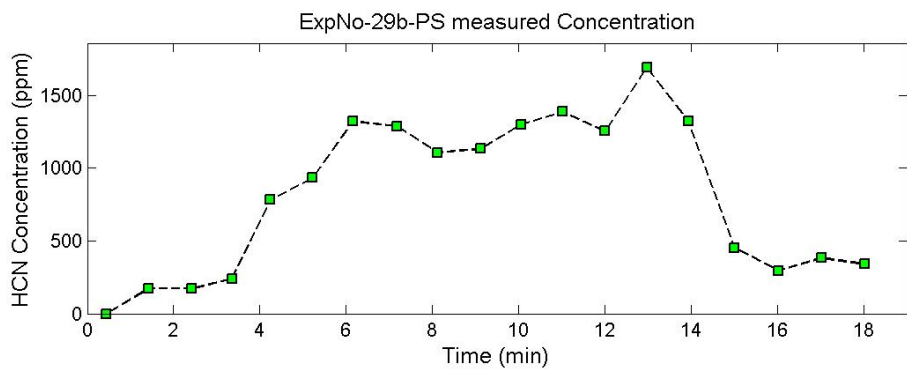
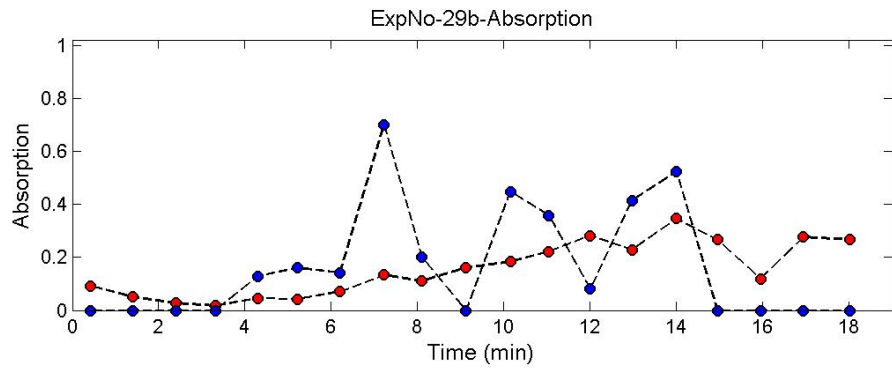
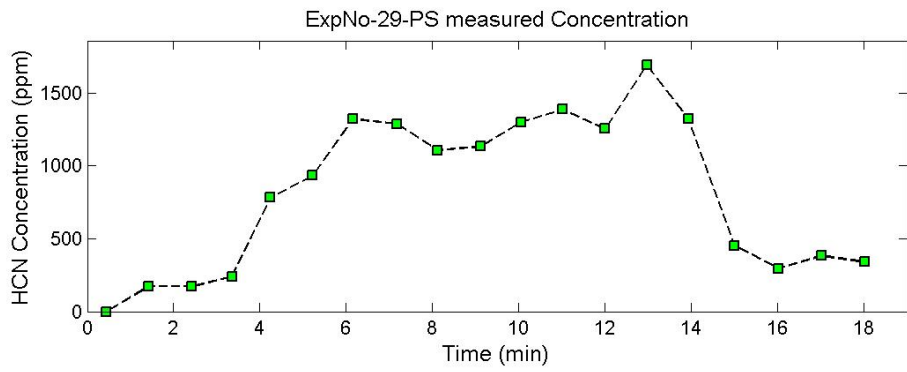
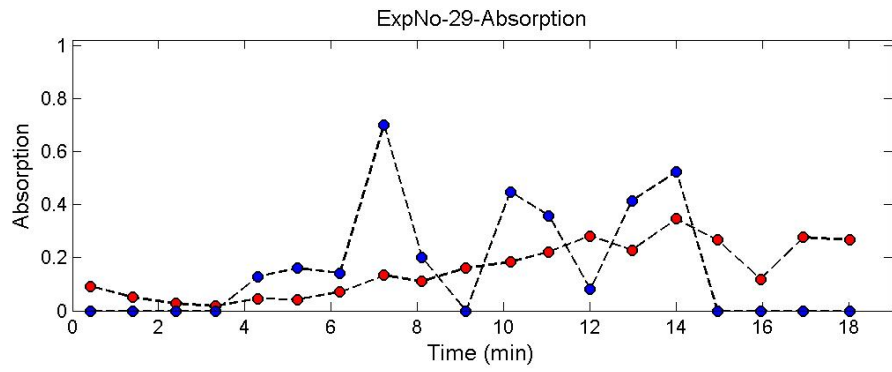


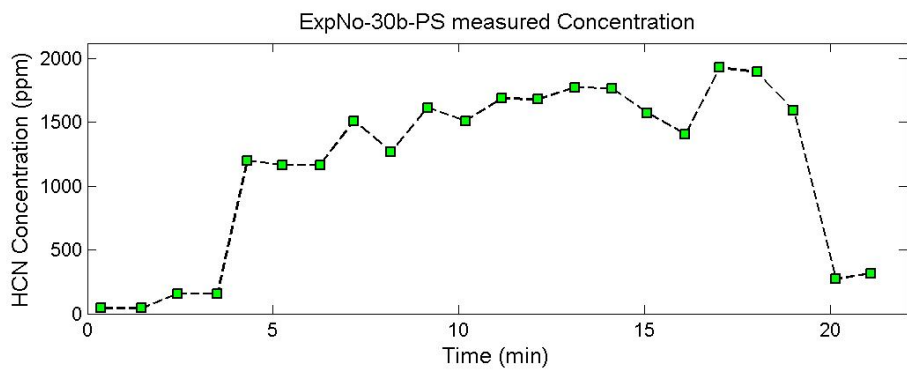
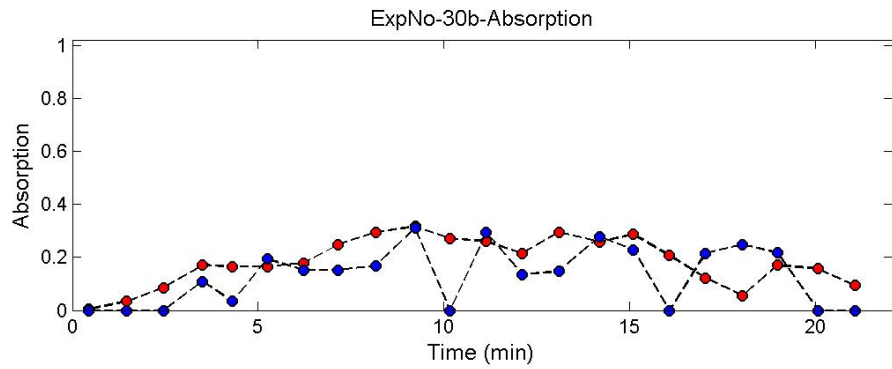
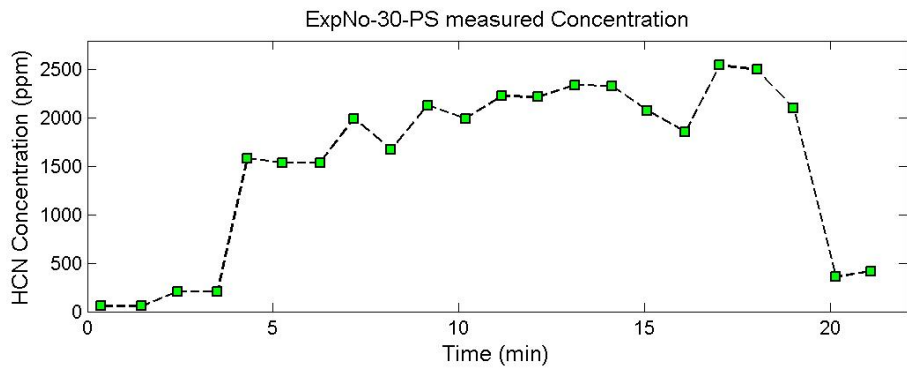
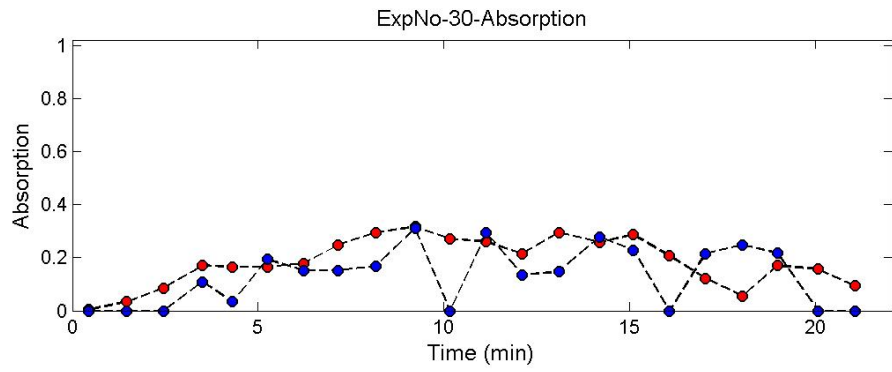


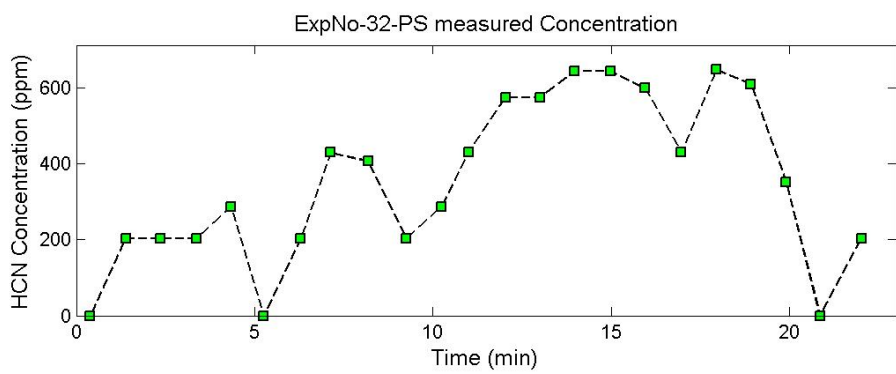
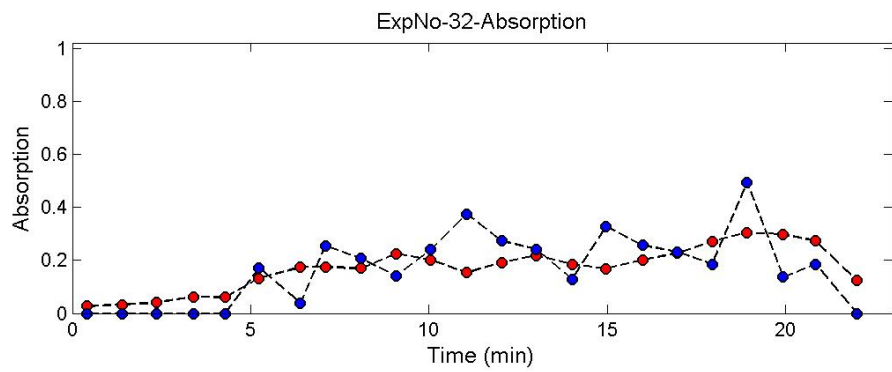
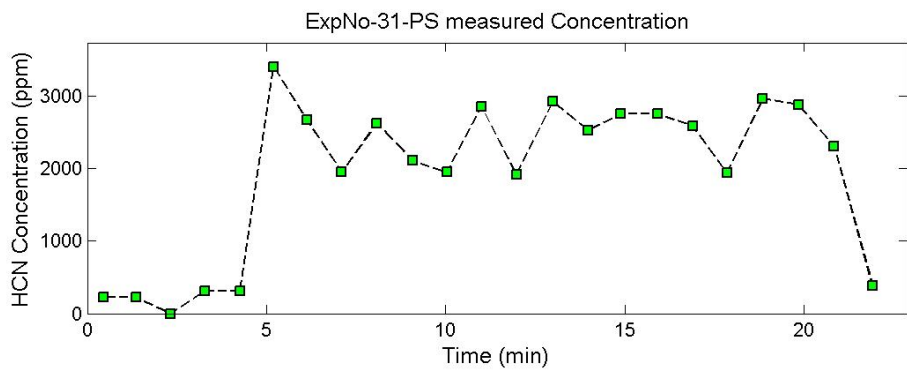
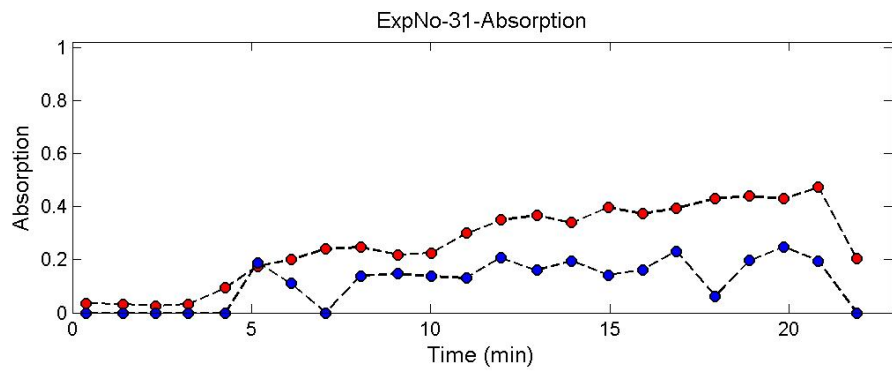




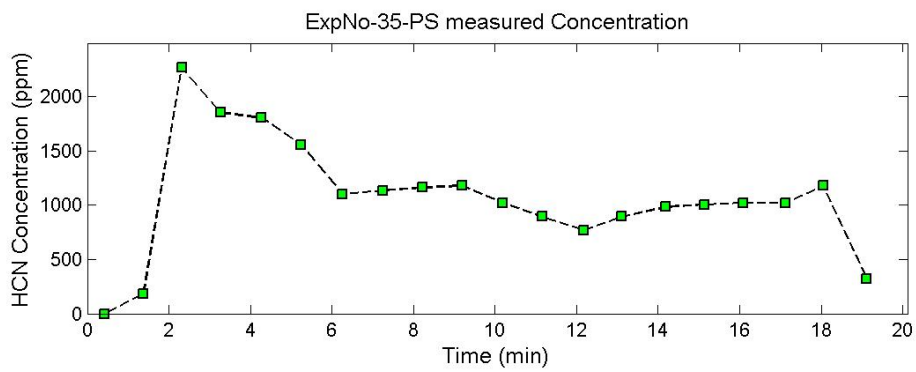
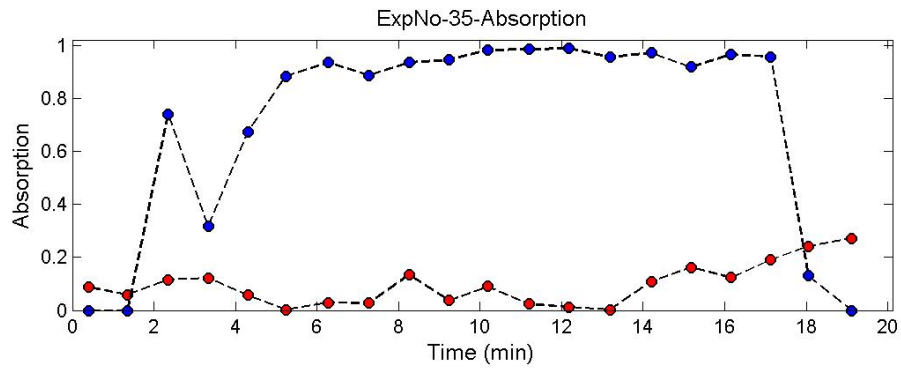
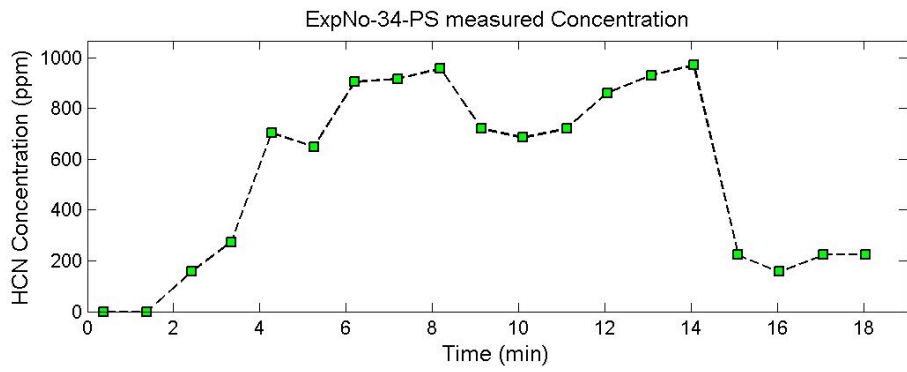
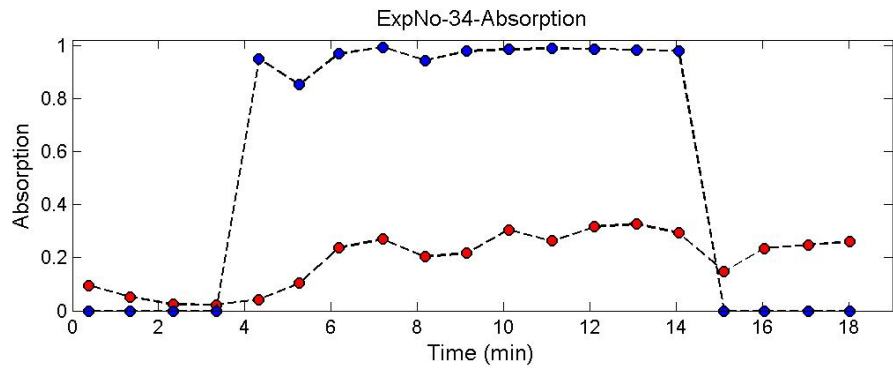


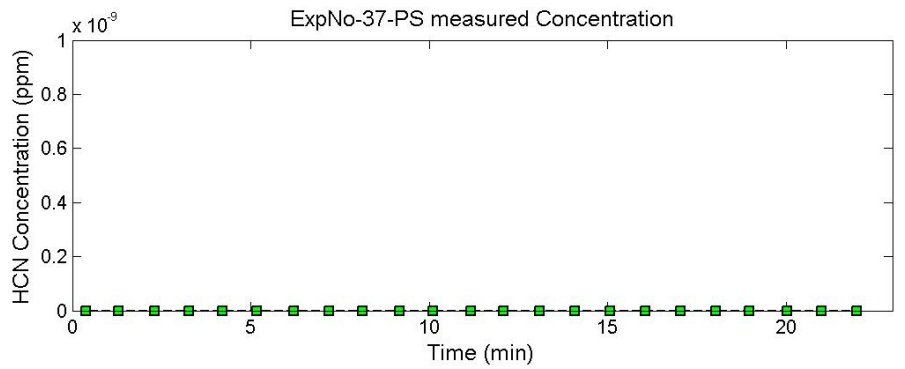
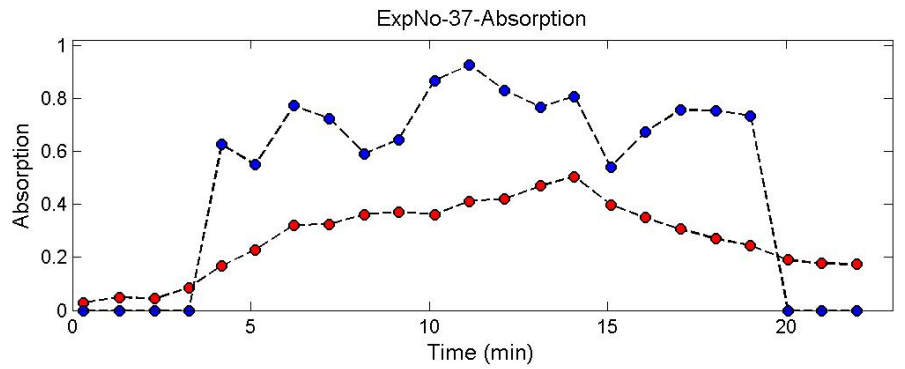
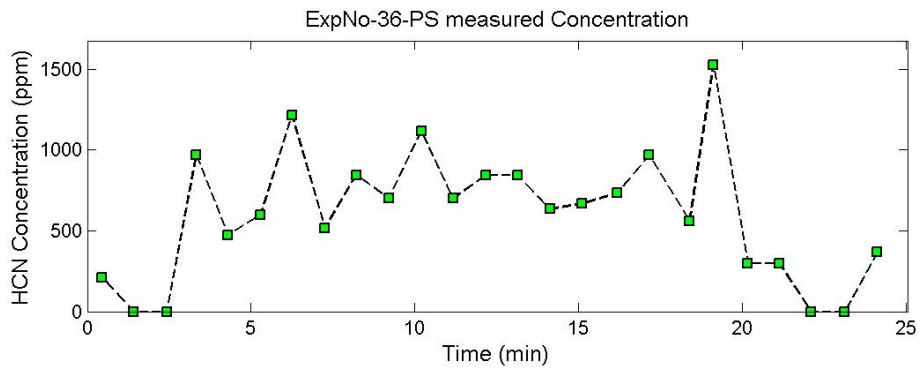
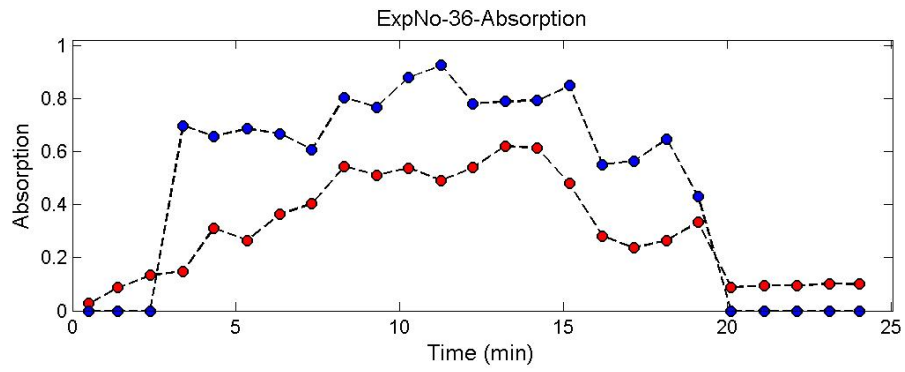


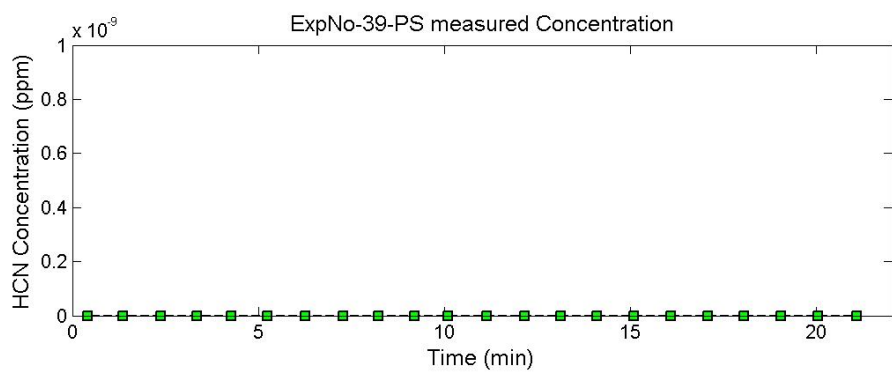
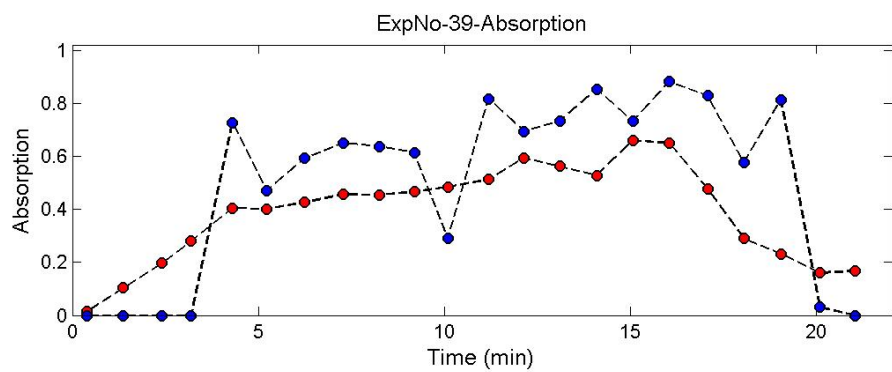
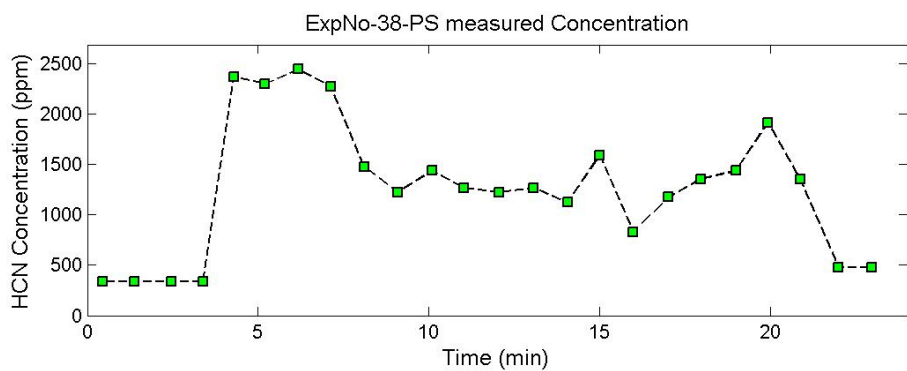
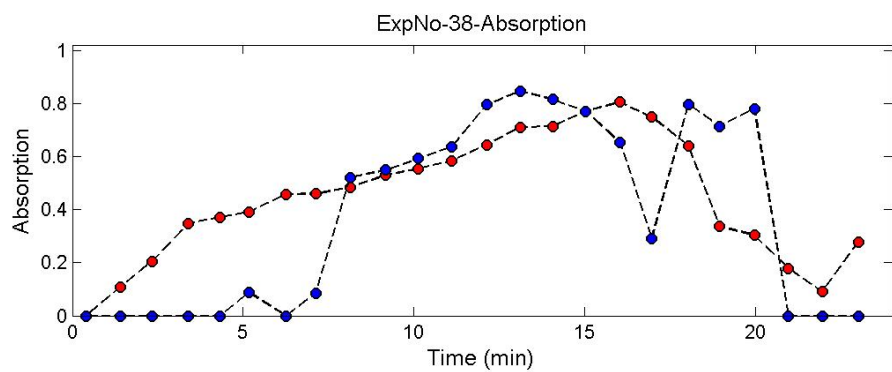


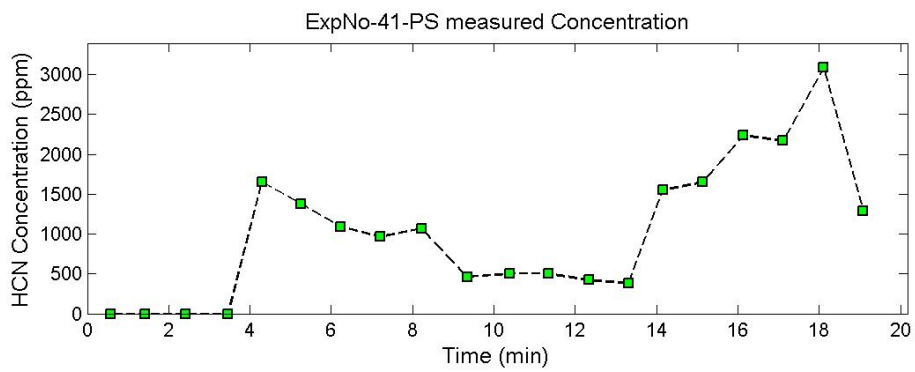
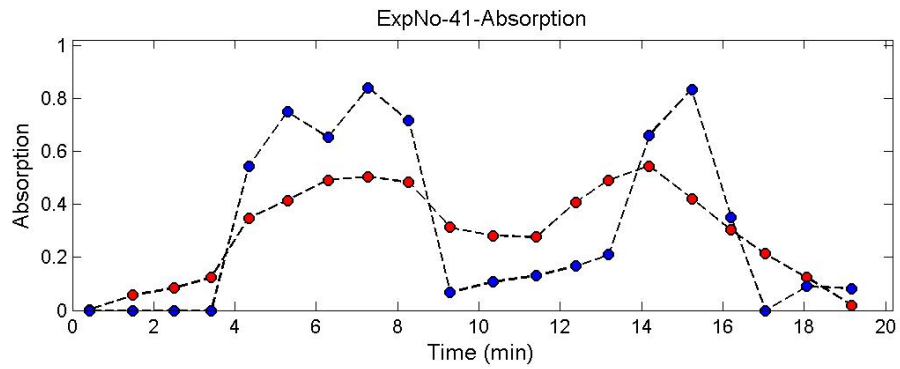
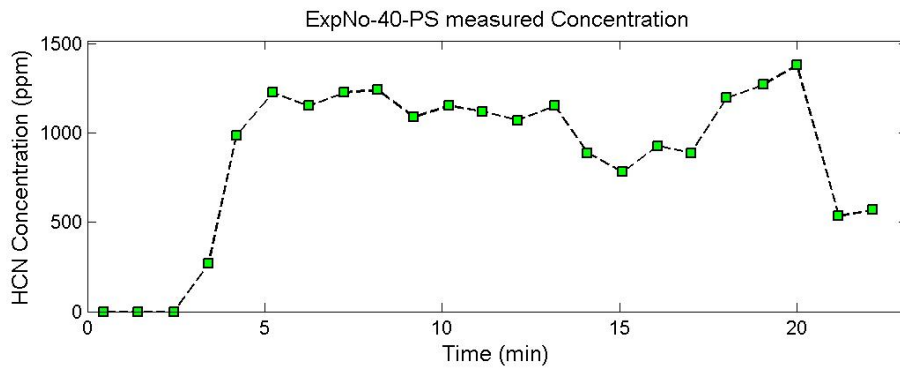
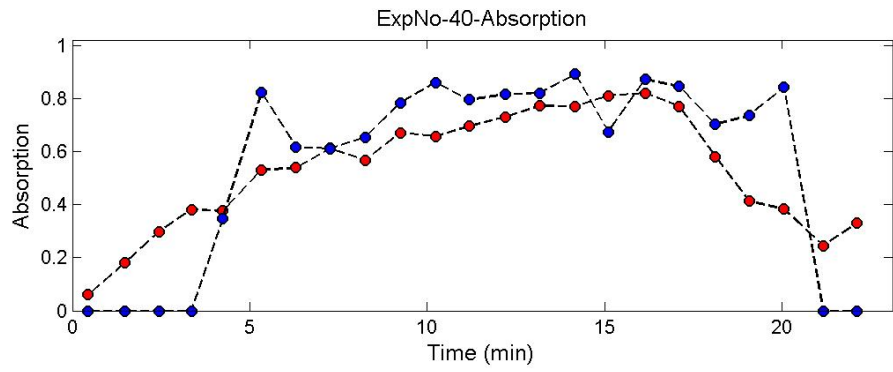


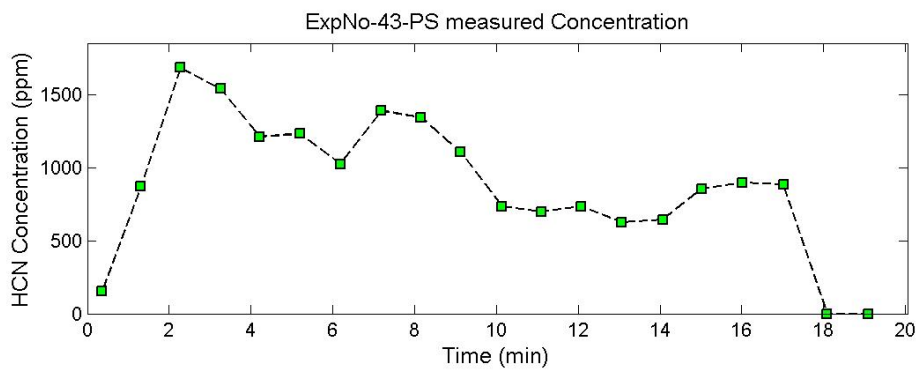
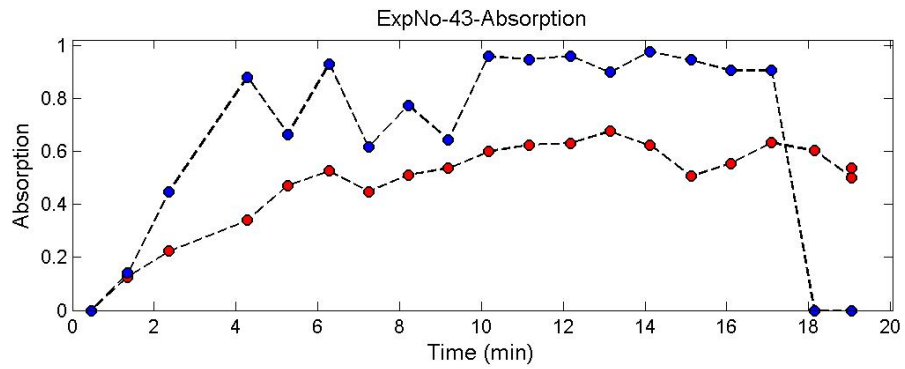
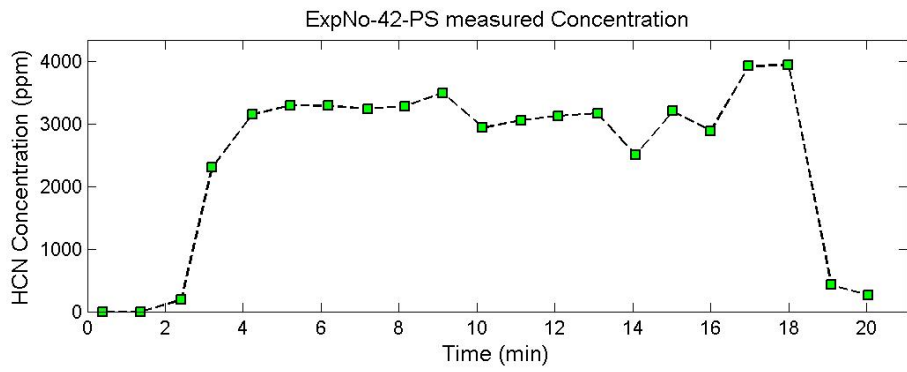
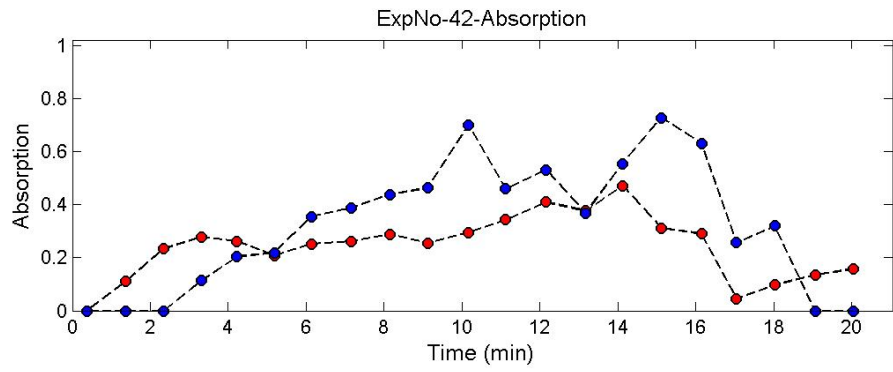


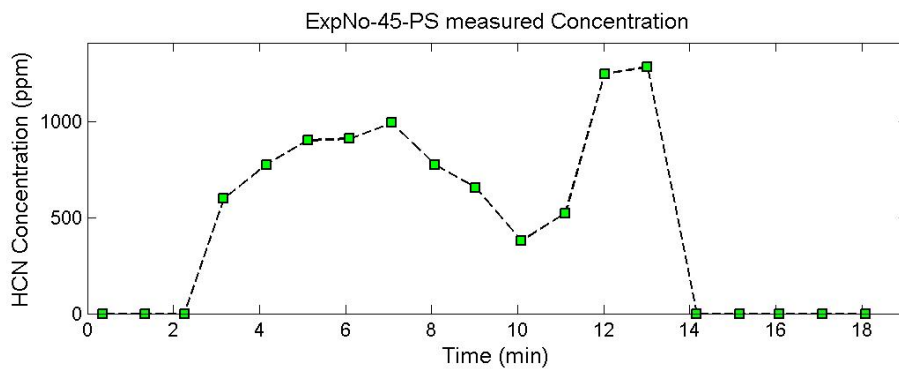
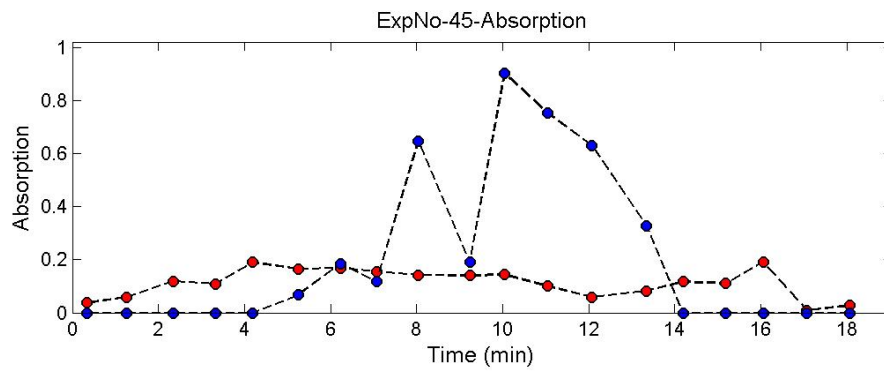
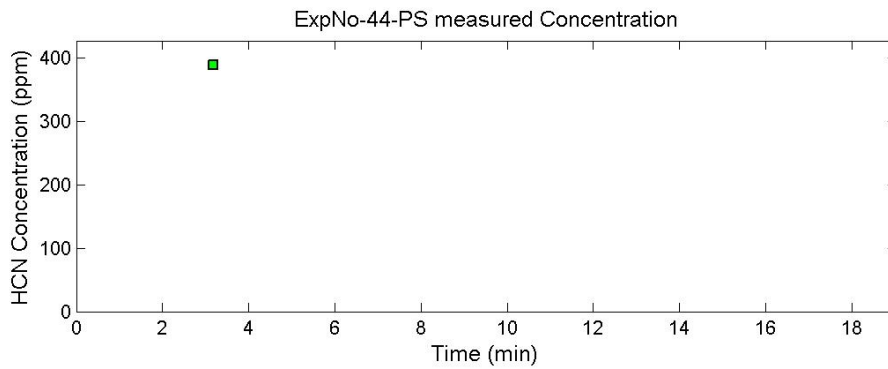
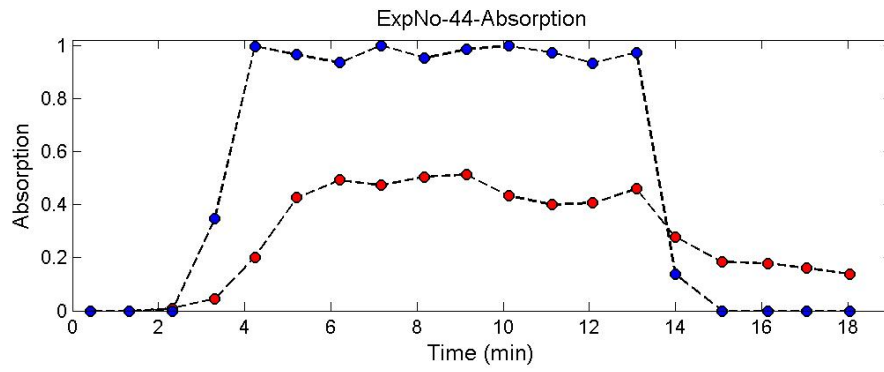






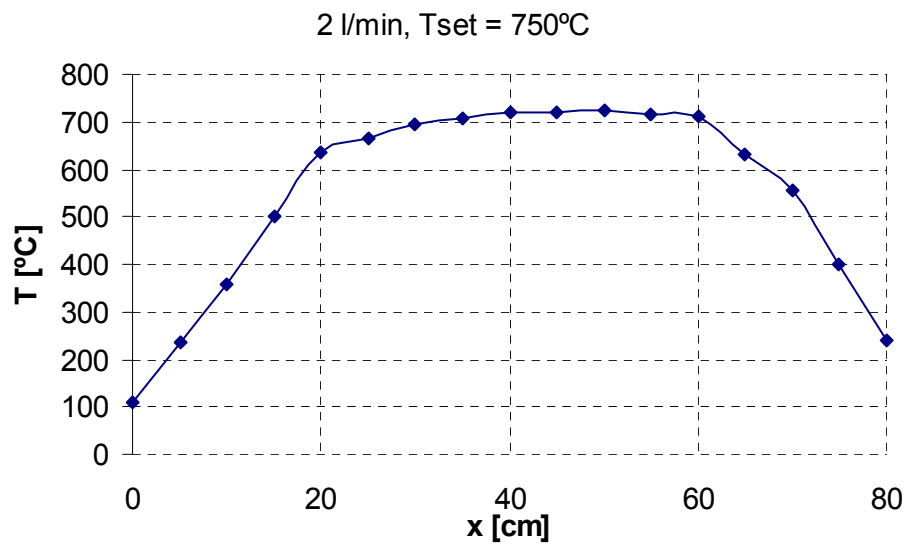
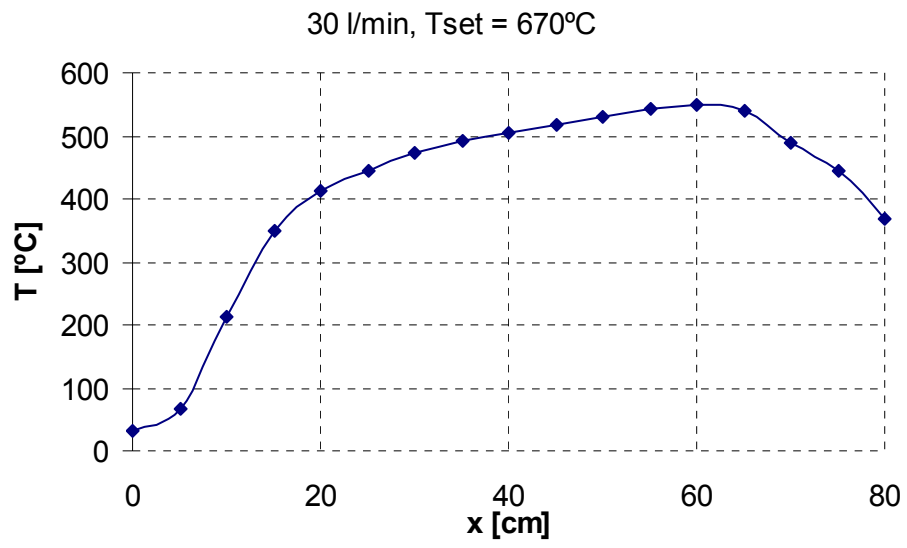


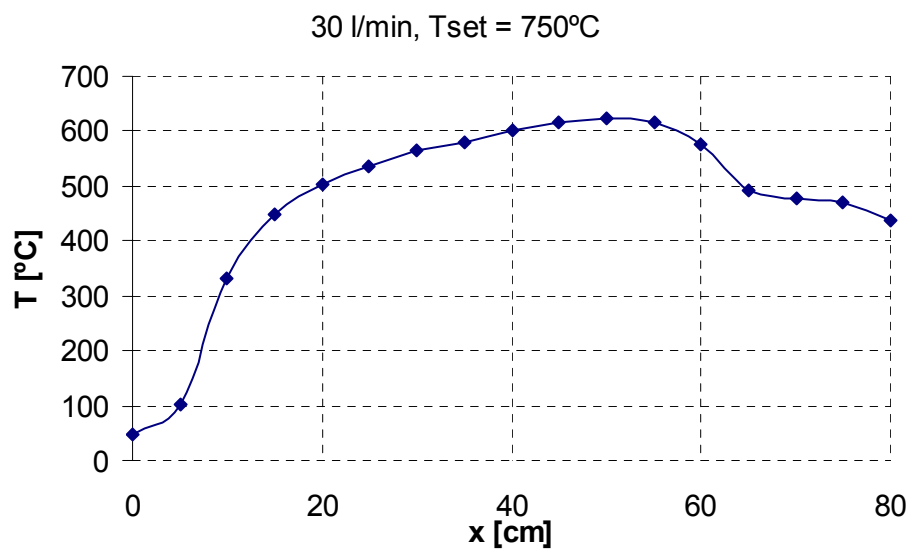
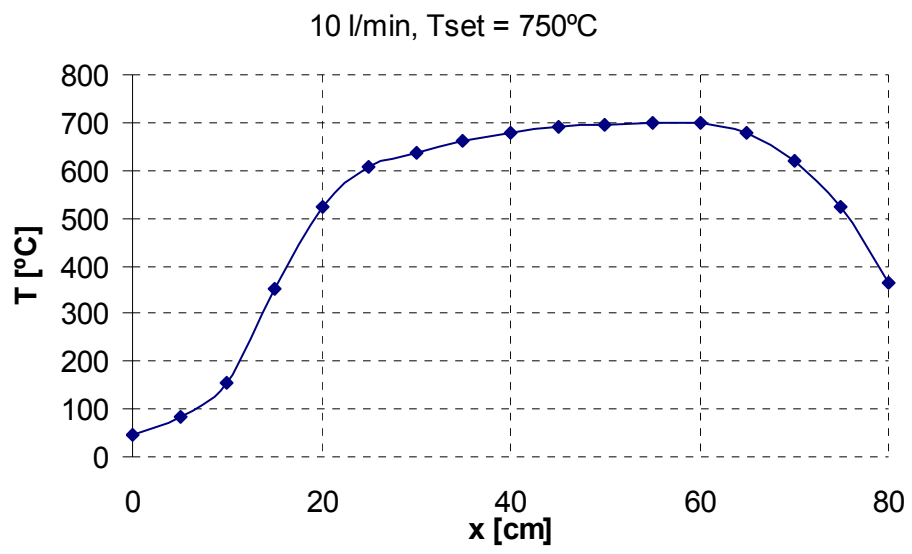




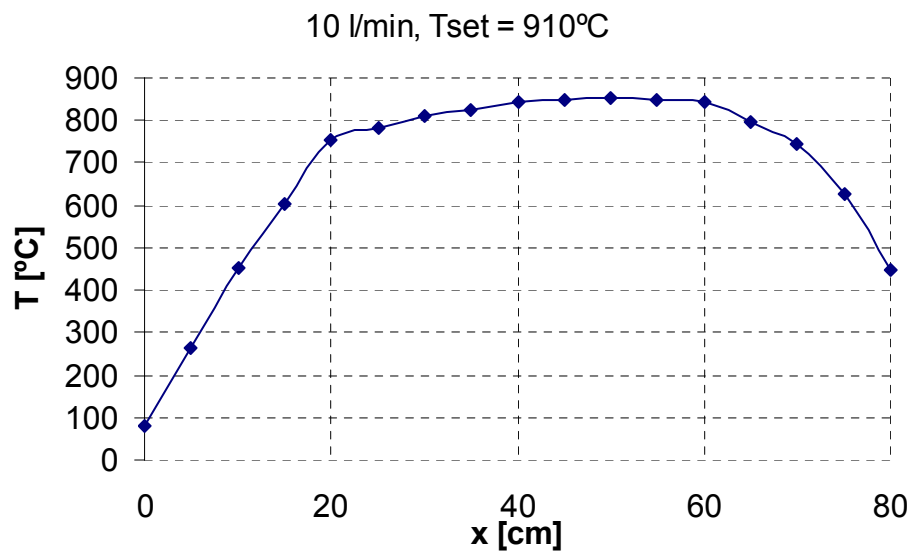
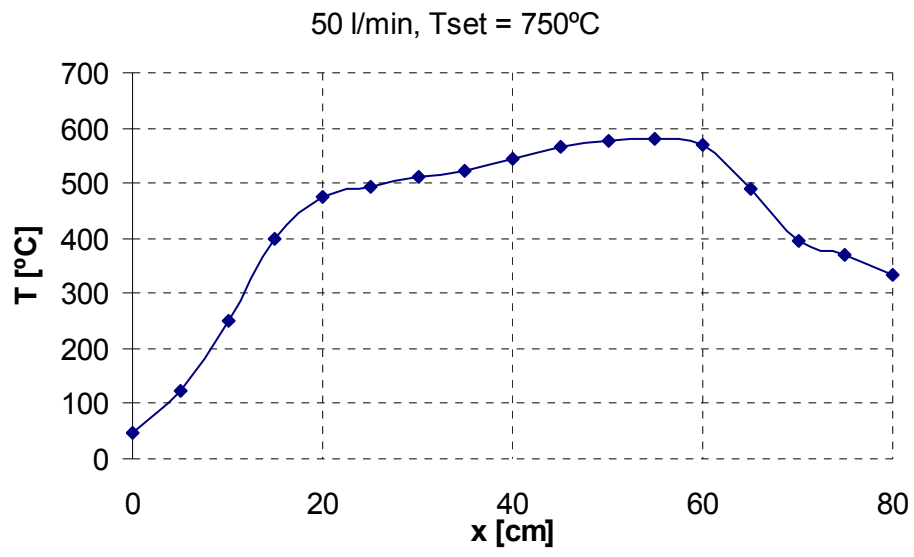
### A.3 Temperature profiles

The measured temperature profiles in the oven for different gas flows and different set temperatures are given below.









## Appendix B Reaction mechanism

SPECIES CONSIDERED	P H A R S G E E	C H A R S G E E	MOLECULAR WEIGHT	TEMPERATURE		ELEMENT COUNT			
				LOW	HIGH	O	H	C	N
1. H2	G	0	2.01594	200	3500	0	2	0	0
2. H	G	0	1.00797	200	3500	0	1	0	0
3. O	G	0	15.99940	200	3500	1	0	0	0
4. O2	G	0	31.99880	200	3500	2	0	0	0
5. OH	G	0	17.00737	200	3500	1	1	0	0
6. H2O	G	0	18.01534	200	3500	1	2	0	0
7. HO2	G	0	33.00677	200	3500	2	1	0	0
8. H2O2	G	0	34.01474	200	3500	2	2	0	0
9. C	G	0	12.01115	200	3500	0	0	1	0
10. CH	G	0	13.01912	200	3500	0	1	1	0
11. CH2	G	0	14.02709	200	3500	0	2	1	0
12. CH2*	G	0	14.02709	200	3500	0	2	1	0
13. CH3	G	0	15.03506	200	3500	0	3	1	0
14. CH4	G	0	16.04303	200	3500	0	4	1	0
15. CO	G	0	28.01055	200	3500	1	0	1	0
16. CO2	G	0	44.00995	200	3500	2	0	1	0
17. HCO	G	0	29.01852	200	3500	1	1	1	0
18. CH2O	G	0	30.02649	200	3500	1	2	1	0
19. CH2OH	G	0	31.03446	200	3500	1	3	1	0
20. CH3O	G	0	31.03446	300	3000	1	3	1	0
21. CH3OH	G	0	32.04243	200	3500	1	4	1	0
22. C2H	G	0	25.03027	200	3500	0	1	2	0
23. C2H2	G	0	26.03824	200	3500	0	2	2	0
24. C2H3	G	0	27.04621	200	3500	0	3	2	0
25. C2H4	G	0	28.05418	200	3500	0	4	2	0
26. C2H5	G	0	29.06215	200	3500	0	5	2	0
27. C2H6	G	0	30.07012	200	3500	0	6	2	0
28. HCCO	G	0	41.02967	300	4000	1	1	2	0
29. CH2CO	G	0	42.03764	200	3500	1	2	2	0
30. HCCOH	G	0	42.03764	300	5000	1	2	2	0
31. C2H3O	G	0	43.04561	300	5000	1	3	2	0
32. N2	G	0	28.01340	300	5000	0	0	0	2
33. C2O	G	0	40.02170	300	5000	1	0	2	0
34. C3H2	G	0	38.04939	300	5000	0	2	3	0
35. C3H3	G	0	39.05736	300	4000	0	3	3	0
36. PC3H4	G	0	40.06533	300	5000	0	4	3	0
37. AC3H4	G	0	40.06533	300	5000	0	4	3	0
38. C4H	G	0	49.05257	300	3000	0	1	4	0
39. C4H2	G	0	50.06054	300	3000	0	2	4	0
40. H2C4O	G	0	66.05994	300	4000	1	2	4	0
41. n-C4H3	G	0	51.06851	300	3000	0	3	4	0
42. i-C4H3	G	0	51.06851	300	3000	0	3	4	0
43. C4H4	G	0	52.07648	300	3000	0	4	4	0
44. n-C4H5	G	0	53.08445	300	3000	0	5	4	0
45. i-C4H5	G	0	53.08445	300	3000	0	5	4	0
46. C4H6	G	0	54.09242	300	3000	0	6	4	0
47. C4H612	G	0	54.09242	300	3000	0	6	4	0
48. C5H2	G	0	62.07169	300	5000	0	2	5	0
49. C5H3	G	0	63.07966	300	5000	0	3	5	0
50. C6H	G	0	73.07487	300	3000	0	1	6	0
51. C6H2	G	0	74.08284	300	3000	0	2	6	0
52. C6H3	G	0	75.09081	300	3000	0	3	6	0
53. l-C6H4	G	0	76.09878	300	3000	0	4	6	0
54. c-C6H4	G	0	76.09878	300	3000	0	4	6	0
55. n-C6H5	G	0	77.10675	300	3000	0	5	6	0
56. i-C6H5	G	0	77.10675	300	3000	0	5	6	0
57. l-C6H6	G	0	78.11472	300	3000	0	6	6	0
58. n-C6H7	G	0	79.12269	300	3000	0	7	6	0
59. i-C6H7	G	0	79.12269	300	3000	0	7	6	0
60. c-C6H7	G	0	79.12269	300	3000	0	7	6	0
61. C6H8	G	0	80.13066	300	3000	0	8	6	0
62. A1	G	0	78.11472	300	3000	0	6	6	0
63. A1-	G	0	77.10675	300	3000	0	5	6	0
64. C6H5O	G	0	93.10615	300	5000	1	5	6	0
65. C6H5OH	G	0	94.11412	300	5000	1	6	6	0



1.	H+O2=O+OH		8.30E+13	0.0	14413.0
2.	O+H2=H+OH		5.00E+04	2.7	6290.0
3.	OH+H2=H+H2O		2.16E+08	1.5	3430.0
4.	OH+OH=O+H2O		3.57E+04	2.4	-2110.0
5.	H+H+M=H2+M		1.00E+18	-1.0	0.0
	H2	Enhanced by	0.000E+00		
	H2O	Enhanced by	0.000E+00		
	CH4	Enhanced by	2.000E+00		
	CO2	Enhanced by	0.000E+00		
	C2H6	Enhanced by	3.000E+00		
6.	H+H+H2=H2+H2		9.00E+16	-0.6	0.0
7.	H+H+H2O=H2+H2O		6.00E+19	-1.2	0.0
8.	H+H+CO2=H2+CO2		5.50E+20	-2.0	0.0
9.	H+OH+M=H2O+M		2.20E+22	-2.0	0.0
	H2	Enhanced by	7.300E-01		
	H2O	Enhanced by	3.650E+00		
	CH4	Enhanced by	2.000E+00		
	C2H6	Enhanced by	3.000E+00		
10.	O+H+M=OH+M		5.00E+17	-1.0	0.0
	H2	Enhanced by	2.000E+00		
	H2O	Enhanced by	6.000E+00		
	CH4	Enhanced by	2.000E+00		
	CO	Enhanced by	1.500E+00		
	CO2	Enhanced by	2.000E+00		
	C2H6	Enhanced by	3.000E+00		
11.	O+O+M=O2+M		1.20E+17	-1.0	0.0
	H2	Enhanced by	2.400E+00		
	H2O	Enhanced by	1.540E+01		
	CH4	Enhanced by	2.000E+00		
	CO	Enhanced by	1.750E+00		
	CO2	Enhanced by	3.600E+00		
	C2H6	Enhanced by	3.000E+00		
12.	H+O2+M=HO2+M		2.80E+18	-0.9	0.0
	O2	Enhanced by	0.000E+00		
	H2O	Enhanced by	0.000E+00		
	CO	Enhanced by	7.500E-01		
	CO2	Enhanced by	1.500E+00		
	C2H6	Enhanced by	1.500E+00		
	N2	Enhanced by	0.000E+00		
13.	H+O2+O2=HO2+O2		3.00E+20	-1.7	0.0
14.	H+O2+H2O=HO2+H2O		9.38E+18	-0.8	0.0
15.	H+O2+N2=HO2+N2		3.75E+20	-1.7	0.0
16.	OH+OH(+M)=H2O2(+M)		7.40E+13	-0.4	0.0
	Low pressure limit:	0.23000E+19	-0.90000E+00	-0.17000E+04	
	TROE centering:	0.73460E+00	0.94000E+02	0.17560E+04	0.51820E+04
	H2	Enhanced by	2.000E+00		
	H2O	Enhanced by	6.000E+00		
	CH4	Enhanced by	2.000E+00		
	CO	Enhanced by	1.500E+00		
	CO2	Enhanced by	2.000E+00		
	C2H6	Enhanced by	3.000E+00		
17.	HO2+H=O+H2O		3.97E+12	0.0	671.0
18.	HO2+H=O2+H2		2.80E+13	0.0	1068.0
19.	HO2+H=OH+OH		1.34E+14	0.0	635.0
20.	HO2+O=OH+O2		2.00E+13	0.0	0.0
21.	HO2+OH=O2+H2O		2.90E+13	0.0	-500.0
22.	HO2+HO2=O2+H2O2		1.30E+11	0.0	-1630.0
	Declared duplicate reaction...				
23.	HO2+HO2=O2+H2O2		4.20E+14	0.0	12000.0
	Declared duplicate reaction...				
24.	H2O2+H=HO2+H2		1.21E+07	2.0	5200.0
25.	H2O2+H=OH+H2O		1.00E+13	0.0	3600.0
26.	H2O2+O=OH+HO2		9.63E+06	2.0	4000.0
27.	H2O2+OH=HO2+H2O		1.75E+12	0.0	320.0
	Declared duplicate reaction...				
28.	H2O2+OH=HO2+H2O		5.80E+14	0.0	9560.0
	Declared duplicate reaction...				
29.	CO+O+M=CO2+M		6.02E+14	0.0	3000.0
	H2	Enhanced by	2.000E+00		
	O2	Enhanced by	6.000E+00		
	H2O	Enhanced by	6.000E+00		
	CH4	Enhanced by	2.000E+00		
	CO	Enhanced by	1.500E+00		
	CO2	Enhanced by	3.500E+00		
	C2H6	Enhanced by	3.000E+00		
30.	CO+OH=CO2+H		4.76E+07	1.2	70.0

31.	CO+H2 (+M)=CH2O (+M)			4.30E+07	1.5	79600.0
	Low pressure limit:	0.50700E+28	-0.34200E+01	0.84350E+05		
	TROE centering:	0.93200E+00	0.19700E+03	0.15400E+04	0.10300E+05	
	H2	Enhanced by	2.000E+00			
	H2O	Enhanced by	6.000E+00			
	CH4	Enhanced by	2.000E+00			
	CO	Enhanced by	1.500E+00			
	CO2	Enhanced by	2.000E+00			
	C2H6	Enhanced by	3.000E+00			
32.	CO+O2=CO2+O			2.50E+12	0.0	47800.0
33.	CO+HO2=CO2+OH			1.50E+14	0.0	23600.0
34.	C+OH=CO+H			5.00E+13	0.0	0.0
35.	C+O2=CO+O			5.80E+13	0.0	576.0
36.	CH+H=C+H2			1.10E+14	0.0	0.0
37.	CH+O=CO+H			5.70E+13	0.0	0.0
38.	CH+OH=HCO+H			3.00E+13	0.0	0.0
39.	CH+H2=CH2+H			1.11E+08	1.8	1670.0
40.	CH+H2O=CH2O+H			5.71E+12	0.0	-755.0
41.	CH+O2=HCO+O			3.30E+13	0.0	0.0
42.	CH+CO (+M)=HCCO (+M)			5.00E+13	0.0	0.0
	Low pressure limit:	0.26900E+29	-0.37400E+01	0.19360E+04		
	TROE centering:	0.57570E+00	0.23700E+03	0.16520E+04	0.50690E+04	
	H2	Enhanced by	2.000E+00			
	H2O	Enhanced by	6.000E+00			
	CH4	Enhanced by	2.000E+00			
	CO	Enhanced by	1.500E+00			
	CO2	Enhanced by	2.000E+00			
	C2H6	Enhanced by	3.000E+00			
43.	CH+CO2=HCO+CO			3.40E+12	0.0	690.0
44.	HCO+H (+M)=CH2O (+M)			1.09E+12	0.5	-260.0
	Low pressure limit:	0.13500E+25	-0.25700E+01	0.14250E+04		
	TROE centering:	0.78240E+00	0.27100E+03	0.27550E+04	0.65700E+04	
	H2	Enhanced by	2.000E+00			
	H2O	Enhanced by	6.000E+00			
	CH4	Enhanced by	2.000E+00			
	CO	Enhanced by	1.500E+00			
	CO2	Enhanced by	2.000E+00			
	C2H6	Enhanced by	3.000E+00			
45.	HCO+H=CO+H2			7.34E+13	0.0	0.0
46.	HCO+O=CO+OH			3.00E+13	0.0	0.0
47.	HCO+O=CO2+H			3.00E+13	0.0	0.0
48.	HCO+OH=CO+H2O			5.00E+13	0.0	0.0
49.	HCO+M=CO+H+M			1.87E+17	-1.0	17000.0
	H2	Enhanced by	2.000E+00			
	H2O	Enhanced by	1.200E+01			
	CH4	Enhanced by	2.000E+00			
	CO	Enhanced by	1.500E+00			
	CO2	Enhanced by	2.000E+00			
	C2H6	Enhanced by	3.000E+00			
50.	HCO+O2=CO+HO2			7.60E+12	0.0	400.0
51.	CH2+H (+M)=CH3 (+M)			2.50E+16	-0.8	0.0
	Low pressure limit:	0.32000E+28	-0.31400E+01	0.12300E+04		
	TROE centering:	0.68000E+00	0.78000E+02	0.19950E+04	0.55900E+04	
	H2	Enhanced by	2.000E+00			
	H2O	Enhanced by	6.000E+00			
	CH4	Enhanced by	2.000E+00			
	CO	Enhanced by	1.500E+00			
	CO2	Enhanced by	2.000E+00			
	C2H6	Enhanced by	3.000E+00			
52.	CH2+O=HCO+H			8.00E+13	0.0	0.0
53.	CH2+OH=CH2O+H			2.00E+13	0.0	0.0
54.	CH2+OH=CH+H2O			1.13E+07	2.0	3000.0
55.	CH2+H2=H+CH3			5.00E+05	2.0	7230.0
56.	CH2+O2=CO2+H+H			1.32E+13	0.0	1500.0
57.	CH2+HO2=CH2O+OH			2.00E+13	0.0	0.0
58.	CH2+C=C2H+H			5.00E+13	0.0	0.0
59.	CH2+CO (+M)=CH2CO (+M)			8.10E+11	0.5	4510.0
	Low pressure limit:	0.26900E+34	-0.51100E+01	0.70950E+04		
	TROE centering:	0.59070E+00	0.27500E+03	0.12260E+04	0.51850E+04	
	H2	Enhanced by	2.000E+00			
	H2O	Enhanced by	6.000E+00			
	CH4	Enhanced by	2.000E+00			
	CO	Enhanced by	1.500E+00			
	CO2	Enhanced by	2.000E+00			
	C2H6	Enhanced by	3.000E+00			
60.	CH2+CH=C2H2+H			4.00E+13	0.0	0.0
61.	CH2+CH2=C2H2+H2			3.20E+13	0.0	0.0

62.	CH2*+N2=CH2+N2		1.50E+13	0.0	600.0
63.	CH2*+H=CH+H2		3.00E+13	0.0	0.0
64.	CH2*+O=CO+H2		1.50E+13	0.0	0.0
65.	CH2*+O=HCO+H		1.50E+13	0.0	0.0
66.	CH2*+OH=CH2O+H		3.00E+13	0.0	0.0
67.	CH2*+H2=CH3+H		7.00E+13	0.0	0.0
68.	CH2*+O2=H+OH+CO		2.80E+13	0.0	0.0
69.	CH2*+O2=CO+H2O		1.20E+13	0.0	0.0
70.	CH2*+H2O (+M)=CH3OH (+M)		2.00E+13	0.0	0.0
	Low pressure limit:	0.27000E+39	-0.63000E+01	0.31000E+04	
	TROE centering:	0.15070E+00	0.13400E+03	0.23830E+04	0.72650E+04
	H2	Enhanced by	2.000E+00		
	H2O	Enhanced by	6.000E+00		
	CH4	Enhanced by	2.000E+00		
	CO	Enhanced by	1.500E+00		
	CO2	Enhanced by	2.000E+00		
	C2H6	Enhanced by	3.000E+00		
71.	CH2*+H2O=CH2+H2O		3.00E+13	0.0	0.0
72.	CH2*+CO=CH2+CO		9.00E+12	0.0	0.0
73.	CH2*+CO2=CH2+CO2		7.00E+12	0.0	0.0
74.	CH2*+CO2=CH2O+CO		1.40E+13	0.0	0.0
75.	CH2O+H (+M)=CH2OH (+M)		5.40E+11	0.5	3600.0
	Low pressure limit:	0.12700E+33	-0.48200E+01	0.65300E+04	
	TROE centering:	0.71870E+00	0.10300E+03	0.12910E+04	0.41600E+04
	H2	Enhanced by	2.000E+00		
	H2O	Enhanced by	6.000E+00		
	CH4	Enhanced by	2.000E+00		
	CO	Enhanced by	1.500E+00		
	CO2	Enhanced by	2.000E+00		
	C2H6	Enhanced by	3.000E+00		
76.	CH2O+H (+M)=CH3O (+M)		5.40E+11	0.5	2600.0
	Low pressure limit:	0.22000E+31	-0.48000E+01	0.55600E+04	
	TROE centering:	0.75800E+00	0.94000E+02	0.15550E+04	0.42000E+04
	H2	Enhanced by	2.000E+00		
	H2O	Enhanced by	6.000E+00		
	CH4	Enhanced by	2.000E+00		
	CO	Enhanced by	1.500E+00		
	CO2	Enhanced by	2.000E+00		
	C2H6	Enhanced by	3.000E+00		
77.	CH2O+H=HCO+H2		2.30E+10	1.1	3275.0
78.	CH2O+O=HCO+OH		3.90E+13	0.0	3540.0
79.	CH2O+OH=HCO+H2O		3.43E+09	1.2	-447.0
80.	CH2O+O2=HCO+HO2		1.00E+14	0.0	40000.0
81.	CH2O+HO2=HCO+H2O2		1.00E+12	0.0	8000.0
82.	CH2O+CH=CH2CO+H		9.46E+13	0.0	-515.0
83.	CH3+H (+M)=CH4 (+M)		1.27E+16	-0.6	383.0
	Low pressure limit:	0.24770E+34	-0.47600E+01	0.24400E+04	
	TROE centering:	0.78300E+00	0.74000E+02	0.29410E+04	0.69640E+04
	H2	Enhanced by	2.000E+00		
	H2O	Enhanced by	6.000E+00		
	CH4	Enhanced by	2.000E+00		
	CO	Enhanced by	1.500E+00		
	CO2	Enhanced by	2.000E+00		
	C2H6	Enhanced by	3.000E+00		
84.	CH3+O=CH2O+H		8.43E+13	0.0	0.0
85.	CH3+OH (+M)=CH3OH (+M)		6.30E+13	0.0	0.0
	Low pressure limit:	0.27000E+39	-0.63000E+01	0.31000E+04	
	TROE centering:	0.21050E+00	0.83500E+02	0.53980E+04	0.83700E+04
	H2	Enhanced by	2.000E+00		
	H2O	Enhanced by	6.000E+00		
	CH4	Enhanced by	2.000E+00		
	CO	Enhanced by	1.500E+00		
	CO2	Enhanced by	2.000E+00		
	C2H6	Enhanced by	3.000E+00		
86.	CH3+OH=CH2+H2O		5.60E+07	1.6	5420.0
87.	CH3+OH=CH2*+H2O		2.50E+13	0.0	0.0
88.	CH3+O2=O+CH3O		2.68E+13	0.0	28800.0
89.	CH3+O2=OH+CH2O		3.60E+10	0.0	8940.0
90.	CH3+HO2=CH4+O2		1.00E+12	0.0	0.0
91.	CH3+HO2=CH3O+OH		2.00E+13	0.0	0.0
92.	CH3+H2O2=CH4+HO2		2.45E+04	2.5	5180.0
93.	CH3+C=C2H2+H		5.00E+13	0.0	0.0
94.	CH3+CH=C2H3+H		3.00E+13	0.0	0.0
95.	CH3+HCO=CH4+CO		2.65E+13	0.0	0.0
96.	CH3+CH2O=CH4+HCO		3.32E+03	2.8	5860.0
97.	CH3+CH2=C2H4+H		4.00E+13	0.0	0.0
98.	CH3+CH2*=C2H4+H		1.20E+13	0.0	-570.0

99.	CH3+CH3 (+M)=C2H6 (+M)		2.12E+16	-1.0	620.0
	Low pressure limit:	0.17700E+51	-0.96700E+01	0.62200E+04	
	TROE centering:	0.53250E+00	0.15100E+03	0.10380E+04	0.49700E+04
	H2	Enhanced by	2.000E+00		
	H2O	Enhanced by	6.000E+00		
	CH4	Enhanced by	2.000E+00		
	CO	Enhanced by	1.500E+00		
	CO2	Enhanced by	2.000E+00		
	C2H6	Enhanced by	3.000E+00		
100.	CH3+CH3=H+C2H5		4.99E+12	0.1	10600.0
101.	CH3O+H (+M)=CH3OH (+M)		5.00E+13	0.0	0.0
	Low pressure limit:	0.86000E+29	-0.40000E+01	0.30250E+04	
	TROE centering:	0.89020E+00	0.14400E+03	0.28380E+04	0.45569E+05
	H2	Enhanced by	2.000E+00		
	H2O	Enhanced by	6.000E+00		
	CH4	Enhanced by	2.000E+00		
	CO	Enhanced by	1.500E+00		
	CO2	Enhanced by	2.000E+00		
	C2H6	Enhanced by	3.000E+00		
102.	CH3O+H=CH2OH+H		3.40E+06	1.6	0.0
103.	CH3O+H=CH2O+H2		2.00E+13	0.0	0.0
104.	CH3O+H=CH3+OH		3.20E+13	0.0	0.0
105.	CH3O+H=CH2*+H2O		1.60E+13	0.0	0.0
106.	CH3O+O=CH2O+OH		1.00E+13	0.0	0.0
107.	CH3O+OH=CH2O+H2O		5.00E+12	0.0	0.0
108.	CH3O+O2=CH2O+HO2		4.28E-13	7.6	-3530.0
109.	CH2OH+H (+M)=CH3OH (+M)		1.80E+13	0.0	0.0
	Low pressure limit:	0.30000E+32	-0.48000E+01	0.33000E+04	
	TROE centering:	0.76790E+00	0.33800E+03	0.18120E+04	0.50810E+04
	H2	Enhanced by	2.000E+00		
	H2O	Enhanced by	6.000E+00		
	CH4	Enhanced by	2.000E+00		
	CO	Enhanced by	1.500E+00		
	CO2	Enhanced by	2.000E+00		
	C2H6	Enhanced by	3.000E+00		
110.	CH2OH+H=CH2O+H2		2.00E+13	0.0	0.0
111.	CH2OH+H=CH3+OH		1.20E+13	0.0	0.0
112.	CH2OH+H=CH2*+H2O		6.00E+12	0.0	0.0
113.	CH2OH+O=CH2O+OH		1.00E+13	0.0	0.0
114.	CH2OH+OH=CH2O+H2O		5.00E+12	0.0	0.0
115.	CH2OH+O2=CH2O+HO2		1.80E+13	0.0	900.0
116.	CH4+H=CH3+H2		6.60E+08	1.6	10840.0
117.	CH4+O=CH3+OH		1.02E+09	1.5	8600.0
118.	CH4+OH=CH3+H2O		1.00E+08	1.6	3120.0
119.	CH4+CH=C2H4+H		6.00E+13	0.0	0.0
120.	CH4+CH2=CH3+CH3		2.46E+06	2.0	8270.0
121.	CH4+CH2*=CH3+CH3		1.60E+13	0.0	-570.0
122.	CH3OH+H=CH2OH+H2		1.70E+07	2.1	4870.0
123.	CH3OH+H=CH3O+H2		4.20E+06	2.1	4870.0
124.	CH3OH+O=CH2OH+OH		3.88E+05	2.5	3100.0
125.	CH3OH+O=CH3O+OH		1.30E+05	2.5	5000.0
126.	CH3OH+OH=CH2OH+H2O		1.44E+06	2.0	-840.0
127.	CH3OH+OH=CH3O+H2O		6.30E+06	2.0	1500.0
128.	CH3OH+CH3=CH2OH+CH4		3.00E+07	1.5	9940.0
129.	CH3OH+CH3=CH3O+CH4		1.00E+07	1.5	9940.0
130.	C2H+H (+M)=C2H2 (+M)		1.00E+17	-1.0	0.0
	Low pressure limit:	0.37500E+34	-0.48000E+01	0.19000E+04	
	TROE centering:	0.64640E+00	0.13200E+03	0.13150E+04	0.55660E+04
	H2	Enhanced by	2.000E+00		
	H2O	Enhanced by	6.000E+00		
	CH4	Enhanced by	2.000E+00		
	CO	Enhanced by	1.500E+00		
	CO2	Enhanced by	2.000E+00		
	C2H6	Enhanced by	3.000E+00		
131.	C2H+O=CH+CO		5.00E+13	0.0	0.0
132.	C2H+OH=H+HCCO		2.00E+13	0.0	0.0
133.	C2H+O2=HCO+CO		5.00E+13	0.0	1500.0
134.	C2H+H2=H+C2H2		4.90E+05	2.5	560.0
135.	HCCO+H=CH2*+CO		1.00E+14	0.0	0.0
136.	HCCO+O=H+CO+CO		1.00E+14	0.0	0.0
137.	HCCO+O2=OH+2CO		1.60E+12	0.0	854.0
138.	HCCO+CH=C2H2+CO		5.00E+13	0.0	0.0
139.	HCCO+CH2=C2H3+CO		3.00E+13	0.0	0.0
140.	HCCO+HCCO=C2H2+CO+CO		1.00E+13	0.0	0.0
141.	C2H2+H (+M)=C2H3 (+M)		5.60E+12	0.0	2400.0
	Low pressure limit:	0.38000E+41	-0.72700E+01	0.72200E+04	
	TROE centering:	0.75070E+00	0.98500E+02	0.13020E+04	0.41670E+04

	H2	Enhanced by	2.000E+00			
	H2O	Enhanced by	6.000E+00			
	CH4	Enhanced by	2.000E+00			
	CO	Enhanced by	1.500E+00			
	CO2	Enhanced by	2.000E+00			
	C2H6	Enhanced by	3.000E+00			
142.	C2H2+O=HCCO+H			1.02E+07	2.0	1900.0
143.	C2H2+O=C2H+OH			4.60E+19	-1.4	28950.0
144.	C2H2+O=CH2+CO			1.02E+07	2.0	1900.0
145.	C2H2+OH=CH2CO+H			2.18E-04	4.5	-1000.0
146.	C2H2+OH=HCCOH+H			5.04E+05	2.3	13500.0
147.	C2H2+OH=C2H+H2O			3.37E+07	2.0	14000.0
148.	C2H2+OH=CH3+CO			4.83E-04	4.0	-2000.0
149.	CH2CO+H=HCCO+H2			5.00E+13	0.0	8000.0
150.	CH2CO+H=CH3+CO			1.13E+13	0.0	3428.0
151.	CH2CO+O=HCCO+OH			1.00E+13	0.0	8000.0
152.	CH2CO+O=CH2+CO2			1.75E+12	0.0	1350.0
153.	CH2CO+OH=HCCO+H2O			7.50E+12	0.0	2000.0
154.	HCCOH+H=CH2CO+H			1.00E+13	0.0	0.0
155.	C2H3+H(+M)=C2H4(+M)			6.08E+12	0.3	280.0
	Low pressure limit:	0.14000E+31	-0.38600E+01	0.33200E+04		
	TROE centering:	0.78200E+00	0.20750E+03	0.26630E+04	0.60950E+04	
	H2	Enhanced by	2.000E+00			
	H2O	Enhanced by	6.000E+00			
	CH4	Enhanced by	2.000E+00			
	CO	Enhanced by	1.500E+00			
	CO2	Enhanced by	2.000E+00			
	C2H6	Enhanced by	3.000E+00			
156.	C2H3+H=C2H2+H2			4.00E+13	0.0	0.0
157.	C2H3+O=CH2CO+H			3.00E+13	0.0	0.0
158.	C2H3+OH=C2H2+H2O			2.00E+13	0.0	0.0
159.	C2H3+O2=C2H2+HO2			1.12E+08	0.9	200.0
160.	C2H3+O2=C2H3O+O			3.64E+11	0.3	101.0
161.	C2H3+O2=HCO+CH2O			4.58E+16	-1.4	1015.0
162.	C2H4(+M)=H2+C2H2(+M)			8.00E+12	0.4	88770.0
	Low pressure limit:	0.70000E+51	-0.93100E+01	0.99860E+05		
	TROE centering:	0.73450E+00	0.18000E+03	0.10350E+04	0.54170E+04	
	H2	Enhanced by	2.000E+00			
	H2O	Enhanced by	6.000E+00			
	CH4	Enhanced by	2.000E+00			
	CO	Enhanced by	1.500E+00			
	CO2	Enhanced by	2.000E+00			
	C2H6	Enhanced by	3.000E+00			
163.	C2H4+H(+M)=C2H5(+M)			1.08E+12	0.5	1820.0
	Low pressure limit:	0.12000E+43	-0.76200E+01	0.69700E+04		
	TROE centering:	0.97530E+00	0.21000E+03	0.98400E+03	0.43740E+04	
	H2	Enhanced by	2.000E+00			
	H2O	Enhanced by	6.000E+00			
	CH4	Enhanced by	2.000E+00			
	CO	Enhanced by	1.500E+00			
	CO2	Enhanced by	2.000E+00			
	C2H6	Enhanced by	3.000E+00			
164.	C2H4+H=C2H3+H2			1.32E+06	2.5	12240.0
165.	C2H4+O=CH3+HCO			1.92E+07	1.8	220.0
166.	C2H4+OH=C2H3+H2O			3.60E+06	2.0	2500.0
167.	C2H4+CH3=C2H3+CH4			2.27E+05	2.0	9200.0
168.	C2H5+H(+M)=C2H6(+M)			5.21E+17	-1.0	1580.0
	Low pressure limit:	0.19900E+42	-0.70800E+01	0.66850E+04		
	TROE centering:	0.84220E+00	0.12500E+03	0.22190E+04	0.68820E+04	
	H2	Enhanced by	2.000E+00			
	H2O	Enhanced by	6.000E+00			
	CH4	Enhanced by	2.000E+00			
	CO	Enhanced by	1.500E+00			
	CO2	Enhanced by	2.000E+00			
	C2H6	Enhanced by	3.000E+00			
169.	C2H5+H=C2H4+H2			2.00E+12	0.0	0.0
170.	C2H5+O=CH3+CH2O			1.32E+14	0.0	0.0
171.	C2H5+O2=C2H4+HO2			8.40E+11	0.0	3875.0
172.	C2H6+H=C2H5+H2			1.15E+08	1.9	7530.0
173.	C2H6+O=C2H5+OH			8.98E+07	1.9	5690.0
174.	C2H6+OH=C2H5+H2O			3.54E+06	2.1	870.0
175.	C2H6+CH2*=C2H5+CH3			4.00E+13	0.0	-550.0
176.	C2H6+CH3=C2H5+CH4			6.14E+06	1.7	10450.0
177.	HCCO+OH=C2O+H2O			3.00E+13	0.0	0.0
178.	C2O+H=CH+CO			5.00E+13	0.0	0.0
179.	C2O+O=CO+CO			5.00E+13	0.0	0.0
180.	C2O+OH=CO+CO+H			2.00E+13	0.0	0.0



181.	C2O+O2=CO+CO+O	2.00E+13	0.0	0.0
182.	CH2CO+H=C2H3O	5.40E+11	0.5	1820.0
183.	C2H3O+H=CH2CO+H2	1.00E+13	0.0	0.0
184.	C2H3O+O=CH2O+HCO	9.60E+06	1.8	220.0
185.	C2H3O+O=CH2CO+OH	1.00E+13	0.0	0.0
186.	C2H3O+OH=CH2CO+H2O	5.00E+12	0.0	0.0
187.	CH3+HCCO=C2H4+CO	5.00E+13	0.0	0.0
188.	CH3+C2H=C3H3+H	2.41E+13	0.0	0.0
189.	CH4+C2H=C2H2+CH3	1.81E+12	0.0	500.0
190.	C2H2+CH=C3H2+H	3.00E+13	0.0	0.0
191.	C2H2+CH2=C3H3+H	2.40E+13	0.0	6620.0
192.	C2H2+CH2*=C3H3+H	4.00E+13	0.0	0.0
193.	C2H2+CH3=AC3H4+H	5.72E+20	-2.4	31500.0
194.	C2H2+CH3=PC3H4+H	2.72E+18	-2.0	20200.0
195.	C2H2+C2H=C4H2+H	9.60E+13	0.0	0.0
196.	C2H2+C2H=n-C4H3	4.50E+37	-7.7	7100.0
197.	C2H2+C2H=i-C4H3	2.60E+44	-9.5	14650.0
198.	C2H2+C2H3=C4H4+H	2.00E+18	-1.7	10600.0
199.	C2H2+C2H3=n-C4H5	9.30E+38	-8.8	12000.0
200.	C2H2+C2H3=i-C4H5	1.60E+46	-11.0	18600.0
201.	C2H4+C2H=C4H4+H	1.20E+13	0.0	0.0
202.	C2H4+C2H3=C4H6+H	2.80E+21	-2.4	14720.0
203.	C2H2+HCCO=C3H3+CO	1.00E+11	0.0	3000.0
204.	C2H4+O2=C2H3+HO2	4.22E+13	0.0	60800.0
205.	C2H3+H2O2=C2H4+HO2	1.21E+10	0.0	-596.0
206.	C2H3+HCO=C2H4+CO	2.50E+13	0.0	0.0
207.	C2H3+CH3=C2H2+CH4	3.92E+11	0.0	0.0
208.	C2H3+C2H3=C4H6	1.50E+42	-8.8	12483.0
209.	C2H3+C2H3=i-C4H5+H	1.20E+22	-2.4	13654.0
210.	C2H3+C2H3=n-C4H5+H	2.40E+20	-2.0	15361.0
211.	C3H2+O=C2H2+CO	6.80E+13	0.0	0.0
212.	C3H2+OH=HCO+C2H2	6.80E+13	0.0	0.0
213.	C3H2+O2=HCCO+CO+H	5.00E+13	0.0	0.0
214.	C3H2+CH=C4H2+H	5.00E+13	0.0	0.0
215.	C3H2+CH2=n-C4H3+H	5.00E+13	0.0	0.0
216.	C3H2+CH3=C4H4+H	5.00E+12	0.0	0.0
217.	C3H2+HCCO=n-C4H3+CO	1.00E+13	0.0	0.0
218.	C3H3+H(+M)=AC3H4(+M)	3.00E+13	0.0	0.0
	Low pressure limit:	0.14000E+32	-0.50000E+01	-0.60000E+04
	TROE centering:	0.50000E+00	0.20000E+04	0.10000E+02 0.10000E+05
	H2	Enhanced by	2.000E+00	
	H2O	Enhanced by	6.000E+00	
	CH4	Enhanced by	2.000E+00	
	CO	Enhanced by	1.500E+00	
	CO2	Enhanced by	2.000E+00	
	C2H6	Enhanced by	3.000E+00	
219.	C3H3+H(+M)=PC3H4(+M)	3.00E+13	0.0	0.0
	Low pressure limit:	0.14000E+32	-0.50000E+01	-0.60000E+04
	TROE centering:	0.50000E+00	0.20000E+04	0.10000E+02 0.10000E+05
	H2	Enhanced by	2.000E+00	
	H2O	Enhanced by	6.000E+00	
	CH4	Enhanced by	2.000E+00	
	CO	Enhanced by	1.500E+00	
	CO2	Enhanced by	2.000E+00	
	C2H6	Enhanced by	3.000E+00	
220.	C3H3+O=CH2O+C2H	2.00E+13	0.0	0.0
221.	C3H3+OH=C3H2+H2O	2.00E+13	0.0	0.0
222.	C3H3+OH=C2H3+HCO	4.00E+13	0.0	0.0
223.	C3H3+O2=CH2CO+HCO	3.00E+10	0.0	2878.0
224.	C3H3+HO2=AC3H4+O2	1.00E+12	0.0	0.0
225.	C3H3+HO2=PC3H4+O2	1.00E+12	0.0	0.0
226.	C3H3+HCO=AC3H4+CO	2.50E+13	0.0	0.0
227.	C3H3+HCO=PC3H4+CO	2.50E+13	0.0	0.0
228.	C3H3+CH=i-C4H3+H	5.00E+13	0.0	0.0
229.	C3H3+CH2=C4H4+H	2.00E+13	0.0	0.0
230.	i-C4H5+H=C3H3+CH3	2.00E+13	0.0	2000.0
231.	C3H3+CH3(+M)=C4H612(+M)	1.50E+13	0.0	0.0
	Low pressure limit:	0.26000E+59	-0.11940E+02	0.97700E+04
	TROE centering:	0.17500E+00	0.13406E+04	0.60000E+05 0.97698E+04
	H2	Enhanced by	2.000E+00	
	H2O	Enhanced by	6.000E+00	
	CH4	Enhanced by	2.000E+00	
	CO	Enhanced by	1.500E+00	
	CO2	Enhanced by	2.000E+00	
	C2H6	Enhanced by	3.000E+00	
232.	C3H3+C3H3=>A1	5.00E+12	0.0	0.0
233.	AC3H4+H=C3H3+H2	5.75E+07	1.9	7530.0

234.	AC3H4+O=CH2CO+CH2	2.00E+07	1.8	1000.0
235.	AC3H4+OH=C3H3+H2O	5.30E+06	2.0	2000.0
236.	AC3H4+C2H=C2H2+C3H3	1.00E+13	0.0	0.0
237.	PC3H4+H=C3H3+H2	1.15E+08	1.9	7530.0
238.	PC3H4+OH=C3H3+H2O	3.54E+06	2.1	870.0
239.	PC3H4+C2H=C2H2+C3H3	1.00E+13	0.0	0.0
240.	C4H+H(+M)=C4H2(+M)	1.00E+17	-1.0	0.0
	Low pressure limit:	0.37500E+34	-0.48000E+01	0.19000E+04
	TROE centering:	0.64640E+00	0.13200E+03	0.13150E+04 0.55660E+04
	H2	Enhanced by	2.000E+00	
	H2O	Enhanced by	6.000E+00	
	CH4	Enhanced by	2.000E+00	
	CO	Enhanced by	1.500E+00	
	CO2	Enhanced by	2.000E+00	
	C2H6	Enhanced by	3.000E+00	
241.	C4H+C2H2=C6H2+H	9.60E+13	0.0	0.0
242.	C4H+O=C2H+C2O	5.00E+13	0.0	0.0
243.	C4H+O2=HCCO+C2O	5.00E+13	0.0	1500.0
244.	C4H+H2=H+C4H2	4.90E+05	2.5	560.0
245.	C4H2+H=n-C4H3	1.10E+42	-8.7	15300.0
246.	C4H2+H=i-C4H3	1.10E+30	-4.9	10800.0
247.	C4H2+O=C3H2+CO	2.70E+13	0.0	1720.0
248.	C4H2+OH=H2C4O+H	6.60E+12	0.0	-410.0
249.	C4H2+OH=C4H+H2O	3.37E+07	2.0	14000.0
250.	C4H2+CH=C5H2+H	5.00E+13	0.0	0.0
251.	C4H2+CH2=C5H3+H	1.30E+13	0.0	6620.0
252.	C4H2+CH2*=C5H3+H	2.00E+13	0.0	0.0
253.	C4H2+C2H=C6H2+H	9.60E+13	0.0	0.0
254.	C4H2+C2H=C6H3	4.50E+37	-7.7	7100.0
255.	H2C4O+H=C2H2+HCCO	5.00E+13	0.0	3000.0
256.	H2C4O+OH=CH2CO+HCCO	1.00E+07	2.0	2000.0
257.	H2C4O+O=CH2CO+C2O	2.00E+07	1.9	200.0
258.	n-C4H3=i-C4H3	4.10E+43	-9.5	53000.0
259.	n-C4H3+H=i-C4H3+H	2.50E+20	-1.7	10800.0
260.	n-C4H3+H=C2H2+C2H2	6.30E+25	-3.3	10014.0
261.	i-C4H3+H=C2H2+C2H2	2.80E+23	-2.5	10780.0
262.	n-C4H3+H=C4H4	2.00E+47	-10.3	13070.0
263.	i-C4H3+H=C4H4	3.40E+43	-9.0	12120.0
264.	n-C4H3+H=C4H2+H2	1.50E+13	0.0	0.0
265.	i-C4H3+H=C4H2+H2	3.00E+13	0.0	0.0
266.	n-C4H3+OH=C4H2+H2O	2.50E+12	0.0	0.0
267.	i-C4H3+OH=C4H2+H2O	5.00E+12	0.0	0.0
268.	i-C4H3+O2=HCCO+CH2CO	7.86E+16	-1.8	0.0
269.	n-C4H3+C2H2=1-C6H4+H	2.50E+14	-0.6	10600.0
270.	n-C4H3+C2H2=n-C6H5	2.70E+36	-7.6	16200.0
271.	n-C4H3+C2H2=A1-	9.60E+70	-17.8	31300.0
272.	n-C4H3+C2H2=c-C6H4+H	6.90E+46	-10.0	30100.0
273.	C4H4+H=n-C4H5	1.30E+51	-11.9	16500.0
274.	C4H4+H=i-C4H5	4.90E+51	-11.9	17700.0
275.	C4H4+H=n-C4H3+H2	6.65E+05	2.5	12240.0
276.	C4H4+H=i-C4H3+H2	3.33E+05	2.5	9240.0
277.	C4H4+OH=n-C4H3+H2O	3.10E+06	2.0	3430.0
278.	C4H4+OH=i-C4H3+H2O	1.55E+06	2.0	430.0
279.	C4H4+O=PC3H4+CO	3.00E+13	0.0	1808.0
280.	C4H4+C2H3=1-C6H6+H	2.80E+21	-2.4	14720.0
281.	n-C4H5=i-C4H5	1.50E+67	-16.9	59100.0
282.	n-C4H5+H=i-C4H5+H	3.10E+26	-3.4	17423.0
283.	C4H6=i-C4H5+H	5.70E+36	-6.3	112353.0
284.	C4H6=n-C4H5+H	5.30E+44	-8.6	123608.0
285.	n-C4H5+H=C4H4+H2	1.50E+13	0.0	0.0
286.	i-C4H5+H=C4H4+H2	3.00E+13	0.0	0.0
287.	n-C4H5+OH=C4H4+H2O	2.50E+12	0.0	0.0
288.	i-C4H5+OH=C4H4+H2O	5.00E+12	0.0	0.0
289.	n-C4H5+O2=>C2H4+CO+HCO	4.16E+10	0.0	2500.0
290.	i-C4H5+O2=CH2CO+C2H3O	7.86E+16	-1.8	0.0
291.	n-C4H5+C2H2=n-C6H7	1.10E+14	-1.3	2900.0
292.	n-C4H5+C2H2=c-C6H7	5.00E+24	-5.5	4600.0
293.	n-C4H5+C2H2=1-C6H6+H	5.80E+08	1.0	10900.0
294.	n-C4H5+C2H2=A1+H	1.60E+16	-1.3	5400.0
295.	C4H6+H=n-C4H5+H2	1.33E+06	2.5	12240.0
296.	C4H6+H=i-C4H5+H2	6.65E+05	2.5	9240.0
297.	C4H6+OH=n-C4H5+H2O	6.20E+06	2.0	3430.0
298.	C4H6+OH=i-C4H5+H2O	3.10E+06	2.0	430.0
299.	C4H6+C2H3=C6H8+H	2.80E+21	-2.4	14720.0
300.	C4H612+H=C4H6+H	2.00E+13	0.0	4000.0
301.	C4H612+H=i-C4H5+H2	1.70E+05	2.5	2490.0
302.	C4H612+H=AC3H4+CH3	8.00E+13	0.0	1000.0

303.	C4H612+O=CH2CO+C2H4	1.20E+08	1.6	327.0
304.	C4H612+O=i-C4H5+OH	1.80E+11	0.7	5880.0
305.	C4H612+OH=i-C4H5+H2O	3.10E+06	2.0	-298.0
306.	C5H2+OH=>C4H2+H+CO	2.00E+13	0.0	0.0
307.	C5H2+CH=C6H2+H	5.00E+13	0.0	0.0
308.	C5H2+O2=H2C4O+CO	1.00E+12	0.0	0.0
309.	C5H3+OH=C5H2+H2O	1.00E+13	0.0	0.0
310.	C5H3+CH=C6H2+H+H	5.00E+13	0.0	0.0
311.	C5H3+CH2=1-C6H4+H	5.00E+13	0.0	0.0
312.	C5H3+O2=H2C4O+HCO	1.00E+12	0.0	0.0
313.	C6H+H(+M)=C6H2(+M)	1.00E+17	-1.0	0.0
	Low pressure limit:	0.37500E+34	-0.48000E+01	0.19000E+04
	TROE centering:	0.64640E+00	0.13200E+03	0.13150E+04 0.55660E+04
	H2	Enhanced by	2.000E+00	
	H2O	Enhanced by	6.000E+00	
	CH4	Enhanced by	2.000E+00	
	CO	Enhanced by	1.500E+00	
	CO2	Enhanced by	2.000E+00	
	C2H6	Enhanced by	3.000E+00	
314.	C6H2+H=C6H3	1.10E+30	-4.9	10800.0
315.	C6H+O=C4H+C2O	5.00E+13	0.0	0.0
316.	C6H+H2=H+C6H2	4.90E+05	2.5	560.0
317.	C6H2+O=C5H2+CO	2.70E+13	0.0	1720.0
318.	C6H2+OH=>C2H+C2H2+C2O	6.60E+12	0.0	-410.0
319.	C6H2+OH=C6H+H2O	3.37E+07	2.0	14000.0
320.	C6H3+H=C4H2+C2H2	2.80E+23	-2.5	10780.0
321.	C6H3+H=1-C6H4	3.40E+43	-9.0	12120.0
322.	C6H3+H=C6H2+H2	3.00E+13	0.0	0.0
323.	C6H3+OH=C6H2+H2O	5.00E+12	0.0	0.0
324.	C6H3+O2=>CO+C3H2+HCCO	5.00E+11	0.0	0.0
325.	1-C6H4+H=n-C6H5	5.90E+39	-8.2	15600.0
326.	1-C6H4+H=A1-	1.70E+78	-19.7	31400.0
327.	1-C6H4+H=c-C6H4+H	1.40E+54	-11.7	34500.0
328.	1-C6H4+H=C6H3+H2	6.65E+06	2.5	9240.0
329.	1-C6H4+OH=C6H3+H2O	3.10E+06	2.0	430.0
330.	c-C6H4+H=A1-	2.40E+60	-13.7	29500.0
331.	n-C6H5=A1-	5.10E+54	-13.1	35700.0
332.	n-C6H5=c-C6H4+H	1.30E+59	-13.6	62000.0
333.	n-C6H5+H=i-C6H5+H	2.50E+20	-1.7	10800.0
334.	n-C6H5+H=C4H4+C2H2	6.30E+25	-3.3	10014.0
335.	i-C6H5+H=C4H4+C2H2	2.80E+23	-2.5	10780.0
336.	n-C6H5+H=1-C6H6	2.00E+47	-10.3	13070.0
337.	i-C6H5+H=1-C6H6	3.40E+43	-9.0	12120.0
338.	n-C6H5+H=1-C6H4+H2	1.50E+13	0.0	0.0
339.	i-C6H5+H=1-C6H4+H2	3.00E+13	0.0	0.0
340.	n-C6H5+OH=1-C6H4+H2O	2.50E+12	0.0	0.0
341.	i-C6H5+OH=1-C6H4+H2O	5.00E+12	0.0	0.0
342.	n-C6H5+O2=>C4H4+CO+HCO	4.16E+10	0.0	2500.0
343.	i-C6H5+O2=>CH2CO+CH2CO+C2H	7.86E+16	-1.8	0.0
344.	1-C6H6+H=n-C6H7	1.50E+16	-1.7	1600.0
345.	1-C6H6+H=c-C6H7	4.70E+27	-6.1	3800.0
346.	1-C6H6+H=A1+H	4.40E+18	-1.7	4500.0
347.	1-C6H6+H=n-C6H5+H2	6.65E+05	2.5	12240.0
348.	1-C6H6+H=i-C6H5+H2	3.33E+05	2.5	9240.0
349.	1-C6H6+OH=n-C6H5+H2O	6.20E+06	2.0	3430.0
350.	1-C6H6+OH=i-C6H5+H2O	3.10E+06	2.0	430.0
351.	n-C6H7=c-C6H7	1.20E+31	-8.0	8900.0
352.	n-C6H7=A1+H	3.20E+26	-5.0	15500.0
353.	n-C6H7+H=i-C6H7+H	2.40E+49	-10.7	15100.0
354.	i-C6H7+H=C6H8	1.80E+39	-7.6	11000.0
355.	n-C6H7+H=C6H8	5.60E+48	-10.5	14700.0
356.	n-C6H7+H=1-C6H6+H2	1.50E+13	0.0	0.0
357.	i-C6H7+H=1-C6H6+H2	3.00E+13	0.0	0.0
358.	n-C6H7+OH=1-C6H6+H2O	2.50E+12	0.0	0.0
359.	i-C6H7+OH=1-C6H6+H2O	5.00E+12	0.0	0.0
360.	n-C6H7+O2=>C4H6+CO+HCO	4.16E+10	0.0	2500.0
361.	i-C6H7+O2=>CH2CO+CH2CO+C2H3	7.86E+16	-1.8	0.0
362.	C6H8+H=n-C6H7+H2	1.33E+06	2.5	12240.0
363.	C6H8+H=i-C6H7+H2	6.65E+05	2.5	9240.0
364.	C6H8+OH=n-C6H7+H2O	6.20E+06	2.0	3430.0
365.	C6H8+OH=i-C6H7+H2O	3.10E+06	2.0	430.0
366.	A1+H=c-C6H7	1.40E+51	-11.9	16100.0
367.	A1+H=A1-+H2	2.50E+14	0.0	16000.0
368.	A1+OH=A1-+H2O	1.60E+08	1.4	1450.0
369.	A1-+H(+M)=A1(+M)	1.00E+14	0.0	0.0
	Low pressure limit:	0.66000E+76	-0.16300E+02	0.70000E+04
	TROE centering:	0.10000E+01	0.10000E+00	0.58490E+03 0.61130E+04

	H2	Enhanced by	2.000E+00			
	H2O	Enhanced by	6.000E+00			
	CH4	Enhanced by	2.000E+00			
	CO	Enhanced by	1.500E+00			
	CO2	Enhanced by	2.000E+00			
	C2H6	Enhanced by	3.000E+00			
370.	n-C4H3+C4H2=A1C2H-			9.60E+70	-17.8	31300.0
371.	A1+C2H=A1C2H+H			5.00E+13	0.0	0.0
372.	A1-+C2H2=n-A1C2H2			7.00E+38	-8.0	16400.0
373.	A1-+C2H2=A1C2H+H			3.30E+33	-5.7	25500.0
374.	A1C2H+H=n-A1C2H2			3.00E+43	-9.2	15272.0
375.	A1C2H+H=i-A1C2H2			3.00E+43	-9.2	15272.0
376.	A1C2H+H=A1C2H*+H2			2.50E+14	0.0	16000.0
377.	A1C2H+H=A1C2H-+H2			2.50E+14	0.0	16000.0
378.	A1C2H+OH=A1C2H*+H2O			1.60E+08	1.4	1450.0
379.	A1C2H+OH=A1C2H-+H2O			1.60E+08	1.4	1450.0
380.	A1C2H-+H(+M)=A1C2H(+M)			1.00E+14	0.0	0.0
	Low pressure limit:	0.66000E+76	-0.16300E+02	0.70000E+04		
	TROE centering:	0.10000E+01	0.10000E+00	0.58490E+03	0.61130E+04	
	H2	Enhanced by	2.000E+00			
	H2O	Enhanced by	6.000E+00			
	CH4	Enhanced by	2.000E+00			
	CO	Enhanced by	1.500E+00			
	CO2	Enhanced by	2.000E+00			
	C2H6	Enhanced by	3.000E+00			
381.	A1C2H*+H(+M)=A1C2H(+M)			1.00E+14	0.0	0.0
	Low pressure limit:	0.66000E+76	-0.16300E+02	0.70000E+04		
	TROE centering:	0.10000E+01	0.10000E+00	0.58490E+03	0.61130E+04	
	H2	Enhanced by	2.000E+00			
	H2O	Enhanced by	6.000E+00			
	CH4	Enhanced by	2.000E+00			
	CO	Enhanced by	1.500E+00			
	CO2	Enhanced by	2.000E+00			
	C2H6	Enhanced by	3.000E+00			
382.	A1+C2H3=A1C2H3+H			7.90E+11	0.0	6400.0
383.	A1-+C2H4=A1C2H3+H			2.51E+12	0.0	6190.0
384.	A1-+C2H3=A1C2H3			1.20E+27	-4.2	7235.0
385.	A1-+C2H3=i-A1C2H2+H			8.50E-02	4.7	18424.0
386.	A1-+C2H3=n-A1C2H2+H			9.40E+00	4.1	23234.0
387.	A1C2H3=i-A1C2H2+H			5.30E+27	-3.6	109332.0
388.	A1C2H3=n-A1C2H2+H			1.10E+32	-4.8	119483.0
389.	A1C2H3+H=A1C2H3*+H2			2.50E+14	0.0	16000.0
390.	A1C2H3+OH=A1C2H3*+H2O			1.60E+08	1.4	1450.0
391.	A1C2H3*+H(+M)=A1C2H3(+M)			1.00E+14	0.0	0.0
	Low pressure limit:	0.66000E+76	-0.16300E+02	0.70000E+04		
	TROE centering:	0.10000E+01	0.10000E+00	0.58490E+03	0.61130E+04	
	H2	Enhanced by	2.000E+00			
	H2O	Enhanced by	6.000E+00			
	CH4	Enhanced by	2.000E+00			
	CO	Enhanced by	1.500E+00			
	CO2	Enhanced by	2.000E+00			
	C2H6	Enhanced by	3.000E+00			
392.	A1C2H3+H=n-A1C2H2+H2			6.65E+06	2.5	12240.0
393.	A1C2H3+H=i-A1C2H2+H2			3.33E+05	2.5	9240.0
394.	A1C2H3+OH=n-A1C2H2+H2O			3.10E+06	2.0	3430.0
395.	A1C2H3+OH=i-A1C2H2+H2O			1.55E+06	2.0	430.0
396.	n-A1C2H2+H=A1C2H+H2			1.50E+13	0.0	0.0
397.	i-A1C2H2+H=A1C2H+H2			3.00E+13	0.0	0.0
398.	n-A1C2H2+H=i-A1C2H2+H			9.90E+04	3.4	22040.0
399.	n-A1C2H2+OH=A1C2H+H2O			2.50E+12	0.0	0.0
400.	i-A1C2H2+OH=A1C2H+H2O			5.00E+12	0.0	0.0
401.	A1C2H*+C2H2=A2-1			2.20E+62	-14.6	33100.0
402.	A1C2H*+C2H2=A1C2H)2+H			1.80E+19	-1.7	18800.0
403.	A1C2H*+C2H2=naphthyne+H			5.70E+64	-14.4	57000.0
404.	A1C2H)2+H=A2-1			1.40E+64	-14.6	29900.0
405.	A1C2H)2+H=naphthyne+H			1.90E+73	-16.3	60900.0
406.	naphthyne+H=A2-1			4.90E+52	-12.4	33000.0
407.	A1C2H+C2H=A1C2H)2+H			5.00E+13	0.0	0.0
408.	A1C2H3*+C2H2=A2+H			1.60E+16	-1.3	6600.0
409.	n-A1C2H2+C2H2=A2+H			1.60E+16	-1.3	5400.0
410.	A2+H=A2-1+H2			2.50E+14	0.0	16000.0
411.	A2+H=A2-2+H2			2.50E+14	0.0	16000.0
412.	A2+OH=A2-1+H2O			1.60E+08	1.4	1450.0
413.	A2+OH=A2-2+H2O			1.60E+08	1.4	1450.0
414.	A2-1+H(+M)=A2(+M)			1.00E+14	0.0	0.0
	Low pressure limit:	0.38000+128	-0.31434E+02	0.18676E+05		
	TROE centering:	0.20000E+00	0.12280E+03	0.47840E+03	0.54119E+04	

	H2	Enhanced by	2.000E+00			
	H2O	Enhanced by	6.000E+00			
	CH4	Enhanced by	2.000E+00			
	CO	Enhanced by	1.500E+00			
	CO2	Enhanced by	2.000E+00			
	C2H6	Enhanced by	3.000E+00			
415.	A2-2+H(+M)=A2(+M)			1.00E+14	0.0	0.0
	Low pressure limit:	0.95000+130	-0.32132E+02	0.18782E+05		
	TROE centering:	0.87000E+00	0.49270E+03	0.11790E+03	0.56520E+04	
	H2	Enhanced by	2.000E+00			
	H2O	Enhanced by	6.000E+00			
	CH4	Enhanced by	2.000E+00			
	CO	Enhanced by	1.500E+00			
	CO2	Enhanced by	2.000E+00			
	C2H6	Enhanced by	3.000E+00			
416.	A2-1+H=A2-2+H			2.40E+24	-1.8	45281.0
417.	A2+C2H=A2C2HA+H			5.00E+13	0.0	0.0
418.	A2+C2H=A2C2HB+H			5.00E+13	0.0	0.0
419.	A2-1+C2H2=A2C2H2			1.70E+43	-9.1	21100.0
420.	A2-1+C2H2=A2C2HA+H			1.30E+24	-3.1	22600.0
421.	A2C2HA+H=A2C2H2			5.90E+46	-10.0	19100.0
422.	A2C2H2+H=A2C2HA+H2			1.50E+13	0.0	0.0
423.	A2C2H2+OH=A2C2HA+H2O			2.50E+12	0.0	0.0
424.	A2C2HA+H=A2C2HA*+H2			2.50E+14	0.0	16000.0
425.	A2C2HB+H=A2C2HB*+H2			2.50E+14	0.0	16000.0
426.	A2C2HA+OH=A2C2HA*+H2O			1.60E+08	1.4	1450.0
427.	A2C2HB+OH=A2C2HB*+H2O			1.60E+08	1.4	1450.0
428.	A2C2HB*+H(+M)=A2C2HB(+M)			1.00E+14	0.0	0.0
	Low pressure limit:	0.38000+128	-0.31434E+02	0.18676E+05		
	TROE centering:	0.20000E+00	0.12280E+03	0.47840E+03	0.54119E+04	
	H2	Enhanced by	2.000E+00			
	H2O	Enhanced by	6.000E+00			
	CH4	Enhanced by	2.000E+00			
	CO	Enhanced by	1.500E+00			
	CO2	Enhanced by	2.000E+00			
	C2H6	Enhanced by	3.000E+00			
429.	A2C2HA*+H(+M)=A2C2HA(+M)			1.00E+14	0.0	0.0
	Low pressure limit:	0.95000+130	-0.32132E+02	0.18782E+05		
	TROE centering:	0.87000E+00	0.49270E+03	0.11790E+03	0.56520E+04	
	H2	Enhanced by	2.000E+00			
	H2O	Enhanced by	6.000E+00			
	CH4	Enhanced by	2.000E+00			
	CO	Enhanced by	1.500E+00			
	CO2	Enhanced by	2.000E+00			
	C2H6	Enhanced by	3.000E+00			
430.	A2C2HB*+C2H2=A3-1			1.10E+62	-14.6	33100.0
431.	A2C2HB*+C2H2=A2C2H)2+H			1.80E+19	-1.7	18800.0
432.	A2C2H)2+H=A3-1			6.90E+63	-14.6	29900.0
433.	A2C2HA*+C2H2=A3-4			1.10E+62	-14.6	33100.0
434.	A2C2HA*+C2H2=A2C2H)2+H			1.80E+19	-1.7	18800.0
435.	A2C2H)2+H=A3-4			6.90E+63	-14.6	29900.0
436.	A2C2HA+C2H=A2C2H)2+H			5.00E+13	0.0	0.0
437.	A2C2HB+C2H=A2C2H)2+H			5.00E+13	0.0	0.0
438.	A3+H=A3-1+H2			2.50E+14	0.0	16000.0
439.	A3+H=A3-4+H2			2.50E+14	0.0	16000.0
440.	A3+OH=A3-1+H2O			1.60E+08	1.4	1450.0
441.	A3+OH=A3-4+H2O			1.60E+08	1.4	1450.0
442.	A3-1+H(+M)=A3(+M)			1.00E+14	0.0	0.0
	Low pressure limit:	0.40000+149	-0.37505E+02	0.20551E+05		
	TROE centering:	0.10000E+01	0.53630E+03	0.14490E+03	0.56328E+04	
	H2	Enhanced by	2.000E+00			
	H2O	Enhanced by	6.000E+00			
	CH4	Enhanced by	2.000E+00			
	CO	Enhanced by	1.500E+00			
	CO2	Enhanced by	2.000E+00			
	C2H6	Enhanced by	3.000E+00			
443.	A3-4+H(+M)=A3(+M)			1.00E+14	0.0	0.0
	Low pressure limit:	0.21000+140	-0.34803E+02	0.18378E+05		
	TROE centering:	0.10000E-02	0.17140E+03	0.17140E+03	0.49928E+04	
	H2	Enhanced by	2.000E+00			
	H2O	Enhanced by	6.000E+00			
	CH4	Enhanced by	2.000E+00			
	CO	Enhanced by	1.500E+00			
	CO2	Enhanced by	2.000E+00			
	C2H6	Enhanced by	3.000E+00			
444.	A3-1+H=A3-4+H			3.80E+40	-6.3	61782.0
445.	A1-+C4H4=A2+H			3.30E+33	-5.7	25500.0

446.	A2-1+C4H4=A3+H		3.30E+33	-5.7	25500.0
447.	A2-2+C4H4=A3+H		3.30E+33	-5.7	25500.0
448.	A2R5+H=A2R5-+H2		2.50E+14	0.0	16000.0
449.	A2R5+OH=A2R5-+H2O		1.60E+08	1.4	1450.0
450.	A2R5-+H (+M)=A2R5 (+M)		1.00E+14	0.0	0.0
	Low pressure limit:	0.66000E+76	-0.16300E+02	0.70000E+04	
	TROE centering:	0.10000E+01	0.10000E+00	0.58490E+03	0.61130E+04
	H2	Enhanced by	2.000E+00		
	H2O	Enhanced by	6.000E+00		
	CH4	Enhanced by	2.000E+00		
	CO	Enhanced by	1.500E+00		
	CO2	Enhanced by	2.000E+00		
	C2H6	Enhanced by	3.000E+00		
451.	A2-1+C2H2=A2R5+H		9.70E+30	-5.3	21600.0
452.	A2C2HA+H=A2R5+H		4.60E+37	-7.0	23100.0
453.	A2C2H2=A2R5+H		1.56E+46	-10.3	41300.0
454.	A1C2H*+A1=A3+H		1.10E+23	-2.9	15890.0
455.	A1-+A1C2H=A3+H		1.10E+23	-2.9	15890.0
456.	A3+C2H=A3C2H+H		5.00E+13	0.0	0.0
457.	A3-4+C2H2=A3C2H2		8.00E+61	-14.5	34800.0
458.	A3-4+C2H2=A3C2H+H		1.20E+26	-3.4	30200.0
459.	A3-4+C2H2=A4+H		6.60E+24	-3.4	17800.0
460.	A3C2H+H=A3C2H2		1.90E+64	-15.1	29300.0
461.	A3C2H+H=A4+H		9.00E+38	-7.4	20700.0
462.	A3C2H2=A4+H		2.00E+63	-15.3	43200.0
463.	A4+H=A4-+H2		2.50E+14	0.0	16000.0
464.	A4+OH=A4-+H2O		1.60E+08	1.4	1450.0
465.	A4-+H=A4		1.00E+14	0.0	0.0
466.	A1+A1-==P2+H		1.10E+23	-2.9	15890.0
467.	A1+A1-==P2-H		3.70E+32	-6.7	9870.0
468.	P2-H=P2+H		3.80E+37	-8.0	27880.0
469.	A1-+A1-==P2		2.00E+19	-2.0	2900.0
470.	A1-+A1-==P2-+H		2.30E-01	4.6	28950.0
471.	P2=P2-+H		1.10E+25	-2.7	114270.0
472.	P2+H=P2-+H2		2.50E+14	0.0	16000.0
473.	P2+OH=P2-+H2O		1.60E+08	1.4	1450.0
474.	P2-+C2H2=A3+H		4.60E+06	2.0	7300.0
475.	A1+O=C6H5O+H		2.20E+13	0.0	4530.0
476.	A1+OH=C6H5OH+H		1.30E+13	0.0	10600.0
477.	A1-+O2=C6H5O+O		2.10E+12	0.0	7470.0
478.	C6H5O=CO+C5H5		2.50E+11	0.0	43900.0
479.	C6H5O+H=CO+C5H6		3.00E+13	0.0	0.0
480.	C6H5O+O=HCO+2C2H2+CO		3.00E+13	0.0	0.0
481.	C6H5O+H (+M)=C6H5OH (+M)		2.50E+14	0.0	0.0
	Low pressure limit:	0.10000E+95	-0.21840E+02	0.13880E+05	
	TROE centering:	0.43000E-01	0.30420E+03	0.60000E+05	0.58964E+04
	H2	Enhanced by	2.000E+00		
	H2O	Enhanced by	6.000E+00		
	CH4	Enhanced by	2.000E+00		
	CO	Enhanced by	1.500E+00		
	CO2	Enhanced by	2.000E+00		
	C2H6	Enhanced by	3.000E+00		
482.	C6H5OH+H=C6H5O+H2		1.15E+14	0.0	12400.0
483.	C6H5OH+O=C6H5O+OH		2.80E+13	0.0	7352.0
484.	C6H5OH+OH=C6H5O+H2O		6.00E+12	0.0	0.0
485.	C5H5+H (+M)=C5H6 (+M)		1.00E+14	0.0	0.0
	Low pressure limit:	0.44000E+81	-0.18280E+02	0.12994E+05	
	TROE centering:	0.68000E-01	0.40070E+03	0.41358E+04	0.55019E+04
	H2	Enhanced by	2.000E+00		
	H2O	Enhanced by	6.000E+00		
	CH4	Enhanced by	2.000E+00		
	CO	Enhanced by	1.500E+00		
	CO2	Enhanced by	2.000E+00		
	C2H6	Enhanced by	3.000E+00		
486.	C5H5+O=n-C4H5+CO		1.00E+14	0.0	0.0
487.	C5H5+OH=C5H4OH+H		5.00E+12	0.0	0.0
488.	C5H5+HO2=C5H5O+OH		3.00E+13	0.0	0.0
489.	C5H6+H=C5H5+H2		2.20E+08	1.8	3000.0
490.	C5H6+O=C5H5+OH		1.80E+13	0.0	3080.0
491.	C5H6+OH=C5H5+H2O		3.43E+09	1.2	-447.0
492.	C5H5O=n-C4H5+CO		2.50E+11	0.0	43900.0
493.	C5H5O+H=CH2O+2C2H2		3.00E+13	0.0	0.0
494.	C5H5O+O=CO2+n-C4H5		3.00E+13	0.0	0.0
495.	C5H4OH=C5H4O+H		2.10E+13	0.0	48000.0
496.	C5H4OH+H=CH2O+2C2H2		3.00E+13	0.0	0.0
497.	C5H4OH+O=CO2+n-C4H5		3.00E+13	0.0	0.0
498.	C5H4O=CO+C2H2+C2H2		1.00E+15	0.0	78000.0

499.	C5H4O+O=CO2+2C2H2	3.00E+13	0.0	0.0
500.	A1C2H+OH=>A1-+CH2CO	2.18E-04	4.5	-1000.0
501.	A1C2H)2+OH=>A1C2H-+CH2CO	2.18E-04	4.5	-1000.0
502.	A2C2HA+OH=>A2-1+CH2CO	2.18E-04	4.5	-1000.0
503.	A2C2HB+OH=>A2-2+CH2CO	2.18E-04	4.5	-1000.0
504.	A3C2H+OH=>A3-4+CH2CO	2.18E-04	4.5	-1000.0
505.	A1C2H+OH=>C6H5O+C2H2	1.30E+13	0.0	10600.0
506.	A1C2H3+OH=>C6H5O+C2H4	1.30E+13	0.0	10600.0
507.	A1C2H)2+OH=>C4H2+C6H5O	1.30E+13	0.0	10600.0
508.	A2+OH=>A1C2H+CH2CO+H	1.30E+13	0.0	10600.0
509.	A2C2HA+OH=>A1C2H+H2C4O+H	1.30E+13	0.0	10600.0
510.	A2C2HB+OH=>A1C2H+H2C4O+H	1.30E+13	0.0	10600.0
511.	A3+OH=>A2C2HB+CH2CO+H	6.50E+12	0.0	10600.0
512.	A3+OH=>A2C2HA+CH2CO+H	6.50E+12	0.0	10600.0
513.	A3C2H+OH=>A2C2HA+H2C4O+H	6.50E+12	0.0	10600.0
514.	A3C2H+OH=>A2C2HB+H2C4O+H	6.50E+12	0.0	10600.0
515.	A4+OH=>A3-4+CH2CO	1.30E+13	0.0	10600.0
516.	A1C2H+O=>HCCO+A1-	2.04E+07	2.0	1900.0
517.	A1C2H)2+O=>HCCO+A1C2H-	2.04E+07	2.0	1900.0
518.	A1C2H3+O=>A1-+CH3+CO	1.92E+07	1.8	220.0
519.	A2C2HA+O=>HCCO+A2-1	2.04E+07	2.0	1900.0
520.	A2C2HB+O=>HCCO+A2-2	2.04E+07	2.0	1900.0
521.	A1C2H+O=>C2H+C6H5O	2.20E+13	0.0	4530.0
522.	A1C2H3+O=>C2H3+C6H5O	2.20E+13	0.0	4530.0
523.	A1C2H)2+O=>C6H5O+C4H	2.20E+13	0.0	4530.0
524.	A2+O=>CH2CO+A1C2H	2.20E+13	0.0	4530.0
525.	A2C2HA+O=>A1C2H)2+CH2CO	2.20E+13	0.0	4530.0
526.	A2C2HB+O=>A1C2H)2+CH2CO	2.20E+13	0.0	4530.0
527.	A3+O=>A2C2HA+CH2CO	1.10E+13	0.0	4530.0
528.	A3+O=>A2C2HB+CH2CO	1.10E+13	0.0	4530.0
529.	A3C2H+O=>A2C2HA+H2C4O	1.10E+13	0.0	4530.0
530.	A3C2H+O=>A2C2HB+H2C4O	1.10E+13	0.0	4530.0
531.	A4+O=>A3-4+HCCO	2.20E+13	0.0	4530.0
532.	A1C2H*+O2=>1-C6H4+CO+HCO	2.10E+12	0.0	7470.0
533.	A1C2H-+O2=>1-C6H4+CO+HCO	2.10E+12	0.0	7470.0
534.	A1C2H3*+O2=>1-C6H6+CO+HCO	2.10E+12	0.0	7470.0
535.	n-A1C2H2+O2=>A1-+CO+CH2O	1.00E+11	0.0	0.0
536.	A2-1+O2=>A1C2H+HCO+CO	2.10E+12	0.0	7470.0
537.	A2-2+O2=>A1C2H+HCO+CO	2.10E+12	0.0	7470.0
538.	A2C2HA*+O2=>A2-1+CO+CO	2.10E+12	0.0	7470.0
539.	A2C2HB*+O2=>A2-2+CO+CO	2.10E+12	0.0	7470.0
540.	A3-4+O2=>A2C2HB+HCO+CO	2.10E+12	0.0	7470.0
541.	A3-1+O2=>A2C2HA+HCO+CO	2.10E+12	0.0	7470.0
542.	A4-+O2=>A3-4+CO+CO	2.10E+12	0.0	7470.0
543.	CH3NH2+M=CH3+NH2+M	3.16E+15	0.0	85800.0
544.	CH3NH2+OH=CH2NH2+H2O	3.68E+12	0.0	-500.0
545.	CH3NH2+H=CH2NH2+H2	1.08E+13	0.0	5300.0
546.	CH3NH2+O=CH2NH2+OH	3.26E+12	0.0	1700.0
547.	CH3NH2+OH=CH3NH+H2O	2.46E+12	0.0	-500.0
548.	CH3NH2+H=CH3NH+H2	7.20E+12	0.0	5300.0
549.	CH3NH2+O=CH3NH+OH	2.17E+12	0.0	1700.0
550.	CH3NH2+M=CH2NH2+H+M	2.00E+17	0.0	88400.0
551.	CH3NH2+CH3=CH2NH2+CH4	1.00E+11	0.0	8700.0
552.	CH3NH2+NH2=CH2NH2+NH3	1.30E+14	0.0	20100.0
553.	CH3NH2+CH3=CH3NH+CH4	3.55E+09	0.0	5700.0
554.	CH3NH2+O2=CH3NH+HO2	8.00E+12	0.0	39000.0
555.	CH3NH2+H=CH3+NH3	3.90E+14	0.0	11500.0
556.	CH2NH2+OH=H2CNH+H2O	1.00E+08	2.0	0.0
557.	CH2NH2+H=H2CNH+H2	1.00E+08	2.0	0.0
558.	CH2NH2+O=H2CNH+OH	1.00E+08	2.0	0.0
559.	CH2NH2+O2=H2CNH+HO2	1.00E+07	2.0	9200.0
560.	CH2NH2+HO2=CH3NH2+O2	1.00E+07	2.0	1200.0
561.	CH2NH2+H2O2=CH3NH2+HO2	1.00E+07	2.0	10500.0
562.	CH2NH2+O=CH3O+NH	6.00E+13	0.0	0.0
563.	CH2NH2+OH=CH4+HNO	6.00E+12	0.0	0.0
564.	CH2NH2+H=CH3+NH2	6.00E+13	0.0	0.0
565.	CH2NH2+O2=CH3O+HNO	6.00E+12	0.0	4000.0
566.	CH3NH+OH=H2CNH+H2O	1.00E+08	2.0	0.0
567.	CH3NH+H=H2CNH+H2	1.00E+08	2.0	0.0
568.	CH3NH+O=H2CNH+OH	1.00E+08	2.0	0.0
569.	CH3NH+O2=H2CNH+HO2	1.00E+07	2.0	6300.0
570.	CH3NH+H2O2=CH3NH2+HO2	1.00E+07	2.0	7600.0
571.	CH3NH+O=CH3O+NH	6.00E+13	0.0	0.0
572.	CH3NH+OH=CH4+HNO	6.00E+12	0.0	0.0
573.	CH3NH+H=CH3+NH2	6.00E+13	0.0	0.0
574.	CH3NH+O2=CH3O+HNO	6.00E+12	0.0	4000.0
575.	H2CNH+O=CH2O+NH	1.00E+07	2.0	2800.0

576.	H2CNH+O=H2CNO+H	1.00E+07	2.0	6500.0
577.	H2CNH+OH=CH2O+NH2	1.80E+05	2.0	14800.0
578.	H2CNH+O2=HCNH+HO2	3.16E+08	2.0	4800.0
579.	CH3+NH2=H2CNH+H2	6.00E+12	0.0	16500.0
580.	H2CNH+H=H2CN+H2	3.16E+08	2.0	8600.0
581.	H2CNH+O=H2CN+OH	3.16E+08	2.0	6100.0
582.	H2CNH+NH=H2CN+NH2	1.00E+07	2.0	3700.0
583.	H2CN+HO2=H2CNH+O2	7.87E+04	2.0	21700.0
584.	H2CNH+OH=HCNH+H2O	1.00E+07	2.0	5800.0
585.	H2CNH+H=HCNH+H2	4.76E+34	-4.7	38800.0
586.	H2CNH+O=HCNH+OH	3.16E+08	2.0	10000.0
587.	H2CNH+OH=H2CN+H2O	1.00E+07	2.0	4000.0
588.	H2CN=HCN+H	1.59E+13	0.0	56300.0
589.	H2CN+O=HCN+OH	1.00E+07	2.0	6100.0
590.	H2CN+OH=HCN+H2O	1.00E+07	2.0	3700.0
591.	H2CN+H=HCN+H2	3.16E+08	2.0	8600.0
592.	H2CN+O2=HCN+HO2	2.67E+04	2.0	17300.0
593.	H2CN+CH3=HCN+CH4	1.00E+07	2.0	10000.0
594.	H2CN+NO=HCN+HNO	1.00E+07	2.0	4400.0
595.	HCNH=HCN+H	1.59E+13	0.0	71000.0
596.	HCNH+O2=HCN+HO2	3.16E+08	2.0	4800.0
597.	HCNH+OH=HCN+H2O	1.00E+08	2.0	0.0
598.	HCNH+H=HCN+H2	1.00E+08	2.0	0.0
599.	HCNH+O=HCN+OH	1.00E+08	2.0	0.0
600.	CH3NHNHCH3=2CH3NH	3.16E+15	0.0	68400.0
601.	H2CNCNCH2=H2CN+H2CN	3.16E+15	0.0	-400.0
602.	CH+N2=HCN+N	3.00E+11	0.0	13600.0
603.	CN+N=C+N2	1.04E+15	-0.5	0.0
604.	CH2+N2=HCN+NH	1.00E+13	0.0	74000.0
605.	H2CN+N=N2+CH2	2.00E+13	0.0	0.0
606.	H2CN+M=HCN+H+M	3.00E+14	0.0	22000.0
607.	C+NO=CN+O	1.10E+14	0.0	0.0
608.	CH+NO=HCN+O	1.10E+14	0.0	0.0
609.	CH2+NO=HCNO+H	1.39E+12	0.0	-1100.0
610.	CH3+NO=HCN+H2O	1.00E+11	0.0	15000.0
611.	CH3+NO=H2CN+OH	1.00E+11	0.0	15000.0
612.	HCCO+NO=HCNO+CO	2.00E+13	0.0	0.0
613.	CH2+NO=HCN+OH	2.00E+13	0.0	0.0
614.	HCNO+H=HCN+OH	1.00E+14	0.0	12000.0
615.	CH2+N=HCN+H	5.00E+13	0.0	0.0
616.	CH+N=CN+H	1.30E+13	0.0	0.0
617.	CO2+N=NO+CO	1.90E+11	0.0	3400.0
618.	HCCO+N=HCN+CO	5.00E+13	0.0	0.0
619.	CH3+N=H2CN+H	7.10E+13	0.0	0.0
620.	OH+HCN=HOCN+H	5.85E+04	2.4	12500.0
621.	OH+HCN=HNCO+H	1.98E-03	4.0	1000.0
622.	OH+HCN=NH2+CO	7.83E-04	4.0	4000.0
623.	HCN+O=NCO+H	1.38E+04	2.6	5000.0
624.	HCN+O=NH+CO	3.45E+03	2.6	5000.0
625.	CN+OH=NCO+H	6.00E+13	0.0	0.0
626.	CN+N2O=NCO+N2	1.00E+13	0.0	0.0
627.	C2N2+O=NCO+CN	4.57E+12	0.0	8900.0
628.	C2N2+OH=HOCN+CN	1.86E+11	0.0	2900.0
629.	HO2+NO=NO2+OH	2.11E+12	0.0	-500.0
630.	NO2+H=NO+OH	3.50E+14	0.0	1500.0
631.	NO2+O=NO+O2	1.00E+13	0.0	600.0
632.	NCO+H=NH+CO	5.00E+13	0.0	0.0
633.	NCO+N=N2+CO	2.00E+13	0.0	0.0
634.	NCO+OH=NO+CO+H	2.23E+05	2.0	16300.0
635.	NH+OH=HNO+H	2.00E+13	0.0	0.0
636.	NH+OH=N+H2O	5.00E+11	0.5	2000.0
637.	NH+N=N2+H	3.00E+13	0.0	0.0
638.	NH2+O=HNO+H	6.63E+14	-0.5	0.0
639.	NH2+O=NH+OH	6.75E+12	0.0	0.0
640.	NH2+OH=NH+H2O	4.00E+06	2.0	1000.0
641.	NH3+H=NH2+H2	6.36E+05	2.4	10200.0
642.	NNH+NO=N2+HNO	5.00E+13	0.0	0.0
643.	NNH+H=N2+H2	1.00E+14	0.0	0.0
644.	NNH+OH=N2+H2O	5.00E+13	0.0	0.0
645.	NNH+NH2=N2+NH3	5.00E+13	0.0	0.0
646.	NNH+NH=N2+NH2	5.00E+13	0.0	0.0
647.	NNH+O=N2O+H	1.00E+14	0.0	0.0
648.	HNO+M=H+NO+M	1.50E+16	0.0	48700.0
	H2O	Enhanced by	1.000E+01	
	O2	Enhanced by	2.000E+00	
	N2	Enhanced by	2.000E+00	
	H2	Enhanced by	2.000E+00	



649.	HNO+OH=NO+H2O	3.60E+13	0.0	0.0
650.	HNO+NH2=NH3+NO	2.00E+13	0.0	1000.0
651.	N+NO=N2+O	3.27E+12	0.3	0.0
652.	N+O2=NO+O	6.40E+09	1.0	6300.0
653.	N+OH=NO+H	3.80E+13	0.0	0.0
654.	CN+H2=HCN+H	3.60E+08	1.6	3000.0
655.	CN+HCN=C2N2+H	1.50E+07	1.7	200.0
656.	CN+NO2=NCO+NO	2.40E+13	0.0	-400.0
657.	CN+H2O=HCN+OH	8.00E+12	0.0	7500.0
658.	HCN+O=CN+OH	2.70E+09	1.6	29200.0
659.	CN+O=CO+N	7.70E+13	0.0	0.0
660.	CN+O2=NCO+O	7.50E+12	0.0	-400.0
661.	NCN+H=HCN+N	1.00E+14	0.0	0.0
662.	NCN+O=CN+NO	1.00E+14	0.0	0.0
663.	NCN+OH=HCN+NO	5.00E+13	0.0	0.0
664.	NCN+O2=NO+NCO	1.00E+13	0.0	0.0
665.	CN+CO2=NCO+CO	3.70E+06	2.2	26900.0
666.	CN+NO=NCO+N	1.00E+14	0.0	42100.0
667.	CN+HNO=HCN+NO	1.80E+13	0.0	0.0
668.	CN+HONO=HCN+NO2	1.20E+13	0.0	0.0
669.	CN+N2O=NCN+NO	3.80E+03	2.6	3700.0
670.	HOCN+OH=NCO+H2O	6.40E+05	2.0	2600.0
671.	HOCN+O=NCO+OH	1.50E+04	2.6	4000.0
672.	HOCN+H=HNCO+H	2.00E+07	2.0	2000.0
673.	HNCO+M=CO+NH N2	1.10E+16	0.0	86000.0
	Enhanced by	1.500E+00		
674.	HNCO+O=NCO+OH	2.20E+06	2.1	11400.0
675.	HNCO+O=NH+CO2	9.60E+07	1.4	8500.0
676.	NH+CO2=HNO+CO	1.00E+07	2.0	1700.0
677.	HNCO+H=NH2+CO	2.20E+07	1.7	3800.0
678.	HNCO+O=HNO+CO	1.50E+08	1.6	44000.0
679.	HNCO+OH=NCO+H2O	6.40E+05	2.0	2600.0
680.	HNCO+HO2=NCO+H2O2	3.00E+11	0.0	29000.0
681.	HNCO+O2=HNO+CO2	1.00E+12	0.0	35000.0
682.	HNCO+NH2=NH3+NCO	5.00E+12	0.0	6200.0
683.	HNCO+NH=NH2+NCO	3.00E+13	0.0	23700.0
684.	HNCO+CN=HCN+NCO	1.50E+13	0.0	0.0
685.	NCO+OH=HCO+NO	5.00E+12	0.0	15000.0
686.	NCO+O2=NO+CO2	2.00E+12	0.0	20000.0
687.	NCO+O=NO+CO	4.70E+13	0.0	0.0
688.	NCO+M=N+CO+M N2	3.10E+16	-0.5	48000.0
	Enhanced by	1.500E+00		
689.	NCO+NO=N2O+CO	6.20E+17	-1.7	800.0
690.	NCO+H2=HNCO+H	7.60E+02	3.0	4000.0
691.	NCO+HCO=HNCO+CO	3.60E+13	0.0	0.0
692.	NCO+CH2O=HNCO+HCO	6.00E+12	0.0	0.0
693.	NCO+NO=N2+CO2	7.80E+17	-1.7	800.0
694.	NCO+NO2=CO+NO+NO	1.30E+13	0.0	0.0
695.	NCO+NO2=CO2+N2O	5.40E+12	0.0	0.0
696.	NCO+HNO=HNCO+NO	1.80E+13	0.0	0.0
697.	NCO+HONO=HNCO+NO2	3.60E+12	0.0	0.0
698.	NCO+NCO=CO+CO+N2	1.80E+13	0.0	0.0
699.	NCO+CN=NCN+CO	1.80E+13	0.0	0.0
700.	NH3+M=NH2+H+M	2.20E+16	0.0	93500.0
701.	NH3+HO2=NH2+H2O2	3.00E+11	0.0	22000.0
702.	NH3+O=NH2+OH	9.40E+06	1.9	6500.0
703.	NH2+HO2=H2NO+OH	5.00E+13	0.0	0.0
704.	NH2+HO2=NH3+O2	1.00E+13	0.0	0.0
705.	H2NO+O=NH2+O2	4.00E+13	0.0	0.0
706.	NH2+NH2=N2H2+H2	8.50E+11	0.0	0.0
707.	NH2+NH2=NH3+NH	5.00E+13	0.0	10000.0
708.	NH2+NH=N2H2+H	5.00E+13	0.0	0.0
709.	NH2+N=N2+2H	7.20E+13	0.0	0.0
710.	NH2+NO2=N2O+H2O	3.20E+18	-2.2	0.0
711.	NH2+H=NH+H2	4.00E+13	0.0	3700.0
712.	NH2+NO=NNH+OH	2.80E+13	-0.6	0.0
713.	NH2+NO=N2+H2O	1.30E+16	-1.3	0.0
714.	NH+O2=HNO+O	4.60E+05	2.0	6500.0
715.	NH+O2=NO+OH	1.30E+06	1.5	100.0
716.	NH+NO=N2O+H	2.90E+14	-0.4	0.0
717.	NH+H=N+H2	3.00E+13	0.0	0.0
718.	NH+O=NO+H	9.20E+13	0.0	0.0
719.	NH+NH=N2+2H	2.50E+13	0.0	0.0
720.	NH+NO=N2+OH	2.20E+13	-0.2	0.0
721.	NH+NO2=N2O+OH	1.00E+13	0.0	0.0
722.	NNH=N2+H	1.00E+06	0.0	0.0
723.	NO+O+M=NO2+M	7.50E+19	-1.4	0.0

	N2	Enhanced by	1.700E+00			
	O2	Enhanced by	1.500E+00			
	H2O	Enhanced by	1.000E+01			
724.	NO+OH+M=HONO+M			2.00E+12	0.0	-700.0
	N2	Enhanced by	1.000E+00			
	H2O	Enhanced by	5.000E+00			
725.	HCO+NO=CO+HNO			7.20E+12	0.0	0.0
726.	NO2+NO2=NO+NO+O2			1.60E+12	0.0	26100.0
727.	CO+NO2=CO2+NO			9.00E+13	0.0	33800.0
728.	HCO+NO2=CO+HONO			2.10E+00	3.3	2400.0
729.	HCO+NO2=H+CO2+NO			8.40E+15	-0.8	1900.0
730.	HNO+H=H2+NO			4.40E+11	0.7	700.0
731.	HNO+O=NO+OH			1.00E+13	0.0	0.0
732.	HNO+O2=NO+HO2			1.00E+13	0.0	25000.0
733.	HNO+NO=N2O+OH			2.00E+12	0.0	26000.0
734.	HNO+NO2=HONO+NO			6.00E+11	0.0	2000.0
735.	HNO+HNO=N2O+H2O			4.00E+12	0.0	5000.0
736.	HCO+HNO=NO+CH2O			6.00E+11	0.0	2000.0
737.	H2NO+M=HNO+H+M			5.00E+16	0.0	50000.0
738.	H2NO+H=HNO+H2			3.00E+07	2.0	2000.0
739.	H2NO+H=NH2+OH			5.00E+13	0.0	0.0
740.	H2NO+O=HNO+OH			3.00E+07	2.0	2000.0
741.	H2NO+OH=HNO+H2O			2.00E+07	2.0	1000.0
742.	H2NO+NO=HNO+HNO			2.00E+07	2.0	13000.0
743.	H2NO+NH2=HNO+NH3			3.00E+12	0.0	1000.0
744.	HONO+H=NO2+H2			1.20E+13	0.0	7400.0
745.	HONO+O=NO2+OH			1.20E+13	0.0	6000.0
746.	HONO+OH=NO2+H2O			1.30E+10	1.0	100.0
747.	HCO+HONO=NO2+CH2O			1.20E+03	2.4	3900.0
748.	N2H2+M=NNH+H+M			5.00E+16	0.0	50000.0
	H2O	Enhanced by	1.500E+01			
	H2	Enhanced by	2.000E+00			
	N2	Enhanced by	2.000E+00			
	O2	Enhanced by	2.000E+00			
749.	N2H2+H=NNH+H2			5.00E+13	0.0	1000.0
750.	N2H2+O=NH2+NO			1.00E+13	0.0	1000.0
751.	N2H2+O=NNH+OH			2.00E+13	0.0	1000.0
752.	N2H2+OH=NNH+H2O			1.00E+13	0.0	1000.0
753.	N2H2+NH=NNH+NH2			1.00E+13	0.0	1000.0
754.	N2H2+NH2=NNH+NH3			1.00E+13	0.0	1000.0
755.	N2O+OH=N2+HO2			2.00E+12	0.0	40000.0
756.	N2O+H=N2+OH			3.30E+10	0.0	4700.0
757.	N2O+M=N2O+M			4.00E+14	0.0	56100.0
	N2	Enhanced by	1.700E+00			
	O2	Enhanced by	1.400E+00			
	CO2	Enhanced by	3.000E+00			
	H2O	Enhanced by	1.200E+01			
758.	N2O+O=N2+O2			1.40E+12	0.0	10800.0
759.	N2O+O=2NO			2.90E+13	0.0	23200.0
760.	N2O+CO=N2+CO2			2.70E+11	0.0	20200.0
761.	H+H+N2=H2+N2			5.40E+18	-1.3	0.0

NOTE: A units mole-cm-sec-K, E units cal/mole

## References

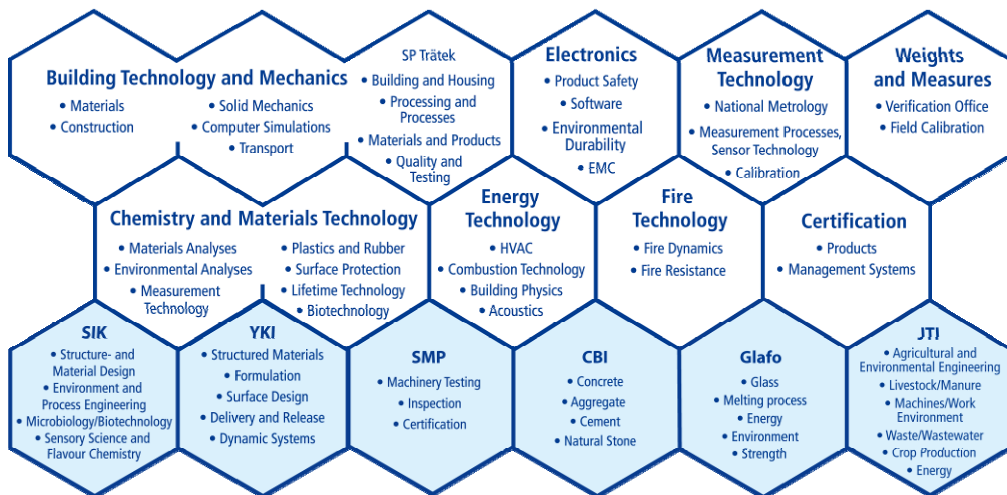
1. ISO 5660-1:2002 Reaction-to-fire tests - Heat release, smoke production and mass loss rate - Part 1: Heat release rate (cone calorimeter method), 2002.
2. ISO 9705 Fire tests - Full-scale room test for surface products, 1993.
3. Savolainen H, Kirchner N (1998) Toxicological Mechanisms Of Fire Smoke. The Internet Journal of Rescue and Disaster Medicine **1**, <http://www.ispub.com/ostia/index.php?xmlFilePath=journals/ijrdm/vol1n1/smoke.xml>
4. Speitel LC, Toxicity Assessment of Combustion Gases and Development of a Survival Model. Federal Aviation Administration, FAA Technical Center, DOT/FAA/AR-95/5, 1995.
5. Hill RG, Brown LJ, Speitel LC, Johnson GR, Sarkos C, Aircraft Seat Fire Blocking Layers - Effectiveness and Benefits Under Various Scenarios. Federal Aviation Administration, FAA Technical Center, DOT/FAA/CT-83/43, 1984.
6. Lestari F, Green AR, Chattopadhyay G, Hayes AJ, An alternative method for smoke toxicity assessment using human lung cells, *Fire Safety Journal*, 2006; **41**: 605-615.
7. Hertzberg T, Blomqvist P, L. L, Influence of HCl and PVC-smoke on isolated and perfused guinea pig lungs. SP Technical Research Institute of Sweden, SP Report 2006:57, 2006.
8. Tuovinen H, Blomqvist P, Effect of residence time on fire gases - experiments and simulations. SP Technical Research Institute of Sweden, SP Report 2007:71, 2007.
9. Dagaut P, Glarborg P, Alzueta MU, The oxidation of hydrogen cyanide and related chemistry, *Progress in Energy and Combustion Science*, 2008; **34**(1): 1-46.
10. Glarborg P, Miller JA, Mechanism and modeling of hydrogen cyanide oxidation in a flow reactor, *Combustion and Flame*, 1994; **99**(3-4): 475-483.
11. Hakkarainen T, Mikkola E, Laperre J, Gensous F, Fardell P, LeTallec Y, Carradori F, Paul K, Simonson M, Deley C, Metcalfe E, Smoke gas analysis by Fourier transform infrared spectroscopy, Final report of the SAFIR project, EU project Contract no. SMT4-CT96-2136. 1999.
12. ISO/TS 19700 Controlled equivalence ratio method for the determination of hazardous components of fire effluents, ISO, 2007.
13. Purser DA, Fardell PJ, Rowley J, Vollam S, Bridgeman B, Ness EM, An improved tube furnace method for the generation and measurement of toxic combustion products under a wide range of fire conditions, *Flame Retardants '94 Conference*, London, 1994.
14. Blomqvist P, Hertzberg T, Tuovinen H, A small-scale controlled equivalence ratio tube furnace method - experiences of the method and the link to large scale fires, *Interflam Conference 2007*, London, 2007.
15. Paul KT, Hull TR, Lebek K, Stec AA, Fire smoke toxicity: The effect on nitrogen oxides, *Fire Safety Journal*, 2008
16. Purser DA, Purser JA, HCN yields and fate of fuel nitrogen for materials under different combustion conditions in the ISO 19700 tube furnace and large -scale fires, *Fire Safety Science* 2008; **9**: 1117-1128.
17. Smith GP, Diagnostics for detailed chemical modeling, in *Applied Combustion Diagnostics*, K. Kohse-Höinghaus and J.B. Jeffries, Editors. 2002, Taylor & Francis.
18. Eckbreth AC, Laser Diagnostics for Combustion Temperature and Species. 2 ed. Combustion Science and Technology Book Series, ed. W.A. Sirignano, Vol. 3, Amsterdam, Gordon and Breach Science Publishers SA, 1996.

19. Kohse-Höinghaus K, Jeffries JB, Applied Combustion Diagnostics, Taylor & Francis, 2002.
20. Aldén M, Laser spectroscopic techniques for combustion diagnostics, *Combustion Science and Technology*, 1999; **149**: 1-18.
21. Demtröder W, Laser Spectroscopy: Basic concepts and instrumentation. 2 ed, Springer Verlag, 1996.
22. Wieman C, Hänsch TW, Doppler-Free Laser Polarization Spectroscopy, *Physical Review Letters*, 1976; **34**.
23. Farrow RL, Rakestraw DJ, Detection of Trace Molecular-Species Using Degenerate 4-Wave-Mixing, *Science*, 1992; **257**(5078): 1894-1900.
24. Vanderwal RL, Holmes BE, Jeffries JB, Danehy PM, Farrow RL, Rakestraw DJ, Detection of Hf Using Infrared Degenerate 4-Wave-Mixing, *Chemical Physics Letters*, 1992; **191**(3-4): 251-258.
25. Germann GJ, Rakestraw DJ, Multiplex Spectroscopy - Determining the Transition Moments and Absolute Concentrations of Molecular-Species, *Science*, 1994; **264**(5166): 1750-1753.
26. Germann GJ, Farrow RL, Rakestraw DJ, Infrared Degenerate 4-Wave-Mixing Spectroscopy of Polyatomic-Molecules - CH<sub>4</sub> and C<sub>2</sub>H<sub>2</sub>, *Journal of the Optical Society of America B-Optical Physics*, 1995; **12**(1): 25-32.
27. Dreier T, Ewart P, eds. *Coherent techniques for measurements with intermediate concentrations*. Applied combustion diagnostics, ed. K. Kohse-Höinghaus and J.B. Jeffries. 2002, Taylor & Francis: New York. 69.
28. Reichardt TA, Lucht RP, Theoretical calculation of line shapes and saturation effects in polarization spectroscopy, *Journal of Chemical Physics*, 1998; **109**(14): 5830-5843.
29. Li ZS, Rupinski M, Zetterberg J, Alwahabi ZT, Alden M, Mid-infrared polarization spectroscopy of polyatomic molecules: Detection of nascent CO<sub>2</sub> and H<sub>2</sub>O in atmospheric pressure flames, *Chemical Physics Letters*, 2005; **407**(4-6): 243-248.
30. Roy S, Lucht RP, Mcilroy A, Mid-infrared polarization spectroscopy of carbon dioxide, *Applied Physics B-Lasers and Optics*, 2002; **75**(8): 875-882.
31. Li ZS, Linvin M, Zetterberg J, Kiefer J, Alden M, Mid-infrared polarization spectroscopy of C<sub>2</sub>H<sub>2</sub>: Non-intrusive spatial-resolved measurements of polyatomic hydrocarbon molecules for combustion diagnostics, *Proceedings of the Combustion Institute*, 2007; **31**: 817-824.
32. Li ZS, Rupinski M, Zetterberg J, Alwahabi ZT, Alden M, Detection of methane with mid-infrared polarization spectroscopy, *Applied Physics B-Lasers and Optics*, 2004; **79**(2): 135-138.
33. Li ZS, Rupinski M, Zetterberg J, Alden M, Mid-infrared PS and LIF detection of CH<sub>4</sub> and C<sub>2</sub>H<sub>6</sub> in cold flows and flames at atmospheric pressure, *Proceedings of the Combustion Institute*, 2005; **30**: 1629-1636.
34. Alwahabi ZT, Li ZS, Zetterberg J, Aldén M, Infrared polarization spectroscopy of CO<sub>2</sub> at atmospheric pressure, *Optics Communications*, 2004; **233**(4-6): 373-381.
35. <http://www.carbolite.com/products.asp?id=5&doc=173>.
36. Controlled equivalence ratio method for the determination of hazardous components of fire effluents, ISO/TS 19700, 2007.
37. Li ZS, Hu CH, Zetterberg J, Linvin M, Alden M, Midinfrared polarization spectroscopy of OH and hot water in low pressure lean premixed flames, *Journal of Chemical Physics*, 2007; **127**(8).
38. Rothman LS, Gordon IE, Barbe A, Benner DC, Bernath PE, Birk M, Boudon V, Brown LR, Campargue A, Champion JP, Chance K, Coudert LH, Dana V, Devi VM, Fally S, Flaud JM, Gamache RR, Goldman A, Jacquemart D, Kleiner I, Lacombe N, Lafferty WJ, Mandin JY, Massie ST, Mikhailenko SN, Miller CE, Moazzen-Ahmadi N, Naumenko OV, Nikitin AV, Orphal J, Perevalov VI, Perrin

- A, Predoi-Cross A, Rinsland CP, Rotger M, Simeckova M, Smith MAH, Sung K, Tashkun SA, Tennyson J, Toth RA, Vandaele AC, Vander Auwera J, The HITRAN 2008 molecular spectroscopic database, *Journal of Quantitative Spectroscopy & Radiative Transfer*, 2009; **110**(9-10): 533-572.
39. Kee RJ, Rupley FM, Miller JA, Chemkin-II: A Fortran Chemical Kinetics Package for the Analysis of Gas Phase Chemical Kinetics. Sandia National Laboratories, Report SAND80-8009B, 1980.
  40. Kee RJ, Rupley FM, Miller JA, The Chemkin Thermodynamic Data Base. Sandia National Laboratories, Report SAND87-8215B, 1987.
  41. Kee RJ, Dixon-Lewis G, Warnatz J, Coltrin ME, Miller JA, A Fortran Computer Code Package for the Evaluation of Gas-Phase Multicomponent Transport Properties. Sandia National Laboratories, Report SAND86-8246, 1986.
  42. Glarborg P, Kee RJ, Grcar JF, Miller JA, PSR: A Fortran Program for Modeling Well-Stirred Reactors. Sandia National Laboratories, Report SAND86-8209, 1986.
  43. Grcar JF, The twopnt Program for Boundary Value Problems. Sandia National Laboratories, Report SAND91-8230, 1991.
  44. Gregory P. Smith, David M. Golden, Michael Frenklach, Nigel W. Moriarty, Boris Eiteneer, Mikhail Goldenberg, C. Thomas Bowman, Ronald K. Hanson, Soonho Song, William C. Gardiner J, Vitali V. Lissianski a, Qin Z. GRI-Mech 3.0. [http://www.me.berkeley.edu/gri\\_mech/](http://www.me.berkeley.edu/gri_mech/).
  45. Kantak MV, De Manrique KS, Aglave RH, Hesketh RP, Methylamine oxidation in a flow reactor: Mechanism and modeling, *Combustion and Flame*, 1997; **108**(3): 235-265.
  46. Xieqi M, Cicek B, Senkan SM, Chemical Structures of Fuel-Rich and Fuel-Lean Flames of Ccl4/Ch4 Mixtures, *Combustion and Flame*, 1993; **94**(1-2): 131-145.
  47. Li Z, Sun Z, Li B, Aldén M, Försth M, Spatially resolved trace detection of HCl in flames with mid-infrared polarization spectroscopy, *Optics Letters*, 2008; **33**(16): 1836-1838.
  48. Li Z, Sun Z, Li B, Aldén M, Försth M, Detection of HCl in a Premixed H2/O2/Ar Flame Seeded with CHCl3 Using Mid-IR Polarization Spectroscopy. 2008, Optical Society of America, St. Petersburg.
  49. Sun Z, Försth M, Li Z, Li B, Aldén M, In situ detection of HCN and HCl as products from burning polymers with spatially resolved mid-infrared polarization spectroscopy (IRPS), *4th European Combustion Meeting*, Vienna, 2009.

**SP Technical Research Institute of Sweden** develops and transfers technology for improving competitiveness and quality in industry, and for safety, conservation of resources and good environment in society as a whole. With Sweden's widest and most sophisticated range of equipment and expertise for technical investigation, measurement, testing and certification, we perform research and development in close liaison with universities, institutes of technology and international partners.

SP is a EU-notified body and accredited test laboratory. Our headquarters are in Borås, in the west part of Sweden.



**SP consists of eight technology units and six subsidiary companies. Three of the companies, CBI, Glafo and JTI are each 60 % owned by SP and 40 % by their respective industries.**



**SP Technical Research Institute of Sweden**

Box 857, SE-501 15 BORÅS, SWEDEN

Telephone: +46 10 516 50 00, Telefax: +46 33 13 55 02

E-mail: info@sp.se, Internet: www.sp.se

[www.sp.se](http://www.sp.se)

Fire Technology

SP Report 2009:50

ISBN 91-7848-

ISSN 0284-5172